Arab Academy for Science & Technology & Maritime Transport
Collage of Engineering and Technology
Department of Electrical & Computer Control Engineering

A Novel Measurement Technique for Extra High Voltage Busbar Fault Detection

A thesis submitted to partial fulfillment for the degree of
Master of Science
In
Electrical & Computer Control Engineering
By

Sherif Hussein Haggag

B.Sc. in Electrical Power & Machines Engineering

Supervised by

Prof. Dr. Rania Metwally El-Sharkawy

Arab Academy for Science and Technology

Dr. Ali Mohamed El-Rifaie

High Voltage Metrology Lab.
National Institute for Standards

2013

ARAB Academy for Science, Technology and Maritime Transport
College of Engineering and Technology

A Novel Measurement Technique for Extra High Voltage Busbar Fault Detection

By

Sherif Hussein Haggag

A Thesis
Submitted in Partial Fulfillment to the Requirements
for the Master's Degree in

Electrical & Computer Control Engineering

Supervisor
Prof. Dr. Rania Metwally El-Sharkawy

_____

Prof. Dr. Yasser Galal
Examiner

_____

Prof. Dr. Sayed Shehab
Examiner

_____

ACKNOWLEDGEMENT

I would like to thank all those who made a valuable contribution to this research one way or the other.

ABSTRACT

In this thesis, a new fault detection tool for Extra High Voltage (EHV) busbars is introduced. The new tool is to be used by extra high speed digital relays to detect busbar faults besides differentiating between close up line faults and busbar ones. The suggested tool uses a new technique that squares both of the instantaneous voltage signal and its complement to produce a unity relation in normal operating conditions. The new tool is then applied on the travelling wave equations to discriminate busbar faults from line ones. The suggested tool is being applied to a 500 KV busbar arrangement chosen from the Egyptian unified network then the relay criteria were applied to a small network lab. model with the true parameters of 500KV grid. The simulation results indicate the capability of the new tool for the detection and discrimination of all types of busbar faults while the practical tests show the capability of implementing such protection technique in reality.

CONTENTS

FIGURES

TABLES

Chapter 1 Introduction

1.1 Background:

An electric power system comprises of generation, transmission and distribution of electric energy [1]. They allow for power to be generated (generators), transformed from one voltage level to another (transformers), transmitted from one location to another (transmission lines), distributed among a number of transmission lines and power transformers (busses), and used by consumers (loads) [2].

Figure 1.1 is a one line graphical representation of the power system, the dashed borders contains the protective zones that covers one or at most two elements of the power system. The protective zones are planned in overlapped way that entire power system is collectively covered by them, and thus, no part of the system is left unprotected [3].

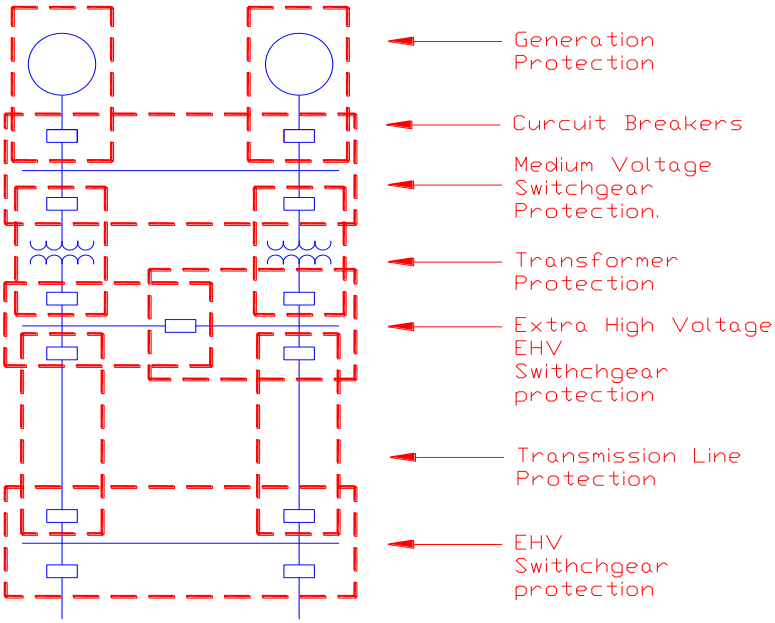

Figure 1.1, Single line diagram of power system.

Usually power system operates in steady state to deliver customers with convenient energy in proper voltage waveform and designated frequency. In up normal operation, system subjects to disturbances that caused by either heavy load changes or by the effect of a fault.

A fault in electric equipment is defined as a defect in its electrical circuit due to which the current is diverted from the intended path. Faults are generally caused by breaking of the conductor or failure of insulation. The other reasons include mechanical failure, accident, excessive internal end external stress, aging, operator mistakes---etc.[4].

On the occurrence of faults, current is relatively high so the fault currents can damage the defected equipment, system three phase voltage become un balanced ,faulted phase voltage decreases, power flow is directed towards the fault and the supply to the neighboring zone is effected [5].

Although proper power system planning and using sophisticated well fabricated component can minimized faults yet they can never prevent it completely therefore, it is necessary to protect power systems from faults.

1.2 Power system protection:

System protection is the actions taken to make sure that faults caused by abnormal operating conditions are detected and the affected part of the system is quickly removed from operation [6].

Modern power system evolves large amount of investment nowadays, so it is very important to avoid damages might happened to equipment of the utility as they take much time and cost to repair. Also service failure of a large

portion of the system is not acceptable. It is significant to keep the impaired component and the isolated part as minimum as possible.

1.2.1 Parameters of protective system

Protective system should have certain Parameters that are very important and should be considered [7]. The qualities of the protective systems are named as:

Reliability: assurance that the protection will perform correctly.

Selectivity: maximum continuity of service with minimum system disconnection.

Speed of operation: minimum fault duration and consequent equipment damage and system instability.

Simplicity: minimum protective equipment and associated circuitry to achieve the protection objectives.

Economics: maximum protection at minimal total cost knowing that a better protective system costs more.

1.2.1.1 Reliability

Reliability has two aspects, dependability and security. Dependability is defined as ''the degree of certainty that a relay or relay system will operate correctly'' (IEEE C 37.2). Security ''relates to the degree of certainty that a relay or relay system will not operate incorrectly'' (IEEE C 37.2). In other words, dependability indicates the ability of the protection system to perform correctly when required, whereas security is its ability to avoid unnecessary operation during normal day after-day operation, and faults and problems outside the designated zone of operation.

1.2.1.2 Selectivity-Coordination

Relays have an assigned area known as the primary protection zone, but they may properly operate in response to conditions outside this zone. In these instances, they provide backup protection for the area outside their primary zone. This is designated as the backup or overreached zone. Selectivity (also known as relay coordination) is the process of applying and setting the protective relays that overreach other relays such that they operate as fast as possible within their primary zone, but have delayed operation in their backup zone.

1.2.1.3 Speed

System should operate promptly interrupting the designated zone when it is required to do so to minimize the damages on the faulted equipment and provide the most possible human safety. Although speed action is inherently desired, sometimes where coordination quality engaged very fast or zero delay operation can cause of false tripping and losing of security. In general the faster the operation, the higher the probability of incorrect operation.

1.2.1.4 Sensitivity

Sensitivity in protective systems is the ability of the system to identify an abnormal condition that exceeds a nominal "pickup" or detection threshold value and which initiates protective action when the sensed quantities exceed that threshold.

1.2.1.5 Economics

It is fundamental to obtain the maximum protection for the minimum cost, and cost is always a major factor however we can't ignore the fact that a better protective system costs more.

1.2.2 Elements of a protection system

Although, in common usage, a protection system may mean only the relays, the actual protection system consists of many other subsystems which contribute to the detection and removal of faults. As shown in Figure 1.2, the major subsystems of the protection system are the transducers, relays, battery and circuit breakers. The transducers, i.e. the current and voltage transformers, constitute a major component of the protection system. Relays are the logic elements which initiate the tripping and closing operations, and we will, of course, discuss relays in the next section.

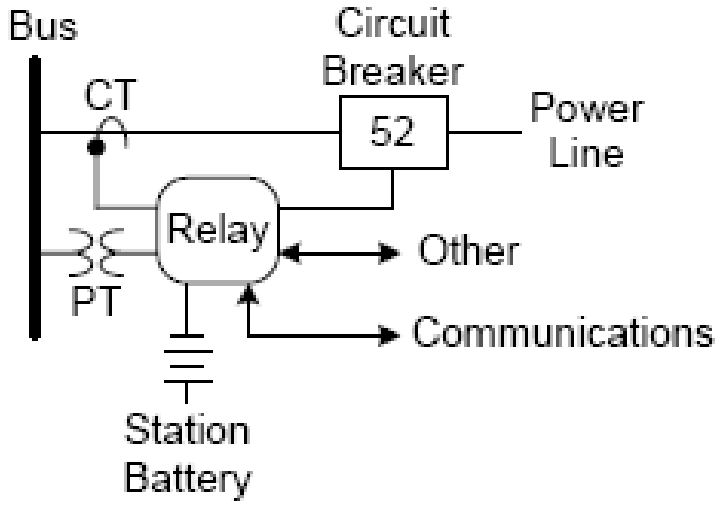

Figure 1.2, Protection system components.

1.3 Relays:

Protective relays can be classified into various ways depending on their scheme such as over current protection, distance protection, differential protection or it can be classified according to their function like over current, under voltages, impedance relays [8]. In the following categorization the classification of protective relays based on technology.

1. Electromagnetic Relays.
2. Static Relays.
3. Digital Relays.
4. Numerical relays.

In the previous century, protective relays have gone through major transitions with the change in technology. Electromechanical relays, the oldest in the family of protective relays, served the power system quite reliably. With the development in electronics, solid-state relays were developed. Small size, light weight and quiet operation are the advantages of solid-state relays over the electromechanical relays. Microprocessors technology made the relays even more compact, multifunctional and flexible.

1.3.1 Electromechanical relays

These relays were the earliest forms of relay used for the protection of power systems, and they date back nearly 100 years. They work on the principle of a mechanical force causing operation of a relay contact in response to a stimulus. The mechanical force is generated through current flow in one or more windings on a magnetic core or cores, hence the term electromechanical relay.

1.3.2 Solid-State Relays

Solid-state or static relays began in the early 1960's.they are semiconductor devices composed of electronic components like resistors, diodes, transistors…etc. These relays do not have moving parts which make them lighter and smaller than electromagnetic relays. Solid-state relays perform the same functions as electromagnetic relays except that they need less voltage to operate and switching can be performed in very short times.

1.3.3 Digital relays

Microprocessors and microcontrollers replaced analogue circuits used in static relays to implement relay functions. Early examples began to be introduced into service around 1980, and, with improvements in processing capacity, can still be regarded as current technology for many relay applications. However, such technology will be completely superseded within the next five years by numerical relays. Digital relays introduce A/D conversion of all measured analogue quantities and use a microprocessor to implement the protection algorithm. The microprocessor may use some kind of counting technique, or use the Discrete Fourier Transform (DFT) to implement the algorithm. However, the typical microprocessors used have limited processing capacity and memory compared to that provided in numerical relays. The functionality tends therefore to be limited and restricted largely to the protection function itself.

1.3.4 Numerical relays

The difference between digital and numerical relay can be viewed as natural developments of digital relays as a result of advances in technology. Typically, they use a specialized digital signal processor (DSP) as the computational hardware, together with the associated software tools. The input

analogue signals are converted into a digital representation and processed according to the appropriate mathematical algorithm.

1.4 Fault Detection based on Transient Analysis Techniques

Fault detection using fault transient analysis has been successfully applied as a scheme on extra high-voltage protection. Fault transient signals are high frequency signals superimposed on the steady state voltage and currents. The transient signals hold plenty of useful information regarding the fault that can help in detecting all its parameters; they can then be extracted from the power frequency signals by applying a suitable tool. A number of methods are available for transient analysis; these methods can be categorized as time domain methods, frequency domain or time frequency domain [9, 10].

1.4.1 Time Domain Approach

There have been a lot of attempts to determine the fault occurrence using signal analysis in the time domain because of its simplicity. In this section, a review of some of these techniques is presented.

1.4.1.1 Statistical Analysis

The objective of signal feature extraction is to represent the signal in terms of a set of properties or parameters. The most common measurements in statistics are the arithmetic mean, standard deviation, and variance. All these parameters actually compute the value about which the data are centered. In fact, all measures of central tendency may be considered estimates of mean. The arithmetic mean of a sample may be computed as:

$$\bar{x} = \frac{1}{n}\sum_{i=1}^{n} x_i \qquad (1.1)$$

Where: x_i is the samples signal, $\bar{x}$ is the signal mean and n is the number of samples.

The standard deviation measures the dispersion of set of samples. It is most often measured by the deviation of the samples from their average. The sum of these deviations will be zero and the sum of squares of the deviations is positive. The standard deviation of a sample is computed as:

$$s = \sqrt{\frac{1}{n-1}\sum_{i=1}^{n}\left(x_i - \bar{x}\right)^2} \qquad (1.2)$$

The variance is the average of the squared deviations as in the form:

$$s^2 = \frac{1}{n-1}\sum_{i=1}^{n}\left(x_i - \bar{x}\right)^2 \qquad (1.3)$$

Another important parameter in statistical estimation method is called the auto correlation coefficient, which measures the correlation between samples at different distance apart. It is closely related to convolution and, when applied to signals, provides a method of measuring the "similarity" between corresponding signals. The concept of cross-correlation analysis (CCA) is similar to ordinary correlation coefficient, namely that given N pairs of samples on two variables x and y, the correlation coefficient is given by

$$R_{\mathrm{xy}}(\tau) = \frac{1}{n}\sum_{k=1}^{n}\left(x_{k\Delta t+\tau} - \bar{x}\right)\left(y_{k\Delta t} - \bar{y}\right) \qquad (1.4)$$

Where R_{xy} is the cross correlation function of the signals x and y, n is the number of samples, $\bar{x}$ is x mean, $\bar{y}$ is y mean and Δt is sampling interval. The mean is removed to attenuate any exponential or power frequency signal. Correlation is a common operation in many signal processing techniques.

1.4.1.2 Signal Derivative

The use of the first derivative of the current or voltage signals has been reported since a long time. This kind of filtering is based on a data window of two samples for extracting the abrupt changes of the monitored signal. The first differences of the current samples can be expressed as:

$$\Delta I_n = I_{n+1} - I_n \qquad (1.5)$$

Where In is the nth sample of the signal I.

A three sample sequence filter, which is based on the second difference of the current samples, is considered. The second difference filter; with three samples window; can be expressed as:

$$\Delta I_n = I_{n+1} - 2I_n + I_{n-1} \qquad (1.6)$$

where n is the sample number.

1.4.2 Frequency Domain Approach

Fourier transform-based fault location algorithms have been proposed for a long time. Most of the proposed algorithms use voltages and currents between fault initiation and fault clearing. To find out the frequency contents of the fault signal, several transformations can be applied, namely, Fourier, wavelet, Wigner, etc., among which the Fourier transform is the most popular and easy to use.

1.4.2.1 Fourier Transform

Fourier transform (FT) is the most popular transformation that can be applied to transient signals to obtain their frequency components appearing in the fault signal. Usually, the information that cannot be readily seen in the time domain can be seen in the frequency domain. The FT and its inverse give a one-to-one relationship between the time domain *x(t)* and the frequency domain *X(ω)*.

Given a signal *I(t)*, the Fourier Transform *FT(ω)* is defined by the following equation:

$$FT(\omega) = \int_{-\infty}^{\infty} I(t).e^{-j\omega t} dt \qquad (1.7)$$

Where ω is the continuous frequency variable. This transform is very suitable for stationary signal, where every frequency components occur in all time. The discrete form of the FT can be written as

$$DFT[k] = \frac{1}{N} \sum_{n=1}^{N} I[n].e^{-j\frac{2\pi kn}{N}} \qquad (1.8)$$

Where $1 \leq k \leq N$.

The FT gives the frequency information of the signal, but it does not tell us when in time these frequency components exist. The information provided by the integral corresponds to all time instances because the integration is done for all time intervals. It means that no matter where in time the frequency *f* appears, it will affect the result of the integration equally. This is why FT is not suitable for non-stationary signals.

1.4.3 Time - Frequency Domain Approach

Fourier transform assumes that the signal is stationary, but fault superimposed signals such as travelling wave signal is always non-stationary. To overcome this deficiency, modified method-short times Fourier transform and Wavelet Transform allows representing the signal in both time and frequency domain through time windowing function. The window length determines a constant time and frequency resolution. Thus, a shorter time windowing is used in order to capture the transient behavior of a signal; we sacrifice the frequency resolution. The nature of the real fault signals is non-periodic; such signals cannot easily be analyzed by conventional transforms. So, an alternative mathematical tool- wavelet transform must be selected to extract the relevant time-amplitude information from a signal. In the meantime, we can improve the signal to noise ratio based on prior knowledge of the signal characteristics.

1.4.3.1 Short Time Fourier Transform

In the STFT, the signal is divided into small segments which can be assumed to be stationary. The signal is multiplied by a window function within the Fourier integral. If the window length is infinite, it becomes the DFT. In order to obtain the stationarity, the window length must be short enough. Narrower windows afford better time resolution and better stationarity, but at the cost of poorer frequency resolution. One problem with the STFT is that one cannot determine what spectral components exist at what points of time. One can only know the time intervals in which certain band of frequencies exist. The STFT is defined by following equation:

$$STFT(t,\omega) = \int_{-\infty}^{\infty} I(t).W(t-\tau).e^{-j\omega t}dt \qquad (1.9)$$

Where I(t) is the measured signal, ω is frequency, W(t- τ) is a window function, τ is the translation, and t is time.

To separate the negative property of the DFT described above, the signal is to be divided into small enough segments, where these segments (portion) of the signal can be assumed to be stationary. These transforms can be displayed in a three dimensional system (Amplitude of transform, frequency, time). And it is clearly seen in time and frequency domain. To get better information in time or frequency domain, parameters of the window can be changed. As aforementioned, narrow windows give good time resolution, but poor frequency resolution. Wide windows give good frequency resolution, but poor time resolution. Thus, it is required to compromise between the time and frequency resolutions.

1.4.3.2 Wavelet Transform

Signal-cutting problem in Fourier-based techniques are overcome in wavelet analysis by using a fully scalable modulated window. The window is shifted along the signal and for every location the spectrum is calculated. This process then repeated several times with a shorter or longer window for every cycle. Eventually a collection of time-frequency representations of the signal is obtained with different resolutions. Due to the nature of this collection this analysis is often called multi-resolution analysis [11, 12].

Wavelets derived from one mother wavelet which is a prototype function by translation in space and dilation (changes of the scale and space simultaneously).

A. Continuous Wavelet Transformation (CWT)

The mother wavelet W(t) given in the following Equation:

$$W_{d,\tau}(t) = \frac{1}{\sqrt{d}}.W(\frac{t-\tau}{d}) \qquad (1.10)$$

Where d stands for the dilation (scaling) parameter and τ is the translation parameter of the mother function Wd,τ (t) to generate wavelets. The scale index d indicates the wavelet's width, and the location index τ gives its position. The 1/√d factor is for energy normalization at different scales. Once the mother wavelet function is known, a CWT of a function, f(t), is given in following Equation:

$$CWT(f,d,\tau) = \int_{-\infty}^{\infty} f(t).W_{d,\tau}^{*}(t)dt \qquad (1.11)$$

Where * stands for complex conjugation. Equation (1.1) shows how to decompose a function into a set of basis functions, wavelets as represented by Wd,τ (t), which are derived from one mother wavelet W(t).

As presented in Equation (1.11), the CWT of a function, f(t), is obtained by continuously shifting a continuously scalable function, W(t) over f(t) and calculating the correlation between the two. However, continuously translating and scaling a wavelet function results in an infinite number of wavelets and eventually leads to a redundant number of wavelet coefficients and an enormous computational burden. In order to overcome this redundancy Discrete Wavelet Transform is introduced.

2. *Discrete Wavelet Transformation (DWT)*

Discrete wavelets are not continuously scalable and translatable but they are dilated and translated in discrete time steps. In DWT, filters of different cutoff frequencies are utilized in order to decompose the signal at different scales. A series of high-pass filters are repeatedly applied to a signal to extract

the high frequencies and another series of low-pass filters are applied to the signal to analyze the low frequencies.

A general form of the discrete mother wavelet function used in DWT is given in the following Equation:

$$W_{j,k}(t) = \frac{1}{\sqrt{j_0^j}} .W(\frac{t - k\tau_0 d_0^j}{d_0^j}) \qquad (1.12)$$

where j and k are integers and d0 > 1 is a fixed dilation step. _0 is the translation factor and depends on the dilation step, d0.

1.5 Thesis Objective

The following are the major objectives of the work reported in this thesis.

1. To develop a digital technique for detecting the occurrence and the parameters of a fault on a busbar.
2. To apply the proposed protection technique on a network that is simulated with actual parameters on the Alternating Transient program (ATP).
3. To implement the fault detection practically using a lab model and National Instrument (NI) logic controller and to check the performance of the techniques.

1.6 Outline of the Thesis

This thesis is organized in seven chapters and five appendices.

The first chapter provides a background on the power system and basics on high voltage protection; it also provides a brief to protective relays. Then the chapter outlines the material presented in the thesis. In addition, digital protection techniques using signal processing are introduced in this chapter.

The second chapter introduces the history of busbar protection besides different connections (configuration) of it. It also presents the obsoleted and contemporary methods that are used in bus protection.

The third chapter presents a new proposed technique which can be used to detect bus faults. The new technique is based on Cos-Sin algorithm. The technique is applied to a small network as a test.

The forth chapter presents extra two algorithms that helps to detect fault type and location. One of them is based on the average of the unity obtained from Cos-Sin technique while the other is depending on the travelling wave phenomena. The chapter contains the complete scenarios of the operating criteria and the final flow chart.

In the fifth chapter the implementation of a new digital relay to be used with extra high voltage network is done. The Egyptian Unified 500 KV network is simulated using the Alternative Transient Program (ATP), while the relays software program is constructed using the MATLAB language. The simulation results of different fault cases, at different fault inception angles and fault resistances and the suggested relay responses for each one of them are also included.

The sixth chapter introduces a 380 V lab model for a 500 KV transmission line based on the Egyptian unified network parameters and investigated using the Lab View program, where a high speed interface card is used. A node that is modeling the busbar and the line model itself are practically protected using the

Cos-Sin and associated tools. A comparison is made between the theoretical and practical results.

The seventh chapter presents the conclusion of the work done in the thesis. It also provides expectations of the available future work that can be done on the light of this thesis.

Chapter 2 Busbar protection

2.1 History:

Up to the mid 1930s, no wide scale efforts had been made to protect busbars on a unit basis. Also there was reluctance in arranging one protective equipment to cause simultaneous tripping of a large number of circuits.

Before the British Grid System was built in the early 1930s, many undertakings ran isolated from adjacent ones, and so the power available for busbar faults was often relatively small, and damage due to these faults was generally not extensive.

By the late 1930s, the British Power Systems were extensively interconnected, with a consequent increase in fault power.

A number of busbar faults occurred about this time, but due to their relatively slow clearance from the system by overcurrent and earth-fault relays, considerable damage resulted, especially in indoor stations.

These faults led to efforts being made to produce busbar protection in such a form that it could be widely applied without itself being a further hazard to the system.

Construction of the British 275 KV supergrid system began in about 1953, by which time standard principles of busbar protection had been adopted for outdoor switchgear at the higher voltages. At this time the emphasis was placed on the avoidance of unwanted operations in order to give maximum security of supply.

With the introduction of 400 KV substations in the 1960s, the transient stability of generators became the more important consideration and this led to a

change of emphasis so that fast operating times and reliable operation would be obtained for a fault occurring within the protected zone, which in this case would be the busbars and switchgear [13].

2.2 Bus arrangements

Buses exist throughout the power system and, particularly, wherever two or more circuits are interconnected. The number of circuits that are connected to a bus varies widely. Bus faults can result in severe system disturbances, as high fault current levels are typically available at bus locations and because all circuits supplying fault current must be opened to isolate the problem. Thus, when there are more than six to eight circuits involved, buses are often split by a circuit breaker (bus tie), or a bus arrangement is used that minimizes the number o f circuits, which must be opened for a bus fault. There are many bus arrangements in service dictated by the foregoing and by the economics and flexibility of system operation [14]. The buses are typically illustrated as:

- Single bus–single breaker Figure 2.1.
- Double bus with bus tie–single breaker Figure 2.2.
- Main and transfer bus–single breaker Figure 2.3.
- Double bus–single breaker Figure 2.4.
- Double bus–double breaker Figure 2.5.
- Ring bus Figure 2.6.
- Breaker- and-a-half bus Figure 2.7.

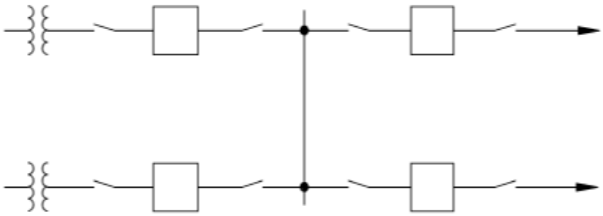

Figure 2.1, Single bus–single breaker.

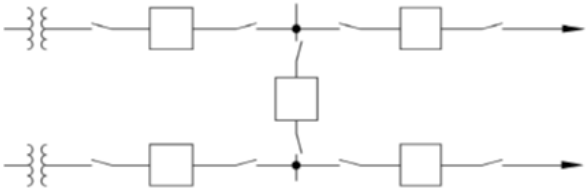

Figure 2.2, Double bus with bus tie–single breaker.

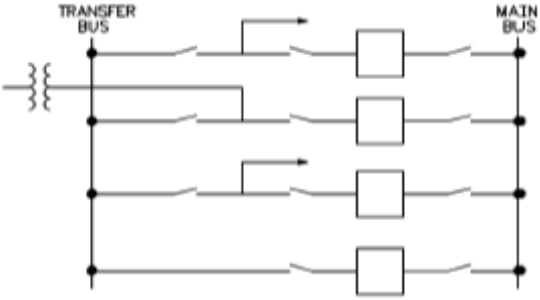

Figure 2.3, Main and transfer bus–single breaker.

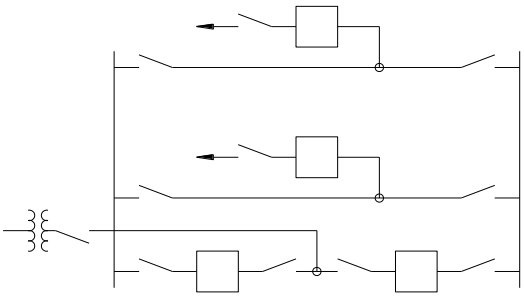

Figure 2.4, Double bus–single breaker.

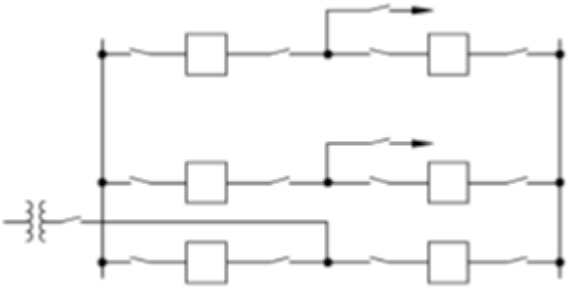

Figure 2.5, Double bus–double breaker.

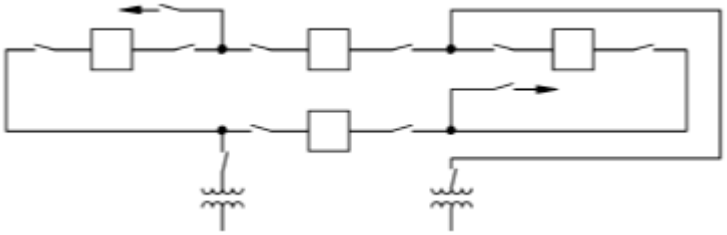

Figure 2.6, Ring bus.

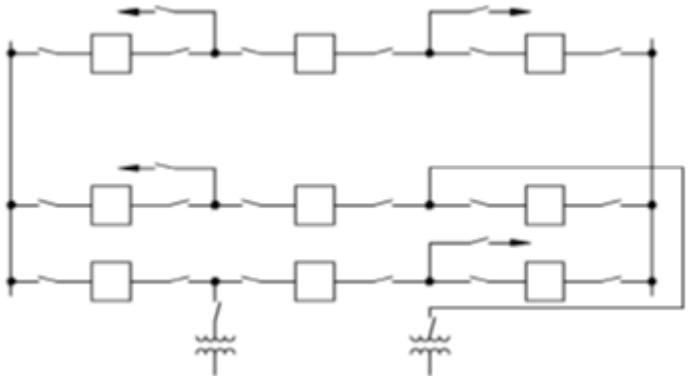

Figure 2.7, Breaker- and-a-half bus.

Table 2.1 presents a summary of advantages and disadvantages of each bus arrangement [11].

Figure	Arrangement		Advantages		Disadvantages
2.1	Single breaker, single bus	1	Basic, simple, economical	1	No operating flexibility
		2	One bus voltage for all circuits	2	One bus voltage for all circuits
				3	Circuit removed for maintenance or problems
2.2	Double bus with bus tie	1	Two power sources to feed two buses	1	Circuit removed for maintenance or problems
		2	One source lost, load transferred	2	Bus tie breaker fault trips both buses
		3	One bus out, partial service available	3	Voltage required on each bus
2.3	Main and transfer bus	1	One differential zone	1	Bus tie breaker protection suitable for each circuit
		2	Only one circuit transferred	2	Bus fault trips all breakers
		3	Breaker, relays transferred for maintenance, etc.	3	Potential for error
		4	Voltage only on main bus	4	Bus tie protection adaptable for all circuits
2.4	Single breaker, double bus	1	High flexibility	1	Complicated (undesirable) switching of protection
		2	Any line operated from either bus	2	Bus tie breaker protection suitable for each circuit
		3	One bus available as a transfer bus	3	With line breaker bypassed differential removed from one bus
				4	Bus tie breaker fault trips all breakers
				5	Voltage required for each bus
2.5	Double breaker, double bus	1	Very high flexibility	1	Protection in service during breaker maintenance
		2	Overlapping protection zones	2	Two breakers per line
		3	Bus fault does not interrupt service	3	Line protection from two CTs
		4	All switching by breakers	4	Requires line side voltage
		5	Either bus can be removed	5	Two breakers trip for line faults
2.6	Ring bus	1	High flexibility	1	Requires line side voltage
		2	Minimum breakers	2	Relays in service during breaker maintenance
		3	Bus section part of line, no bus differentials	3	Line faults trip two breakers
				4	Local backup not applicable
				5	Open ring and subsequent fault may result in undesired system separation
2.7	Breaker and a half bus	1	More operating flexibility	1	Required more breakers
		2	Bus section part of lines	2	Center breaker serves two lines
				3	Requires line side voltage
				4	Two bus differential zones
				5	Local backup not applicable
				6	Line faults trip two breakers

Table 2.1, Advantages and disadvantages of bus arrangement

2.3 Busbar Protection

A variety of methods have been used to implement bus protection system, the most famous schemes are:

1. System protection used to cover busbars.
2. Frame-earth protection.
3. Differential protection.
   a) Over current differential.
   b) Percentage differential.
   c) Linear coupler differential.
   d) High impedance differential
4. Directional interlock protection.

The next sections will present each of them in details.

2.3.1 Schemes cover bus protection

Wherever overcurrent or distance schemes are used in a system protection, busbar's protection is implicitly covered. It is worth to say that overcurrent protection usually applied to relatively simple distribution systems or as a back-up protection, which gives a considerable time delay, whereas distance protection provides cover for busbar faults in its second and possibly subsequent zones [8].

2.3.2 Frame earth protection

The switchgear is lightly insulated from the earth. Primary of the current transformer is connected between metal frame or enclosure of switchgear and an earth point.

Concrete foundation of the switch gear together with all conduits and bolt are insulated from earth, the resistance to earth being about 10 to 12 Ω. In the occurrence of switchgear earth fault, the fault current will flow over through the neutral connection consequently the ground fault relay will be energized [15]. Figure 2.8 illustrates the frame earth connection.

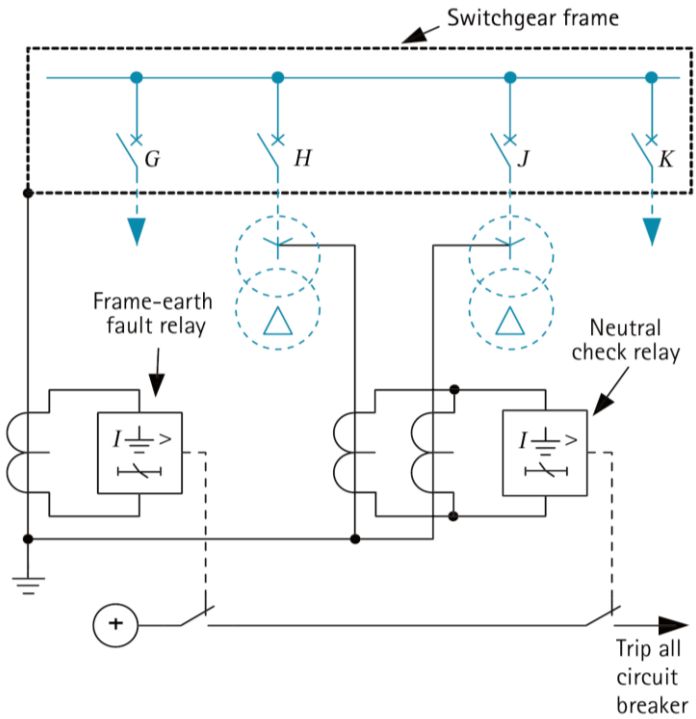

Figure 2.8, Frame earth protection arrangement.

2.3.3 Bus differential protection

Differential protection / Mertz-price is a scheme that is based on Kirchhoff's current law by comparing the vector sum of currents entering and leaving the protected elements (Busbar). In healthy systems the current sum is equal zero, once a fault happens the resultant of that sum deviates from zero and different in currents represents the fault current [16]. Figure 2.9 presents the basic concept of differential protection.

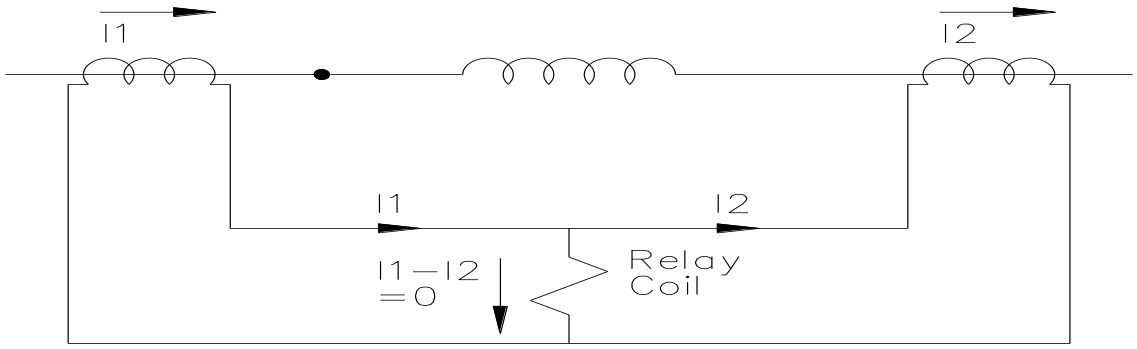

Figure 2.9, Differential protection basic connection.

During faults and especially external ones some problems appears such as [5, 17, 18]:

a) Difference in pilot wires lengths.

Pilot wires that connect measuring current transformers located in different sites to the relay have different lengths and different resistance. This problem can easily be solved by linking series resistors to the pilot wires.

b) CT ratio error.

Current transformers may have almost equal rates, yet during shot circuit, the current increases excessively. Minor inadequacy of current transformers created by different magnetic circuit's characteristic or different saturation conditions can cause false tripping.

c) Current transformer magnetic circuit saturation.

2.3.3.1 Over-current differential protection

Bus fault can be sensed by an over-current relay on the incoming circuit using the arrangement in figure 2.10 [19]. This protection scheme is provided as a primary protection when no other bus protection is available. In case of presence

of other main protection technique, over current and earth fault protection can act as a back up protection.

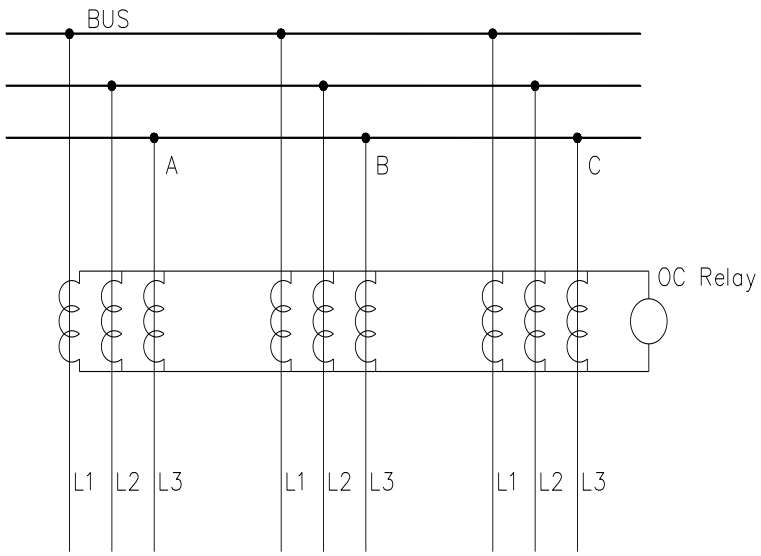

Figure **2.10**, Over-current differential protection.

2.3.3.2 Biased / percentage differential bus zone protection:-

Percentage differential protection overcomes the problem of different CT ratios and solves the problem of false tripping during high current values arising from external faults.

In this relay the operating coil is connected to midpoint of a restraining coil. The circulating current flows through restraining coils while the spill current pass through the operating coil. For external faults, average restraining current increases and thereby the restraining torque increases which prevents the mal-operation of the relay. Figure 2.11 demonstrate the Connections of Multi-restraint Differential Relay [20].

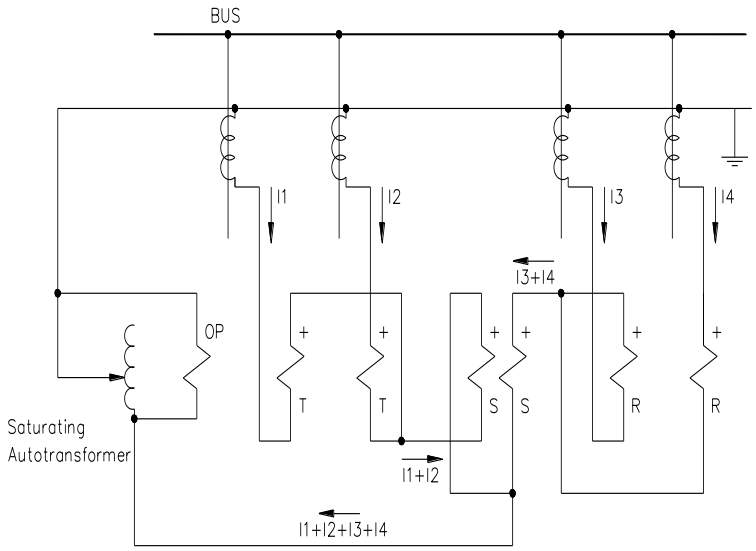

Figure 2.11, Multi-restraint Differential Relay.

2.3.3.3 Bus differential protection with linear coupler

Eliminating the problem of current transformers saturation can be done by eliminating the iron core from the current transducer. This can be performed using linear coupler devices which are an air-cored mutual reactor on a non magnetic toroidal core [8].

Advantage of the linear coupler devices are:

a. Eliminating of saturation in current transducer.
b. High speed performance with negligible transient response.
c. Reliable design.
d. Easy to set and maintain.

2.3.3.4 High impedance bus differential protection

This protection scheme is designed to eliminate both CT ratios mismatch and CT saturation problems. In this scheme of protection difference in balance current passes through high impedance Z_H created by inserting a high resistance

bridge rectifier (of almost 3000Ω) in the current path, that produce high voltage drop on the relay terminals. A series LC circuit is tuned to system fundamental frequency in order to make the relay responsive only to the fundamental component of current, thereby improving the selectivity. The varistor is to limit voltage that is produced when faults occur and an instantaneous overcurrent unit is connected in series with this combination and is set to operate at very high internal fault magnitudes [19, 21].

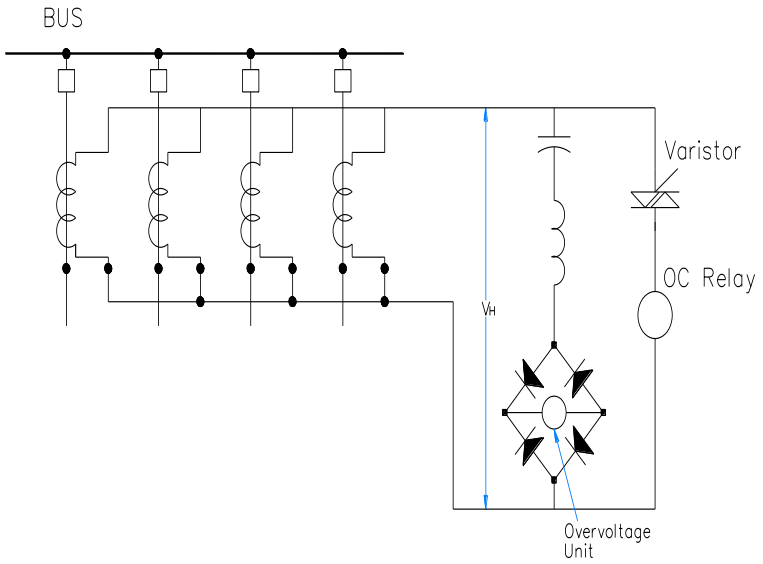

Figure 2.12, High impedance differential protection.

2.3.4 Directional interlock

Directional comparison scheme comprised directional relays in source circuits and overcurrent relays in load circuits. The contacts of these relays are suitably interlocked in such a way that if power flows towards the busbar from the source circuit and the current flowing away from busbars is sufficiently low, the entire zone protection acts and all the circuit breakers on load side and source side are tripped [10].

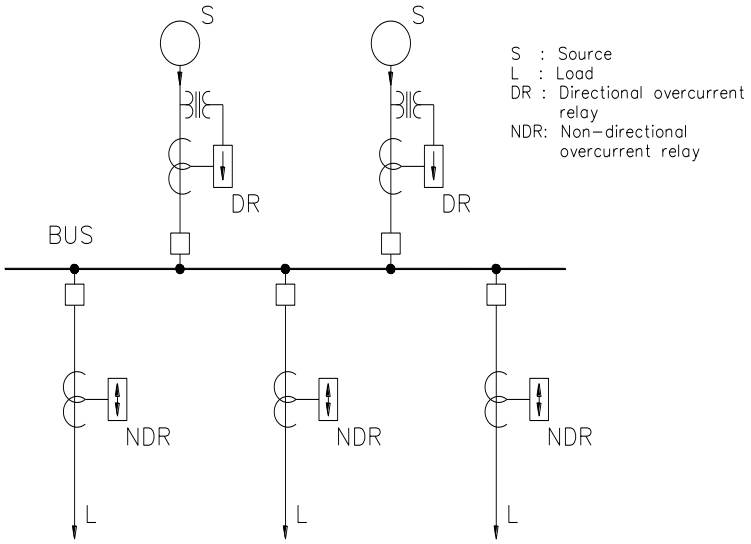

Figure 2.13, Directional comparison.

2.3.5 Digital Busbar Protection

Digital relay application has lagged behind that of other protection functions. Usually static technology is still employed in these schemes, but now digital technology has become mature enough to be considered. Multiple communications paths have provided relays with links to various units.

The philosophy adopted is one of distributed processing of the measured values, as shown in Figure 2.14. Feeders each have their own processing unit, which collects together information on the state of the feeder (currents, voltages, CB and isolator status, etc.) and communicates it over high-speed fiber-optic data links to a central unit. For large substations, more than one central unit may be used, while in the case of small installations, all of the units can be co-located, leading to the appearance of a traditional centralized architecture [22].

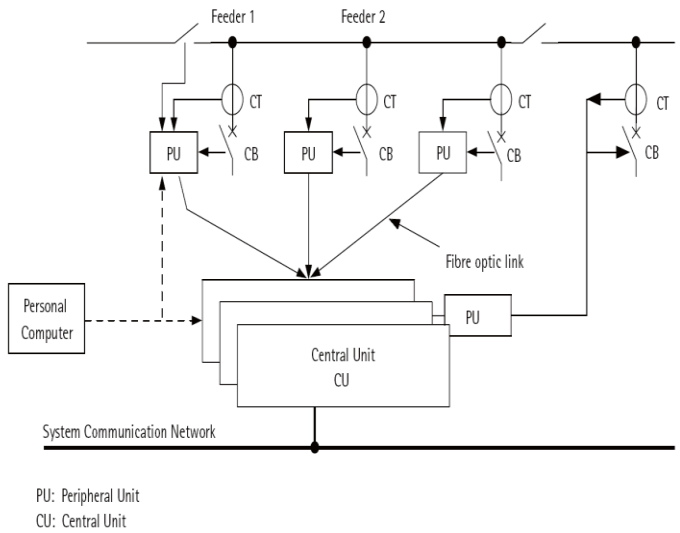

Figure 2.14, Digital protection.

In the next chapter a new technique for busbar fault detection is introduced. The new technique is based on Cos-Sin algorithm.

Chapter 3 COS-SIN Transient Measurement Technique and Some Applications

3.1 Introduction

There are numerous methods available for fault detection in power systems. Earlier methods rely mainly on recording and analyzing of power frequency component of the system while modern relaying depends on fault transient signals which comprise of high frequency signals superimposed on the steady state voltage and current. The transient signals are various and hold different names but the most famous one is the traveling wave that is going to be over viewed later.

The superimposed signals can be filtered by extracting the fundamental frequency component from the measured current and voltage quantities and that can be done using several techniques such as correlation, Fourier analysis and wave let transform [11, 23].

The superimposed high frequency signals hold abundant of information and parameters of the waves that might be useful to identify the fault time, type, direction and even the exact location of it. Such information will never be available through the power frequency components.

Development of computers and processors with respect to speed, power consumption and accuracy accompanied with rapid improvement in modern transformers facilitate fault detection performed in numerical relays [24].

This chapter introduces a new technique to detect transient signals associated to fault and consequently obtain the fault moment. It also presents a limited application on EHV Network as an application sample on that technique.

3.2 Cos-Sin technique

The Cos-Sin algorithm [25, 26] is given as follows: the voltage signal at any instant for a given bus-bar is represented by Va (t) where:

$$V_a(t) = V_{max}\cos(wt + Ø) \qquad (3\text{-}1)$$

On the other hand the complement of this signal could be obtained as Vg(t) where:

$$V_g(t) = V_{max}\sin(wt + Ø) \qquad (3\text{-}2)$$

By squaring, adding and normalizing the above two equations, discrimination signal M(t) can then be introduced as follows:

$$M(t) = \frac{V_a^2(t)}{V_{max}^2} + \frac{V_g^2(t)}{V_{max}^2}$$

$$M(t) = \frac{V_{max}^2\cos^2(wt + Ø)}{V_{max}^2} + \frac{V_{max}^2\sin^2(wt + Ø)}{V_{max}^2}$$

$$M(t) = \cos^2(wt + Ø) + \sin^2(wt + Ø) \qquad (3\text{-}3)$$

3.3 Structuring of discrimination signal M(t)

The voltage signal mentioned is equation (3-1) can be obtained from the system directly by means of measurement. We can call this signal as actual signal Va(t). Generated voltage signal Vg(t) is automatically calculated via equation (3-2).

Max value (Vm) is one of the parameters that should be known prior to getting the generated signal ,it may assumed to be a constant value that have been captured from the first cycle measured of the actual signal V(a). This assumption is valid in power system and especially in extra high voltage networks.

Another missing parameter in the generated signal equation is the phase shift (Ø), it also can be known from analyzing the zero crossing point together with peak value timing of the first cycle of the actual voltage Va(t).

Proper detection of signal peak value, phase shift and frequency will enable us to generate an exact complementary of each sample taken from actual voltage.

Figure 3.1 shows an actual detected voltage signal and its artificial complementary, both signals are totally in sync with each other.

The actual signal contains disturbances due to exposing to a single phase L-G fault occurs in certain time, yet artificial signal kept healthy and undistorted as it was formulated based on pre fault detected information .

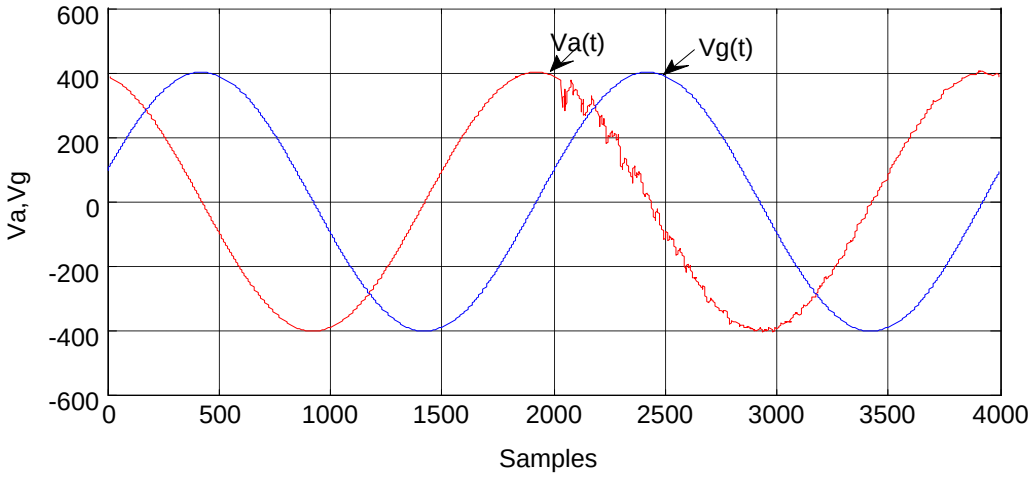

Figure 3.1, Va(t) and Vg(t) signals for one phase during LG fault.

The discrimination signal M(t) is unity signal as long as the detected signal is not distorted however, any distortion in the actual signal, M(t) will deviate away immediately from unity giving a clear indication of improper signal waveform.

To sum up, all necessary information needed will be acquired and gathered from the first cycle of the actual signal Va(t) after that if any sample distorted for any reason, the corresponding fabricated complementary will not follow and it will be kept as it is.

3.4 Applications

The introduced technique is going to be applied on a 500 KV small network as an example. It is going to be tested on normal operation, fault case that locates on busbar and a fault located on transmission line. The recorded results are to be analyzed and compared.

3.4.1 Bus bar fault

A very challenging test to the technique is to apply Cos-Sin tool to the protective digital relay of extra high voltage busbar in 500 KV network.

In such network the peak value of the voltage can be regarded almost constant as the network transformer is normally equipped with an automatic voltage controller, in addition high voltage grids doesn't much affect by dynamic changes of network connections. Figure 3.2 represents a 500 KV small power system that is simulated using ATP software.

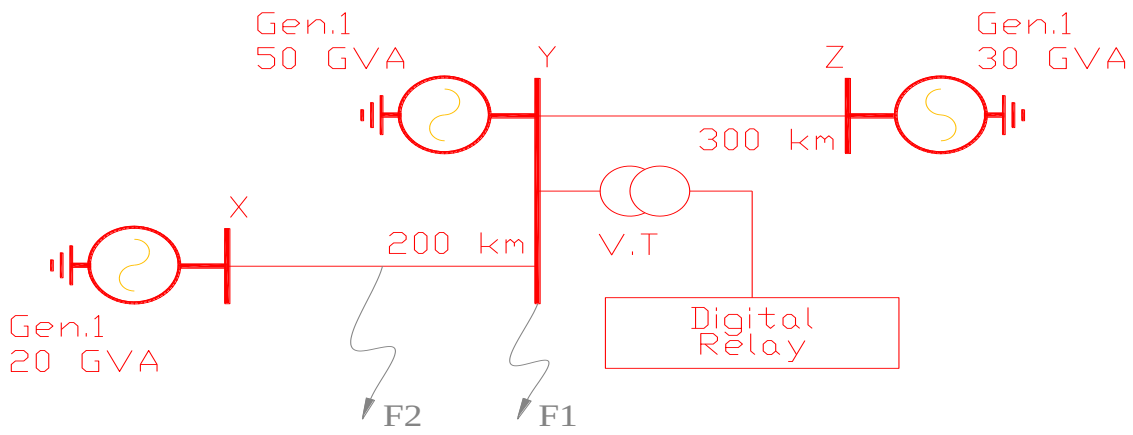

Figure 3.2, 500 KV sample network.

The Cos-Sin technique is applied to the digital relay that is connected to busbar Y via voltage transformer to measure the actual voltage Va(t), the generated voltage Vg(t) is fabricated per each detected sample and consequently the discrimination signal will be obtained.

During normal condition the discrimination signal will almost stick to unity, it will never change unless actual wave starts to distort.

Figure 3.3(a) represents the 3Ø actual voltage detected together with their generated signal computed on bus X whereas, figure 3.3(b) shows the discrimination signal during normal conditions of the same bus.

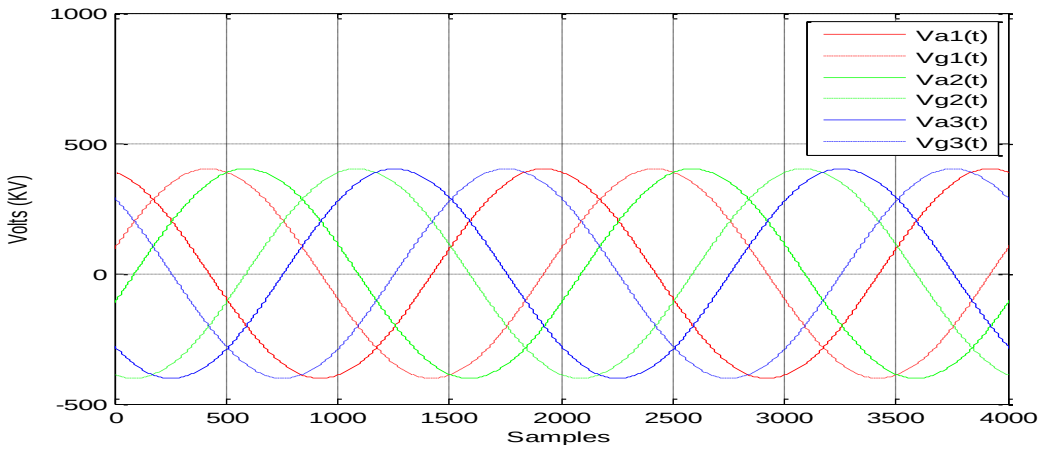

Figure 3.3(a), Va(t) and Vg(t) during normal conditions.

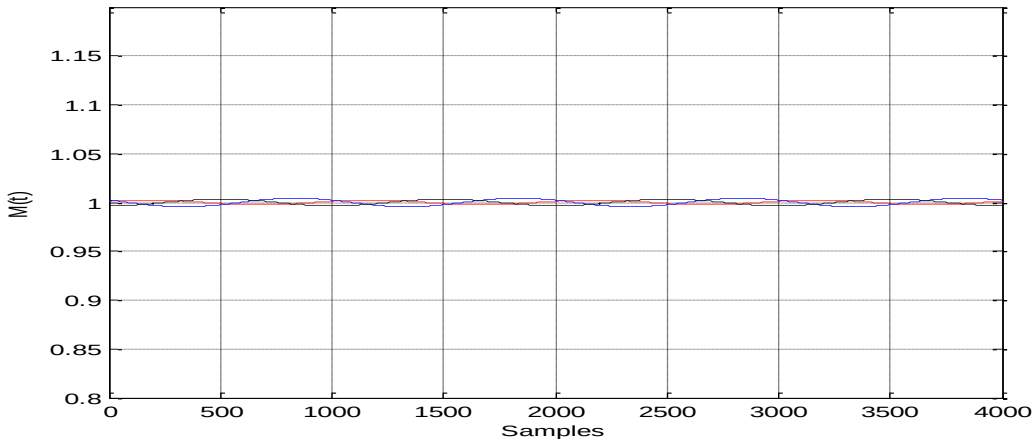

Figure 3.3(b), M(t) during normal conditions.

During abnormal conditions, the actual voltage form will be distorted by occurrence of fault while the generated signal will be kept as it is, therefore the discrimination signals will vary from unity.

Figure 3.4(a) shows actual and generated voltage Va and Vg detected and computed during L-G fault located on the Bus Bar X itself and the corresponding discrimination M (t) signal is shown in figure 3.4(b).

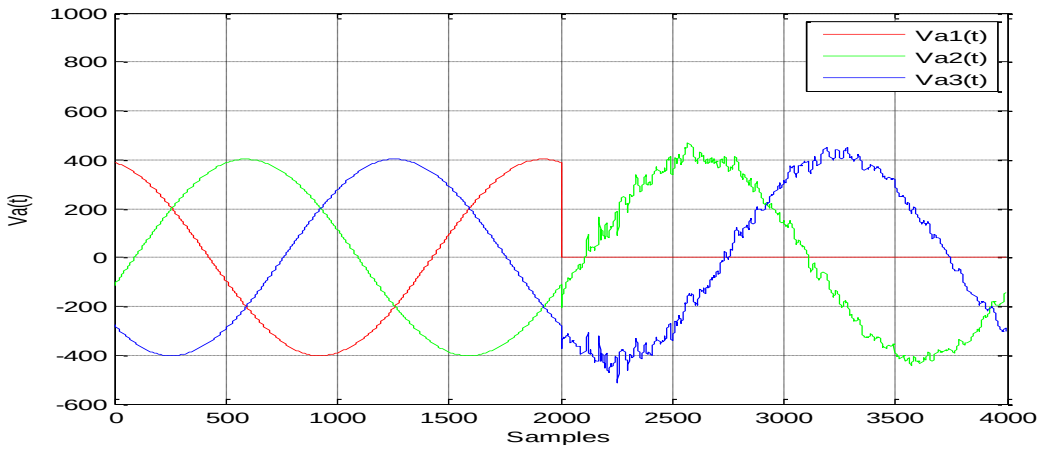

Figure 3.4(a) Va(t)and Vg(t) for a LG-A fault on busbar X

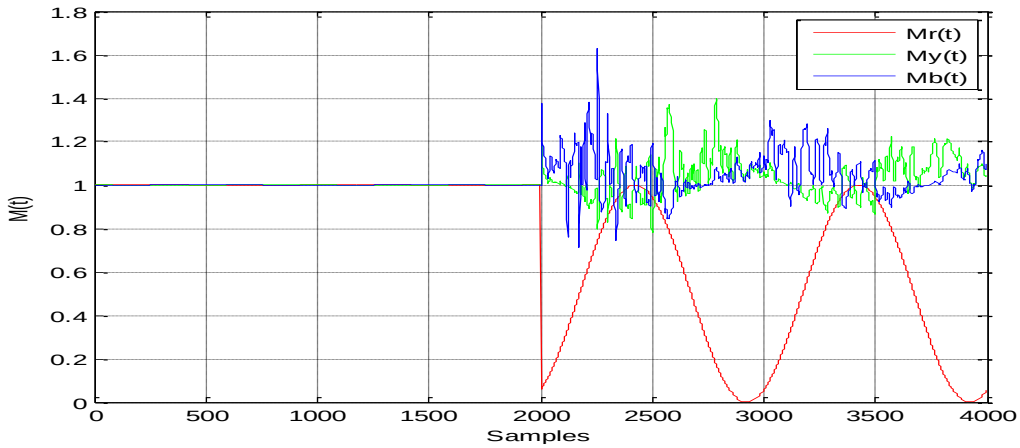

Figure 3.4(b), M(t) for a LG-A fault on busbar X.

Figure 3.5(a) display all phase's voltages when the fault was relocated to the middle of transmission line XY and the corresponding discrimination signal is shown in figure 3.5(b).

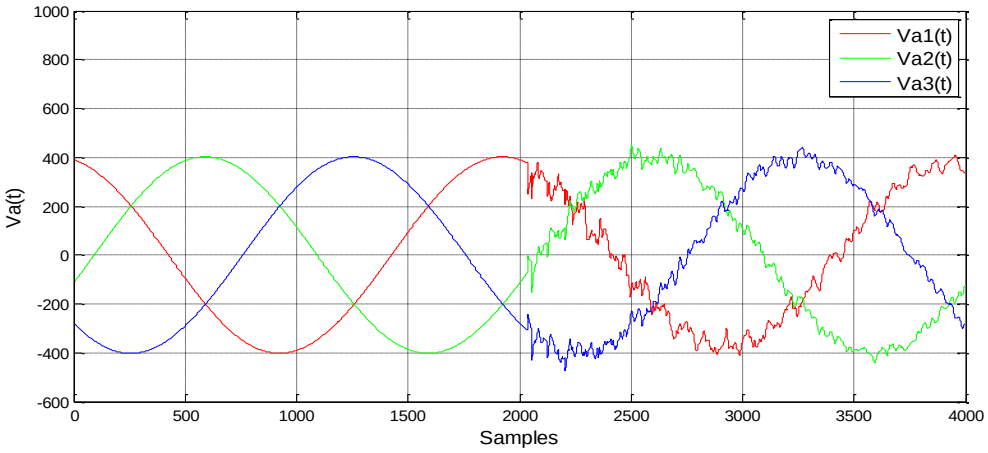

Figure 3.5(a), Va(t) and Vg(t) for a LG-A fault,100 km away from busbar X.

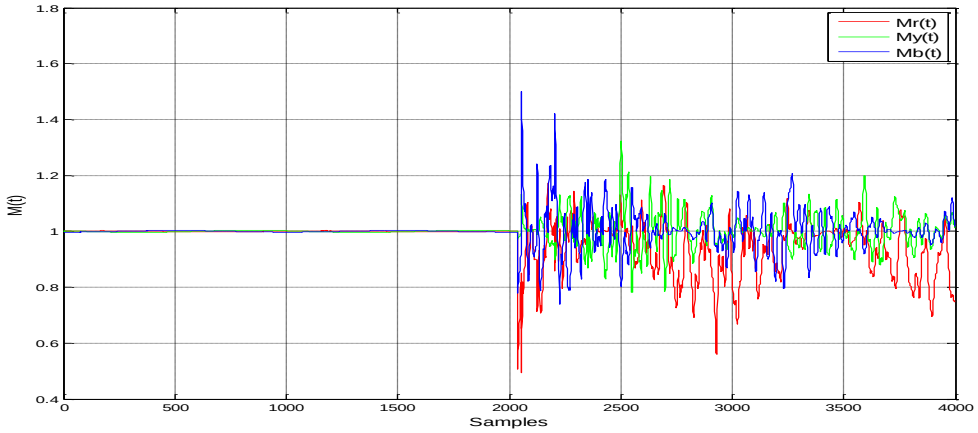

Figure 3.5(b),M(t) for a LG-A fault, 100 km away from busbar X.

3-5 Average deviation

It was noticed from previous section that by using the Cos-Sin technique separately, only the moment that signal started to disturb will be obtained. However, to acquire extra information needed about that fault the average deviation of the discrimination signal M(t) for all three phases will be calculated along a certain period.

This period should be properly considered to avoid any wrong decision that might be taken as a result of transient confusion between fault case and any other cases that might established some transient waves in the network such as switching and heavy load starting which doesn't need the same reactions.

The deviation δ from unity for recorded discrimination signal (M) in certain period can be expressed as:

$$\text{(3-4)}\quad \delta\,\mathrm{M} = \left|1-\frac{1}{n}\sum_{i=1}^{n} M(i)\right|$$

n: is the number of samples obtained in the required period depending on the sampling frequency.

Table 3-1 shows the unity deviation happened in discrimination signal due to single line to ground fault that located on busbar where the relay is connected, also it contains deviations when the same fault located on different place away of busbar. The deviations were computed on a period of one complete cycle as it is long enough time for the relay to have reliable decision regarding the system condition.

Distance from busbar in km	Solid SLG-A			SLG-A via R=100 ohms		
	δ-A	δ-B	δ-C	δ-A	δ-B	δ-C
0	*0.50*	0.039	0.047	*0.094*	0.003	0.001
25	*0.19*	0.008	0.008	*0.012*	0.002	0.000
50	*0.11*	0.004	0.005	*0.011*	0.001	0.000
100	*0.07*	0.002	0.002	*0.009*	0.000	0.000

Table 3.1, Average deviation due to LG faults at phase A on the busbar X & Line XY.

The table shows clearly that the deviation in discrimination signal δM of the faulted phase has much greater value than the un-faulted phases; in addition it is obvious that when the fault location transferred away from the relay, the value of the discrimination deviation decreases.

The above analysis proved that discrimination signal $M(t)$ besides the deviation value δM calculated are holding much information regarding the power system in both healthy and fault cases.

3-6 Conclusions

The suggested tool proved to be sufficient in differentiating between the normal condition and fault conditions however, some problems that could be considered as deficiencies were raised and it should be solved or eliminated. The most important problem is how to discriminate between faults located on busbar itself to that occurs on one of lines connected to that bar as it is known that the effect of both faults are almost similar specially when the line break happened close to the bar. Also fault type should be recognized for proper protection.

Other problems are the effect of fault resistance, fault inception angles and the influences of various short circuit capacities for the generation stations feeding the network under investigation.

In the next chapter our tool will be applied to a certain large network chosen from reality, analysis will be performed besides some amendment and remedies. Moreover supplementary criterion to solve the above mention problems will be provided and demonstration of the final flow chart of a comprehensive digital relay that is capable to protect such grid will be presented.

Chapter 4 Proposed Cos-Sin Digital Relay

4.1 Introduction

In this chapter a multifunction relay for extra high voltage networks is presented. The relay is designed based on new Cos-Sin tool explained previously besides some extra techniques that makes it capable of performing monitoring and protecting jobs in EHV networks perfectly. 500 KV Egyptian network is simulated using computer software where it is done with all actual parameters and the suggested relay is applied on it to test and prove to how extend the relay succeeded in covering protection requirements.

4.2 Simulation

Only a specific part of Cairo zone in the Egyptian unified 500 KV network [27] was simulated using alternating transient software (ATP) [28] as a closed system to apply the analysis on it.

4-3 Network selection

The selection of that part of the grid was done based on several parameters; the most important one is the validity of applying the suggested protection tools completely with all its scenarios on it. Another reason is that the chosen part is relatively wide and it contains many generation points with different short circuit capacities besides different lengths of transmission lines connecting them together, such combination validates having various study

results under all conditions. Also the data availability on the entire grid helps greatly in the simulation step.

4.4 Line's Configuration and Parameters

The parameters of the transmission line may be generally divided into two groups. Power frequency parameters, which are required in order to study load flow, system stability and fault levels. Higher frequency parameters, which are needed for studying the effect of striking voltage, switching and faults during the earliest time. The line parameters needed can be acquired as shown in [App.A]. Table 4-3 shows nodes of the grid in order and relevant capacity of each station.

Ser.	**Bar Tag**	**Cap.**	**Bar Location**
1	Cairo	50 GVA	Cairo
2	C.W.	20 GVA	Cairo west
3	Bas	24.4 GVA	Basous
4	ABAZ	13.26 GVA	Abo Zabal
5	Tip	1.2 GVA	Tippen
6	Kari mat	2 GVA	Korimat
7	Samalut	20 GVA	Samalut

Table 4.1, Nodes of the selected grid.

4.5 Network structure

Figure 4.1 shows the network structure, lengths of lines linking between each bus and the others, capacity of each station of the network, knowing that all indicated parameters are real of the Egyptian network.

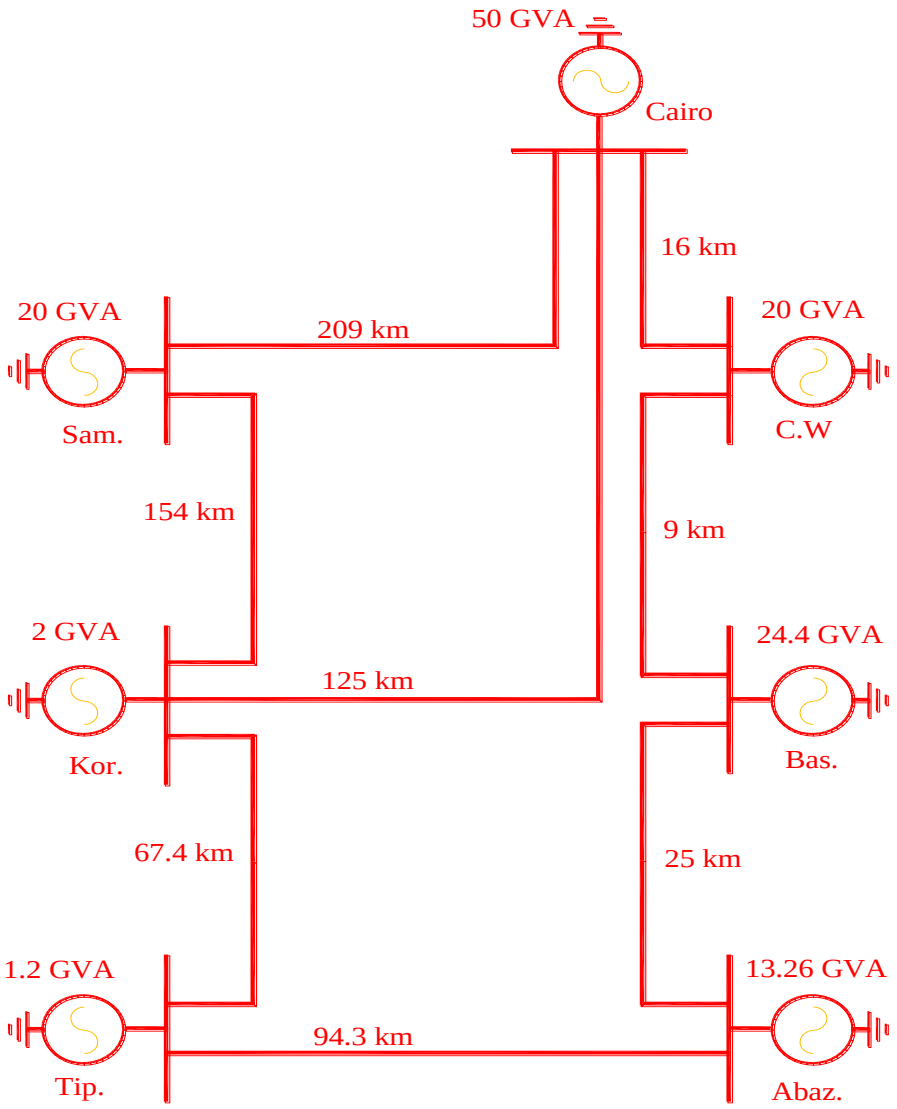

Figure 4.1, Network under investigation.

4.6 Relay connection

Suggested digital relay is placed on Cairo busbar in which it will be able to protect the busbar itself besides monitor all transmission lines connected to this bus.

Figure 4.2 shows the digital relay connected to Cairo busbar. The bus voltage wave is feed to the relay via voltage transformers, in addition current

flows in all transmission lines between Cairo busbar to Cairo West, Korimat and Samalut respectively delivered to the relay via 3 current transformers.

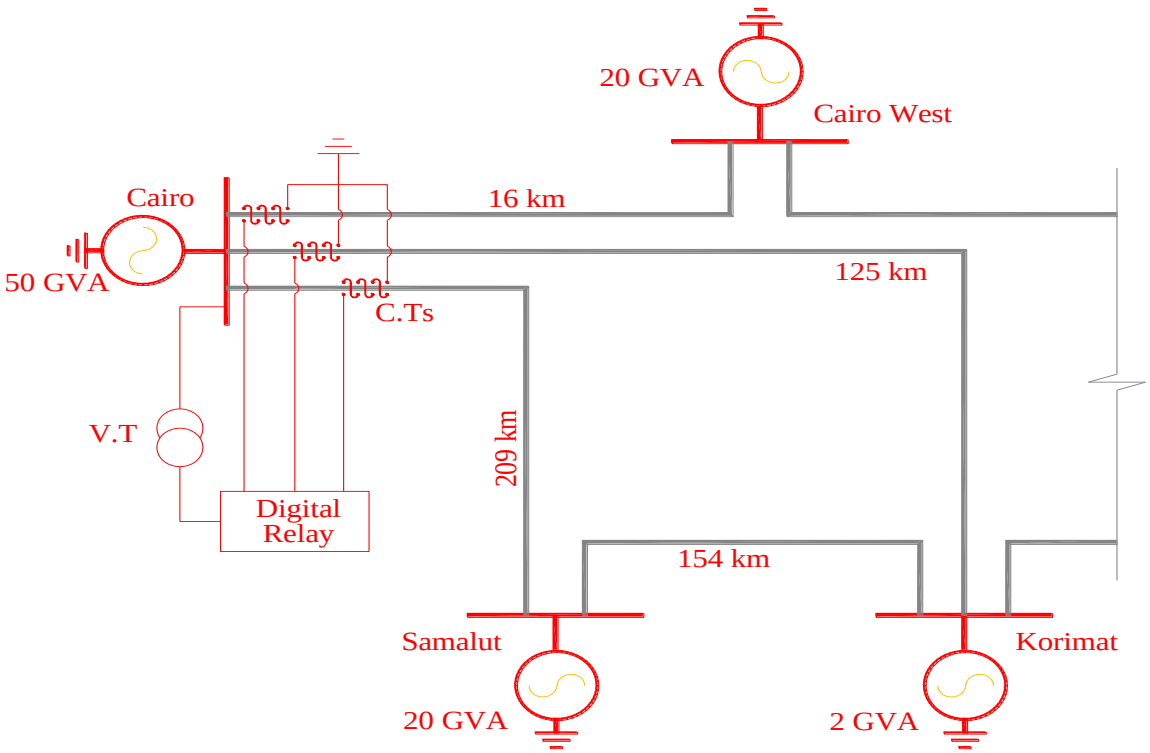

Figure 4.2, The relay connection.

4.7 Simulation parameters

In this section the parameters that should be considered in the simulation will be highlighted.

4.7.1 Sampling frequency

Sampling frequency should be determined to grantee the ability of detecting any small change that might happened to voltage and current wave forms due to faults.

In this section frequency of 100 KHZ is chosen (2000 samples per power frequency cycle 50 HZ) which is high enough to capture the wave deviation moment happened due to forward and backward travelling waves associated to the faults. Obtaining such instant will help to identify whether the fault is on the bar itself or not as we will explain later in this chapter.

4.7.2 Relay operation time

The minimum no. of cycles that should be issued during simulation is two cycles of power frequency signal. Relay technique acquires its initial parameters from the samples of the first cycle obtained, during this cycle the relay is in hold mode. Those initial parameters are wave frequency, peak value and signal phase shift, detection of all of them are necessary to proceed with the protection tool sequence.

The technique criteria also depend on running its analysis on one complete cycle just after receiving initial fault alerts.

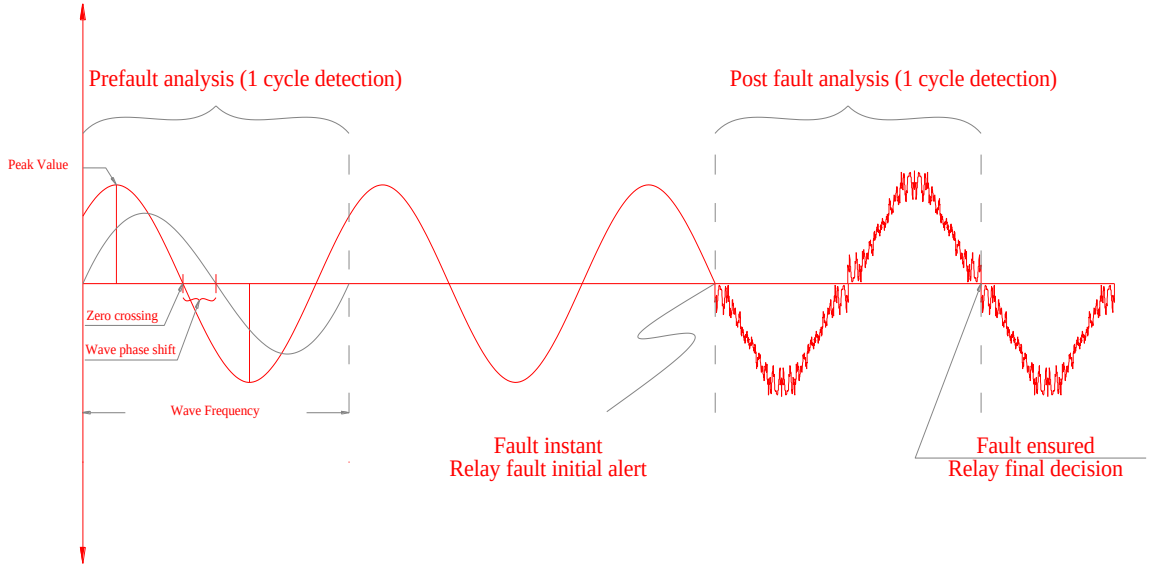

Figure 4-3, Pre-fault and post fault cycles under operation.

It is valid to feed the relay with some of initial conditions instead of obtaining it automatically. That can be done by either inserting certain values via user or recording average values during healthy case. However this might decrease the operation time needed by nearly half cycle but still it will not validate the relay to operation from the first cycle.

Normal operation

Figure 4.4(a) shows the three phase voltage signal feeding the relay. It was obtained from the Cairo Bus Bar of the simulated network, in this figure the network was still healthy and in normal operation. As discussed in the previous chapter this signal is called the actual signal Va (t).

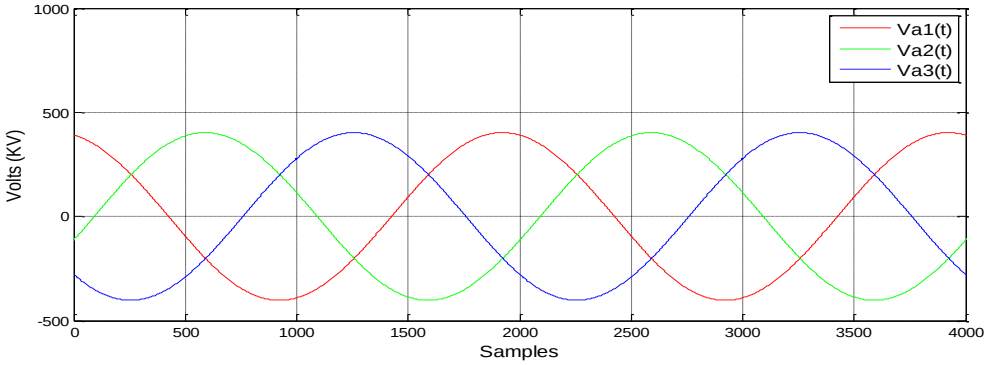

Figure 4.4(a), 3-Phase input Voltage signal V(t)of the local busbar during normal operating conditions.

Figure 4.4(b) shows the same signal after the network exposed to single phase L-G fault on phase A located in the Bas Bar itself.

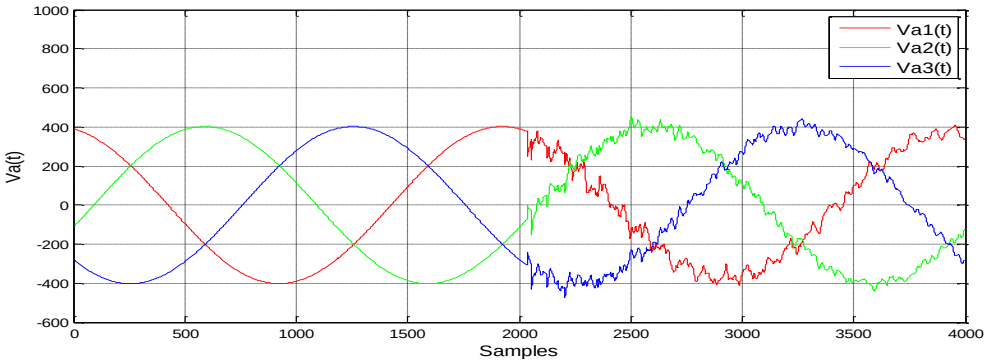

Figure 4.4(b), 3-Phase input Voltage signal V(t)of the local busbar during LG-A fault condition

4.8 Relay criterion:

As the actual of the busbar Va(t) for all 3 phases delivered sample by sample to the digital relay via voltage transformer, the corresponding generated signal Vg(t) is obtained after extracting the necessary pre-fault information required ,accordingly discrimination signal M(t) is digitally calculated using equation (3-3).

The suggested relay has three main operating criterions that applied on the discrimination signals M(t), fault detection criteria, fault analysis criteria and fault discrimination criteria. The combination of three of them by the relay with certain sequence of operation provides complete protection.

4.8.1 Fault detection criteria:

Basic idea of this criterion is to monitor any changes happened to system signal, analyze it to detect if it caused by fault incident or due to any other reason.

During system operation the criteria shall run the following procedures.

1) Read each voltage sample delivered from designated busbar of the observed grid (actual voltage detection Va(t)).
2) Record the first detected voltage cycle and extract voltage peak, signal phase shift and frequency of the wave.
3) Use the obtained information to generate a corresponding complementary value to each sample detected Vg(t) according to equation (3-2).
4) Calculate discrimination signal values for each sample M(t) using the equation (3-3).
5) Retrieve a threshold value that was inserted to the relay by user and compute the threshold limits.
6) Examine if the calculated discrimination value of the current detected sample is within the threshold limits or out of it which leads us to two scenarios.

a) First scenario:

If the discrimination calculated sample is almost stuck to unity and with in threshold limits, that give an indication of healthy system, consequently digital relay DPS should start over from step no.1 with the next sample.

b) Second scenario:

As we mentioned in the last chapter any distortion in the actual voltage signals Va(t) will reflect on the discrimination signal M(t) therefore If the discrimination calculated sample deviated from unity and out of threshold limits, this give an alert of possibility of fault occurrence and criteria procedures shall continue till the end.

7) Provide an initial fault notification and ignite the second stage of the relay analysis to confirm or ignore such alert and to recognize fault type and location.

4.8.1.1 Determination of threshold value (ζ):

At first it should be mentioned that discrimination signal values is not an exact unity. Sampling process of system signals causes errors during developing the generated complementary signal, that error is reflected on each calculate value of the discrimination signal M(t) resulting in small deviation from unity value that should be obtained in normal operation.

This small deviation is inversely proportional with the sampling frequency used in simulation but regardless the sample frequency is high, error is still maintained as a fact.

Figure 4.5 shows unity discrimination signal M(t) that has slight deviation in ripples form.

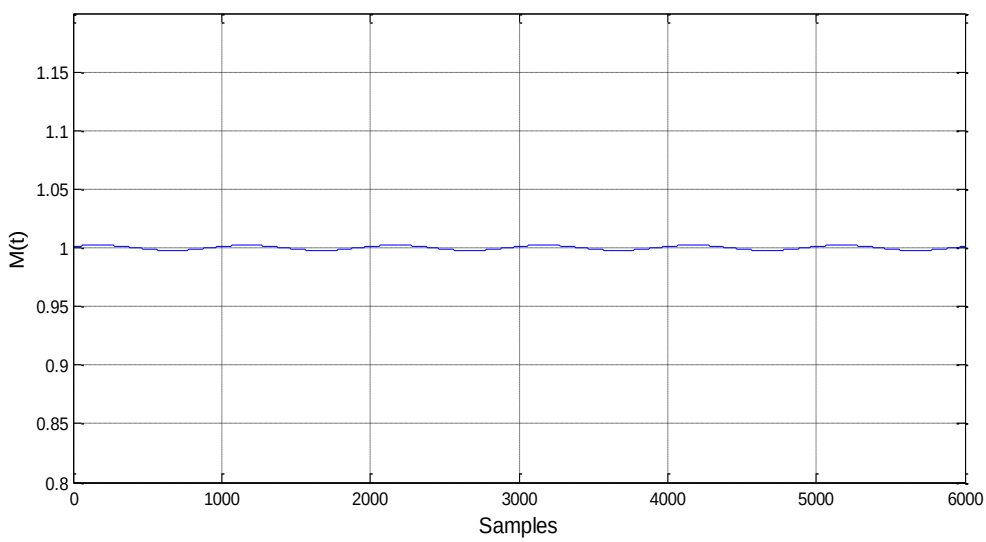

Figure 4.5, Ripples in unity discrimination.

Figure 4.6 shows how sampling can miss the exact detection of pre-fault parameters needed to be capture.

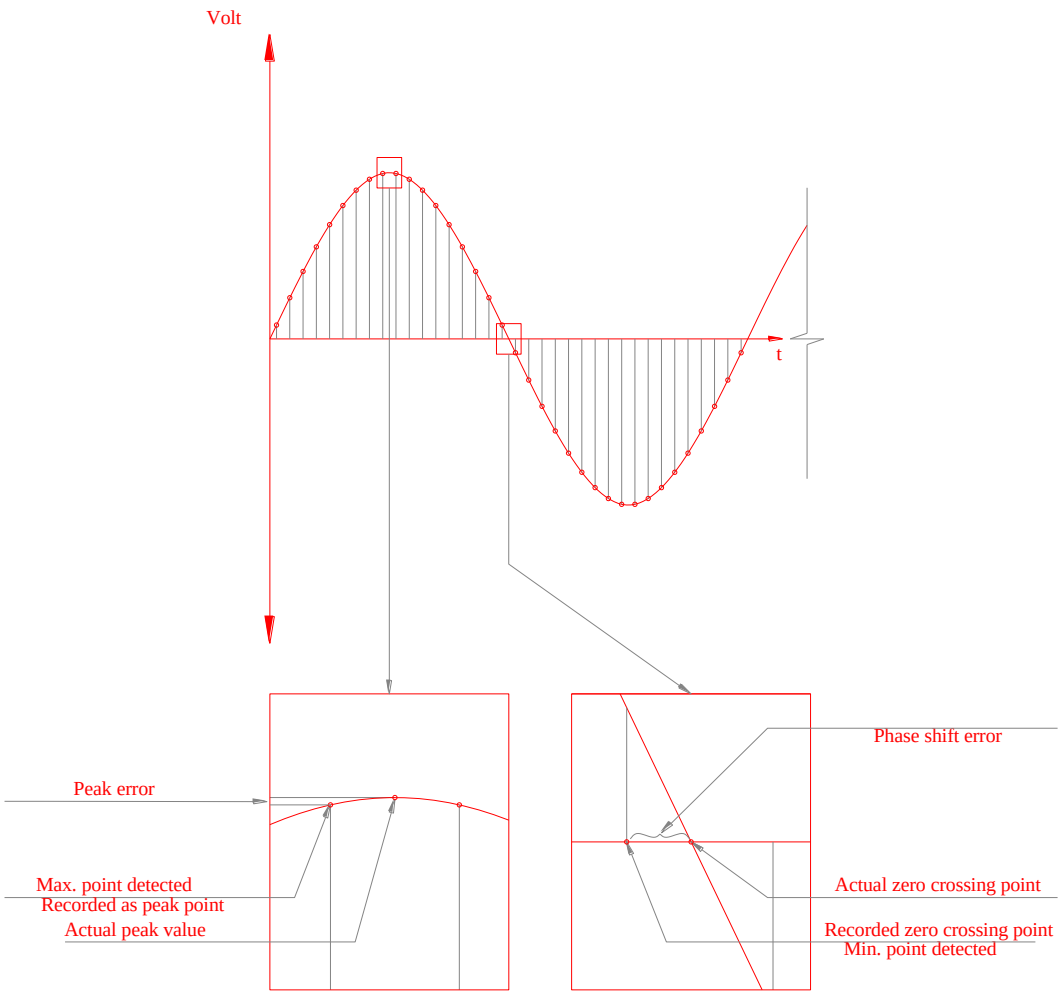

Figure 4.6, Errors in point detection.

The chosen sampling frequency of simulation is 100 KHZ, it can create an error up to 0.018 of the discrimination signal.

The threshold value ζ is a certain constant value determined by the relay user and not affected by any parameters acquired from network signal. Threshold value is used to set limitations of unity tolerance in which any discrimination value falls within these limits can be considered as unity.

The maximum allowable regulation in EHV network is 5%, this value can be considered simply as the constant threshold value ζ and consequently the upper and lower threshold limits are 1.05 and 0.95 respectively.

Figure 4.7(a) shows 3 phase discrimination signal M(t) in normal operation together with threshold limits

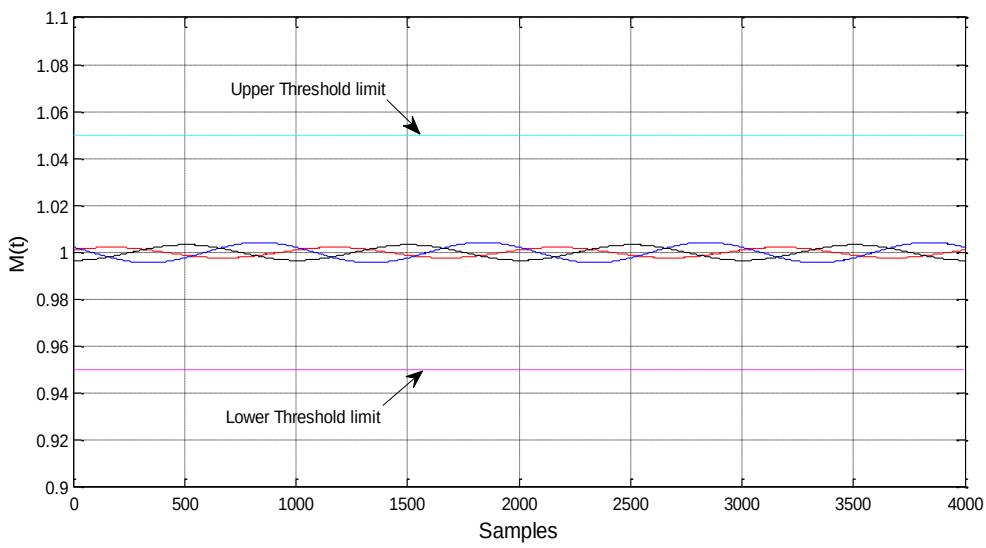

Figure 4.7(a), discrimination unity relation in normal case and the threshold limits.

Figure 4.7(b) shows 3 phase discrimination signal M(t) in single phase L-G fault case together with threshold limits.

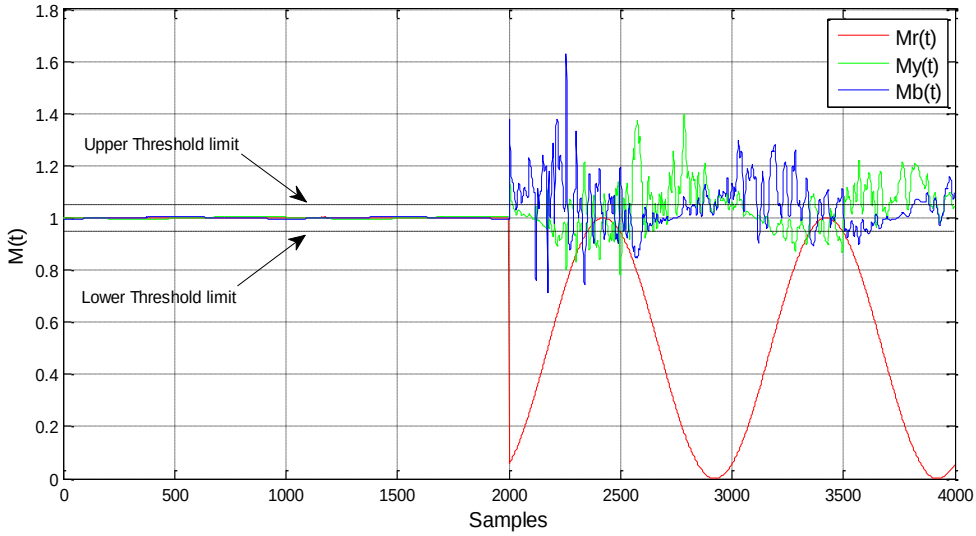

Figure 4.7(b), discrimination unity relation in fault case and the threshold limits.

4.7.2 Fault analysis criteria

The Fault analysis criterion is designed to help obtaining type of fault happened besides an initial speculation of the defected network element in case of fault occurrence.

Currents flow in all lines connected to protected busbar are detected via current transformers, those currents can be named as actual current Ia(t).Signal delivered to the relay where Cos-Sin technique is applied on them providing a current discrimination signal Mi(t) for each phase of all line currents. Equation (4-1) and (4-2) shows how generated current and current discrimination can be calculated from the actual current fed to relay.

$$I_g(t) = I_{max}\sin(wt + Ø) \qquad (4\text{-}1)$$

$$Mi(t) = \frac{I_{max}^2 \sin^2(wt+\varphi) + I_{max}^2 \cos^2(wt+\varphi)}{I_{max}^2} \qquad (4\text{-}2)$$

Where Imax: is the normal operation peak current

During the system operation the criterion shall run the certain following steps knowing that steps 1 to 4 should be done in synchronization with its symmetrical in fault detection criterion:

1) Read each current sample delivered from transmission lines current transformers of the observed grid (actual current detection Ia(t)).
2) Record the first detected current cycle and extract peak value, signal phase shift of the wave.
3) Use the obtained information to generate a corresponding complementary value to each sample detected Ig(t) according to equation (4-1).
4) Calculate discrimination signal values for each sample Mi(t) using the equation (4-2).

The calculated discrimination signals of each phase is almost unity during normal operation of the system, once any type of fault any where in the elements connected to the protected bar occurs the actual current signal will be distorted, relevant generated signal will not follow it resulting in severe change of unity relation.

5) Retrieve the corresponding voltage alert mentioned in fault detection criterion to check whether it is activated or not and that leads us to two scenario.
   a) First scenario:

      If the fault detection criterion gives zero alerts, that consider an indication of normal operation, consequently criterion procedure will start over from step 1 similar to corresponding step in fault detection scenarios.

b) Second scenario:

If the fault detection criterion gives activated alert, that consider an indication of fault occurrence, consequently criterion procedures will carry on to the next step.

6) Calculate the mean value for unity deviation of each phase in all transmission lines δ (i) to detect the faulted component in the network using equation (4-3).

$$\delta \text{ Mi(t)} = \left(\frac{1}{n}\sum_{i=1}^{n} M_I(i) - 1.0\right) \qquad (4\text{-}3)$$

7) Run a comparison between mean values of each phase calculate in the previous step to obtain fault type and defected element.

Figure 4.8 shows the exact connections of all 9 lines phases and the 3 busbar voltages to the relay.

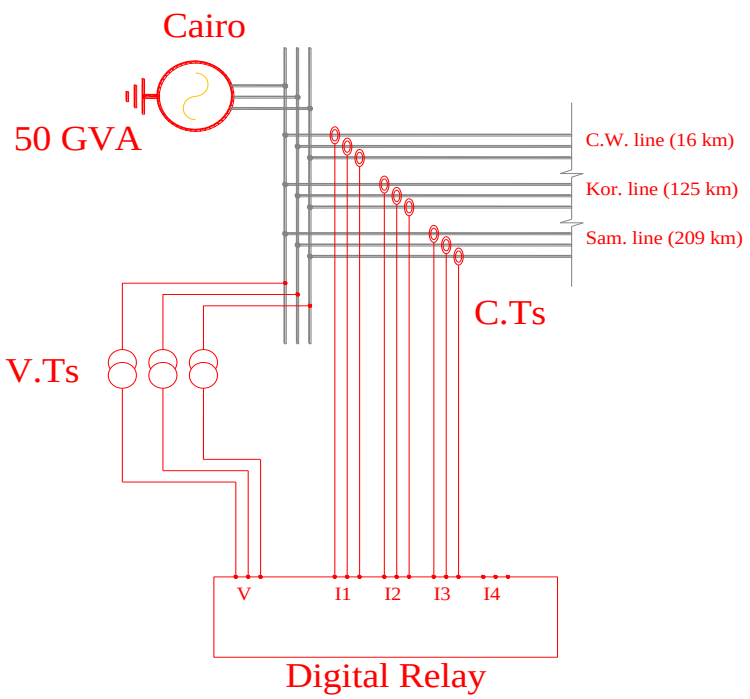

Figure 4.8, all lines connection to the relay.

The fault analysis criterion is sufficient to identify fault type and defected element in the majority of fault cases however in few special cases such as very close faults and faults that happen through high resistance, the criteria might not be totally effective and relay may take a wrong decision which is not acceptable therefore a third criterion is developed to confirm fault information needed.

The new criterion utilizes both voltage and current signals to get fault location in order to avoid mal-function of the relay.

4.8.3 Fault discrimination criteria

This criterion uses fault transient signals superimposed on voltage and current. Voltage sudden change due to fault or switching cases generates a travelling wave that transfers over transmission lines and reflects on each node. Such phenomenon is very useful in identifying the fault location.

In the next section an overview on the travelling wave will be introduced.

4.8.3.1 Travelling waves

When a fault occurs, the abrupt change in voltage at the point of the fault generates a high frequency electromagnetic impulse which propagates along the line in both directions away from the fault point at speeds close to that of light [30-36]. The forward direction wave (Wf (t)) and the backward one (Wb (t)) of this generated travelling waves prove is derived from Telegraph equations of the transmission lines that is going to be explained clearly in [App.B]. They can be given as follows:

$$\mathrm{Wf}\left(\mathrm{t}\right) = V_{0\alpha\beta} + I_{0\alpha\beta} Z_o \qquad (4\text{-}4)$$

$$\mathrm{Wb}\left(\mathrm{t}\right) = V_{0\alpha\beta} - I_{0\alpha\beta} Z_o \qquad (4\text{-}5)$$

Where Z is characteristic impedance of the line and it is given as:

$$\mathrm{Z_o} = \begin{vmatrix} 500.0 & 0.0 & 0.0 \\ 0.0 & 280.0 & 0.0 \\ 0.0 & 0.0 & 280.0 \end{vmatrix} \Omega$$

Vα and Iα are the modal voltages and currents (0, α or β components) at the relay location and can be given by the following equations:

$$\mathrm{T_F}(\mathrm{t}) = \mathrm{V(t)} \times \mathrm{K} - \mathrm{I(t)} \times \mathrm{K} \times \mathrm{Z}o \qquad (4\text{-}6)$$

$$\begin{bmatrix} \mathrm{I}_o \\ \mathrm{I}\alpha \\ \mathrm{I}_\beta \end{bmatrix} = \mathrm{I(t)} \times \left[K\right] \qquad (4\text{-}7)$$

The following lattice figures demonstrate the behavior of forward and backward travelling waves (Wf & Wb) when a fault is applied on two transmission lines system. Several locations have been tested where Tf & Tb is

the time that the forward and backward waves were detected by the digital relay.

It is clear that travelling waves emitted by a line fault are different than those initiated by busbar faults. The faulted line forward and backward waves were detected on almost the same moment ($Tf \cong Tb$) as the wave will be captured just before and just after the collision to the joining busbar while the residual waves propagate in other line connected to same node seems to have different detection times ($Tf \neq Tb$) as the forward wave will be captured in the start of the line, travels along the un-faulted line, reflects on the next bar and then travels back on the same line to be re-captured as backward wave as shown in figures 4.9(a) and 4.9(b). This journey will take a certain travelling time (T) that can be calculated using the following equation:

$$T = Tf - Tb \qquad (4\text{-}8)$$

On the other hand, waves initiated by fault located in the bar itself propagates along all un-faulted lines that is connected to it. They will have different detection times ($Tf \neq Tb$) as the forward waves will be captured in the start of each line Then it will be recaptured again after the reflection occurs on the remote bars. traveling along that line and reflection then travels back again consumes certain time as shown in figure 4.9(c).

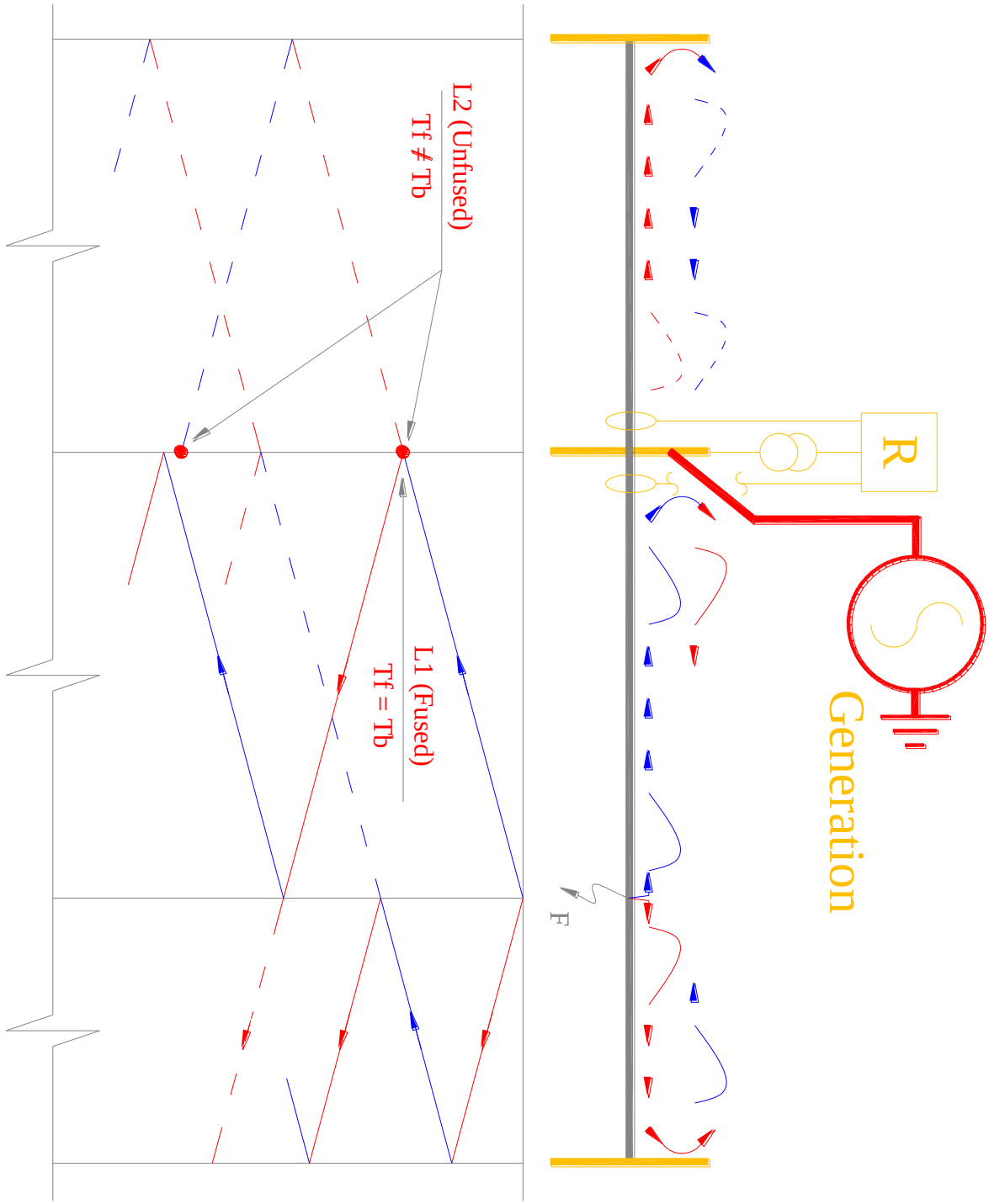

Figure 4.9 (a), travelling waves lattice diagram during line 1 fault.

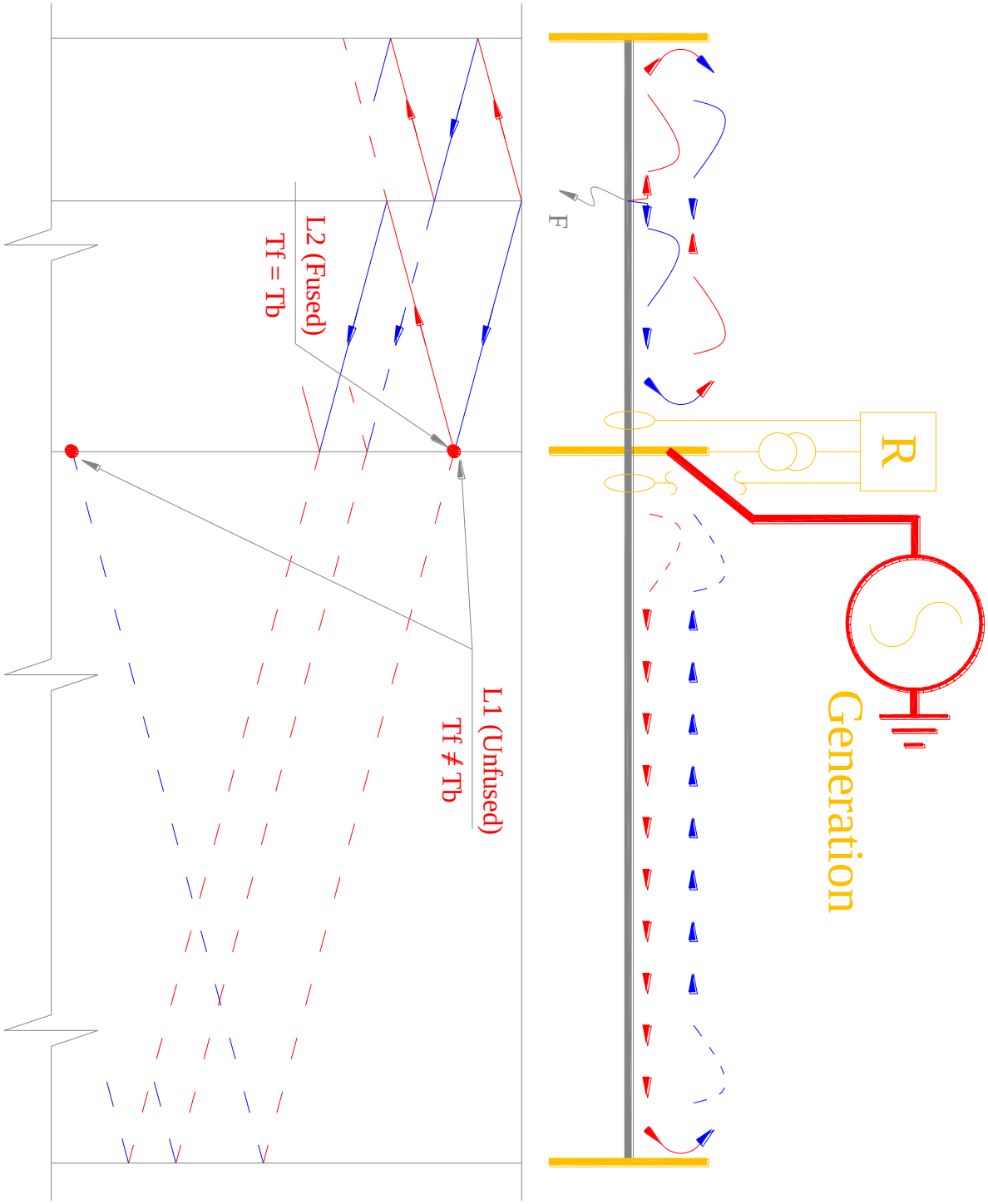

Figure 4.9(b), travelling waves lattice diagram during line 2 fault.

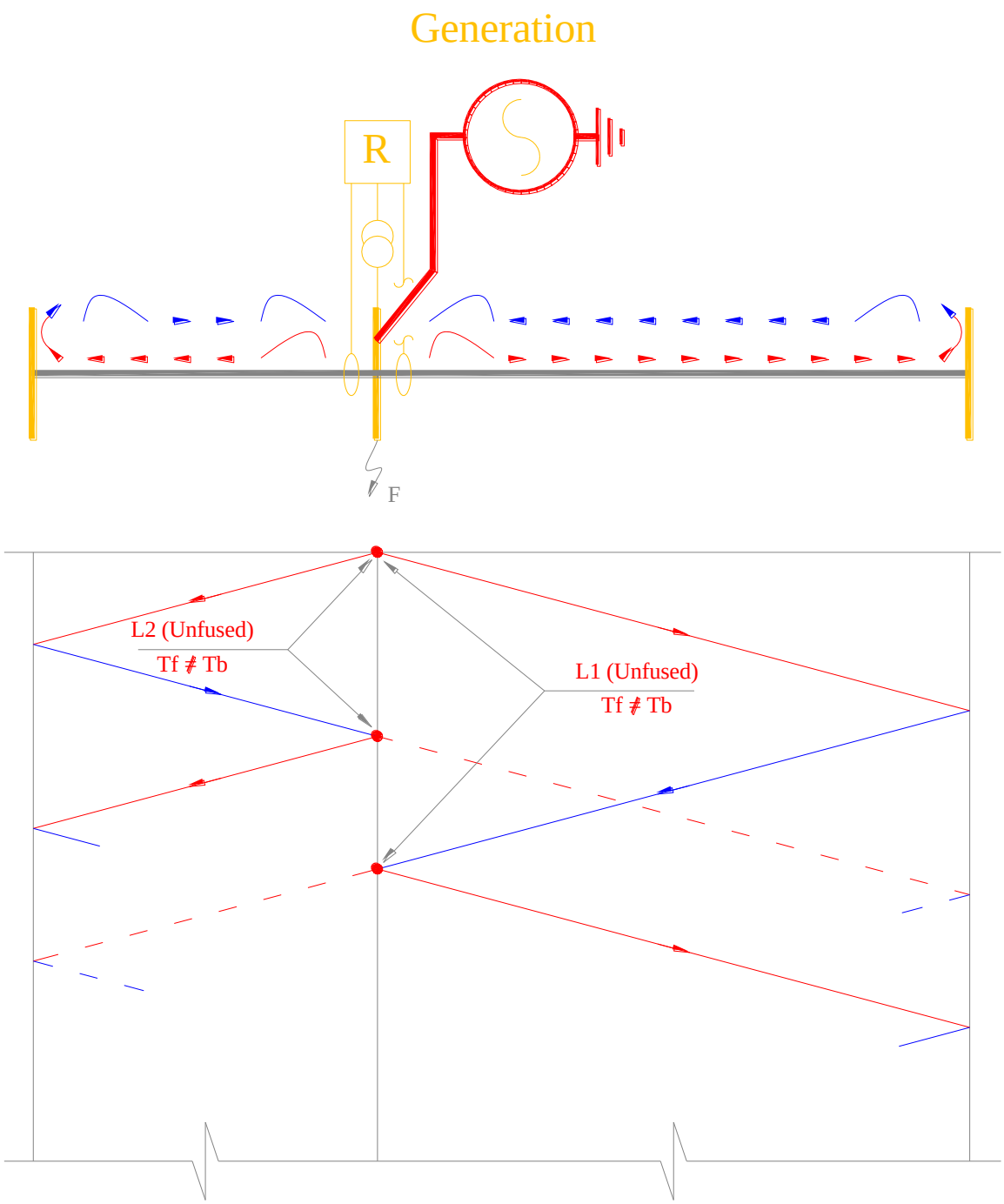

Figure 4.9(c), travelling waves lattice diagram during busbar fault.

During the system operation the criterion shall run the certain following steps taking into consideration that first step should be started after receiving an

alert from fault detection criterion and in synchronization with the start of 6th step in fault analysis criterion:

1) Read each voltage and current sample delivered from transmission lines voltage and current transformers of the observed grid (actual voltage-current detection Va(t)-Ia(t)) .
2) Calculate forward and backward travelling waves (Wf(t) & Wb(t)) for each sample delivered starting from receiving fault detection criterion alert by using equation 4-4 & 4-5.
3) Apply Cos-Sin method on each calculated sample obtained from the previous step completed with all the technique procedures mentioned in chapter 3. This is for having both forward and backward discriminated travelling wave signals (Mwf- Mwb) for all lines attached to the investigated bar and that can be done using the following equations:

$$\text{Mwf}(t) = \frac{W_{f\max}^2 \sin^2(wt+\varphi_1) + W_{f\max}^2 \cos^2(wt+\varphi_1)}{W_{f\max}^2} \tag{4-9}$$

$$\text{Mwb}(t) = \frac{W_{b\max}^2 \sin^2(wt+\varphi_1) + W_{b\max}^2 \cos^2(wt+\varphi_1)}{W_{b\max}^2} \tag{4-10}$$

The value of discriminated travelling wave signals (Mwf & Mwb) obtained will conduct the relay sequence to different scenarios:

a) First scenario:

If (Mwf- Mwb) are maintained unity, that consider an indication of normal operation and that the initial alerts recorded is just false alarm ,consequently criterion with the other ones procedure will skip and start over from step 1.

b) Second scenario:

If (Mwf & Mwb) are deviated from unity, that gives a confirmation of fault occurrence, consequently criterion procedures will carry on to the next step to identify fault location.

4) Capture the moments that both travelling wave discrimination signals Mwf & Mwb deviate from unity Tf and Tb for all lines attached to the joining bar. the calculation should be performed on the Arial mode current and the comparison of the resultant Tf & Tb will determine the location of the fault as the following:

- If Tf = Tb of a certain line while Tf ≠ Tb for the remaining attached lines on the same monitored bar then only that line is faulty and remaining line plus the bar is not.
- If Tf ≠ Tb for the all lines on the investigated bar then fault happened on the bar itself.

5) Determine the value of Mwf and Mwb where they have a non zero value for ground faults only.

4-9 Flow Chart of the Multifunction Digital Relay

The combination of the above three operating criteria would simply construct the relay flowchart. The Fault Detection Criterion acts as an initial fault detector and also energizes the other two criteria to start analyzing the fault case. The Fault Analysis Criterion determines to a great extent the faulted line and fault type; however, it may be deceived by line closed faults where the value of $\delta Mi(t)$ of the faulted line may resemble those of the bar fault ones. The Fault discrimination criteria gives a final decision for the cases that deceive the second criterion and detects busbar faults, where it has the ability of discriminating between busbar faults and line close-up faults. The relay final decision is taken after analyzing the results provided by the three operating criteria. Figure 4.10 shows the flowchart of the proposed relay.

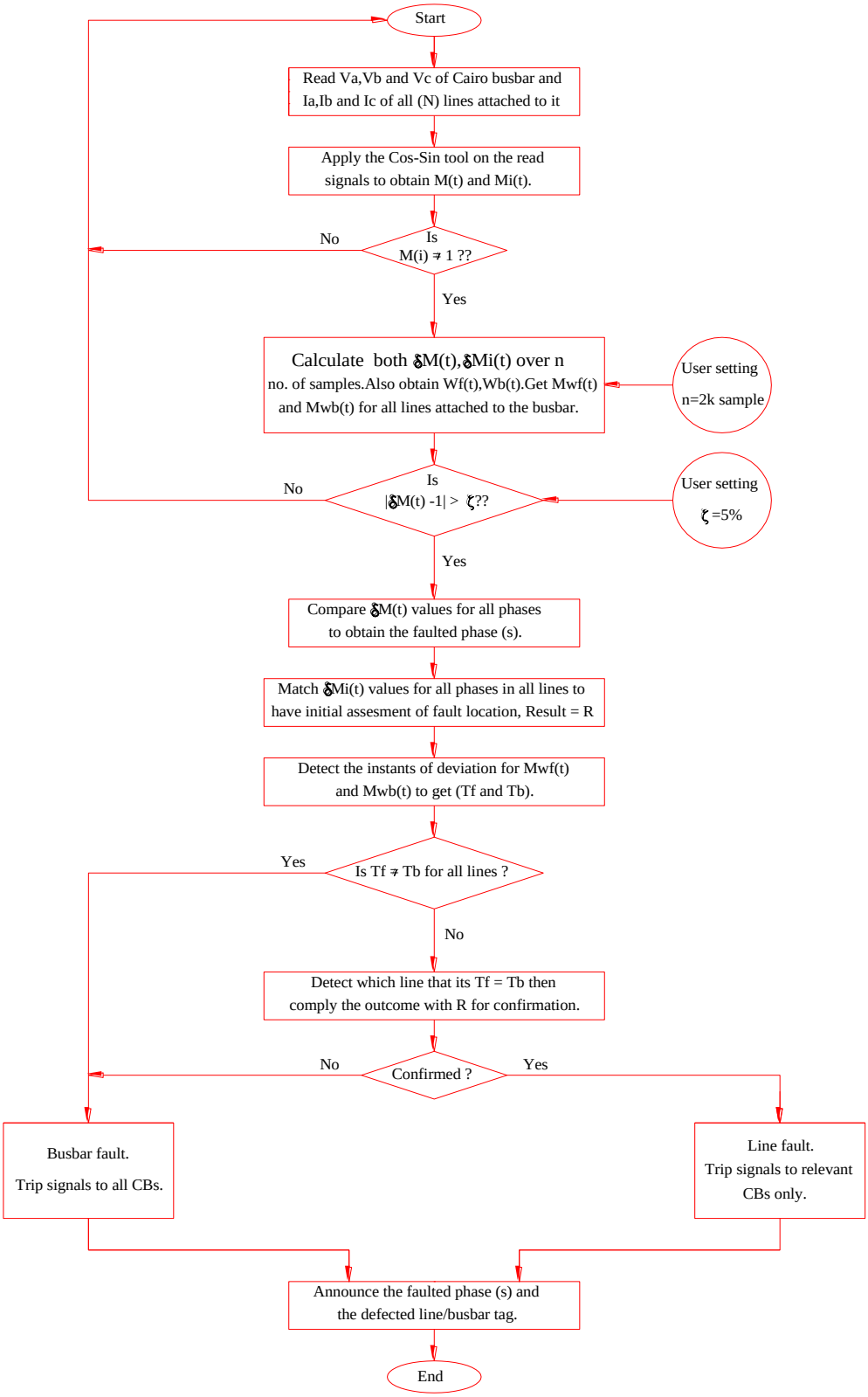

Figure 4.10, relay flow chart.

Chapter 5 Simulated System Studies

5-1 Introduction

In the previous chapter the suggested technique for detecting fault cases besides tools of identifying its type and location on a high voltage network are introduced in details. In this chapter EHV network mentioned earlier is simulated by ATP, then it was subjected to various fault cases, each with different parameters. The relay techniques were programmed using the Matlab [App.C] [37] where they were feed by the ATP simulation outcome data. The output graphs and results are monitored, analyzed and discussed.

5-2 Examined grid

The examined grid modeled on the ATP software [App.D] consists of 7 generating stations with different short circuit capacities as indicated in the last chapter table 4.1, each attached to a busbar and 8 linking transmission lines of different lengths.

The network voltage and frequency are 500 KV and 50 HZ respectively. Cairo busbar besides Cairo-Cairo west line (16 KM) , Cairo-Korimat line (125 KM) and Cairo-Samalut line (209 KM) are specially considered to apply faults on them during these studies [27].

5-3 Simulated fault cases

Plenty of cases were simulated by applying different type of faults on both busbar and attached transmission lines, faults parameters are vary regarding its locations, type, fault resistance and fault inception angle, knowing that the sampling frequency used is 100 KHZ.

5-3-1 Fault location

Fault locations are selected to be on Cairo busbar and in the middle of all transmission lines attached to it. Choosing this part of the grid is made because lines connecting to it vary between short, medium and long lengths which validates studying the effect of different types of faults on different lengths, consequently technique proposed for discrimination can be tested as well.

5-3-2 Fault Type

All types of fault are applied on both busbar and attached transmission lines in the selected part of simulated grid.

The fault types were made in the following order:

1. L-G.
2. L-L-G
3. L-L
4. L-L-L

It is worth to mention that the un-faulted phases are affected by fault presence due to mutual coupling, also fault influences appears in the currents that flow in healthy lines, therefore all lines phases are monitored. Analyzing such data can assist in identifying the exact fault type happened.

5-3-3 Fault Resistance

The value of the obtained discrimination signal and the intensity of the travelling wave are inversely proportional with the fault resistance. Cases under investigations were subjected to the following fault resistance:

1. 0 ohm (negligible fault resistance).
2. 10 ohm (Normal fault resistance).
3. 100 ohm (High fault resistance).

Although high fault resistance simulation introduces a special fault condition that is rare to happen, however it is worth to study it.

5-3-4 Fault inception angle

Both discrimination signal and travelling wave affected severely with fault inception angle as fault happened with angle close to signal peak generates discrimination value and travelling wave intensity much greater than those took place closer to zero crossing points of the wave.

Cases were simulated with fault inception angles in zero crossing points and in peak points that represent special fault conditions besides points in between which represent normal fault angles.

5-4 Case By Case Study

In the up coming section faults case by case will be displayed, studied and discussed. The fault cases are classified according to its location. Busbar fault, short length line faults, medium length faults and long line faults with different parameters and conditions are introduced. Proposed relay is fixed on Cairo busbar and all lines attached to it where it shall monitor the busbar voltage and

current flows in each transmission connected to it. The relay DSP calculates voltage discrimination wave M(t), average deviation values of current that flows in all 3 lines connected to that busbar, and discrimination of travelling wave signal MT(t), analyzes all the above values and provide the trip signal completed with all needed data regarding fault type and location.

The coming results are all cases 3 phase discrimination graphs and current deviation matrix that represents all phases of all lines in the following matrix form:

$$FT = \begin{vmatrix} I_{A1} & I_{B1} & I_{C1} \\ I_{A2} & I_{B2} & I_{C2} \\ I_{A3} & I_{B3} & I_{C3} \end{vmatrix}$$

Also the forward and backward travelling wave graphs of each case are shown.

During faults the voltage discrimination wave M(t) provides the exact instant of fault as it will distort passing over the setted threshold limits , current average deviation matrix (FT) will show the fault type by comparing its columns, also discrimination of travelling wave signal MT(t) graphs can indicate the defected element in the network ,it shows the forward and backward travelling wave of all 3 lines protected by the relay and its capture times (Tf - Tb) then it decides the fault place according to the following criteria:

If	$Tf_1 \neq Tb_1$	&	$Tf_2 \neq Tb_2$	&	$Tf_3 \neq Tb_3$	Then	Busbar fault
Else if	$Tf_1 = Tb_1$	&	$Tf_2 \neq Tb_2$	&	$Tf_3 \neq Tb_3$	Then	Line 1 fault
Else if	$Tf_1 \neq Tb_1$	&	$Tf_2 = Tb_2$	&	$Tf_3 \neq Tb_3$	Then	Line 2 fault
Else if	$Tf_1 \neq Tb_1$	&	$Tf_2 \neq Tb_2$	&	$Tf_3 = Tb_3$	Then	Line 3 fault

Table 5.1, Travelling waves timing scenarios followed to detect fault place.

5-4-1 Busbar fault

Faults of any type that happened directly to the busbar have significant effect specially on the generation station connected to this bar .Unlike the transmission line faults, the isolation of busbars requires disconnection of breakers linking all attached lines which leads to trip a vast part of the network. Therefore caution is highly required before such action.

5-4-1-1 L-G B.B fault

A) R=0 Ω

Figure 5.1(a,b,c & d) and Matrix 5-1 show the effect of applying phase A to ground fault on Cairo busbar. Fault inception angle is 0.0425 and fault resistance is negligible.

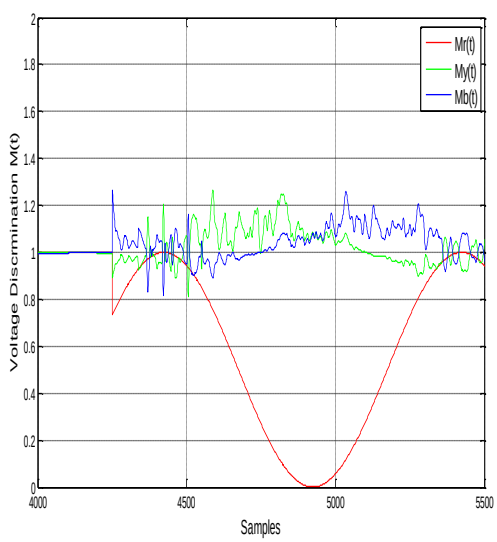

Figure 5.1(a), M(t) of LA-G fault on B.B.

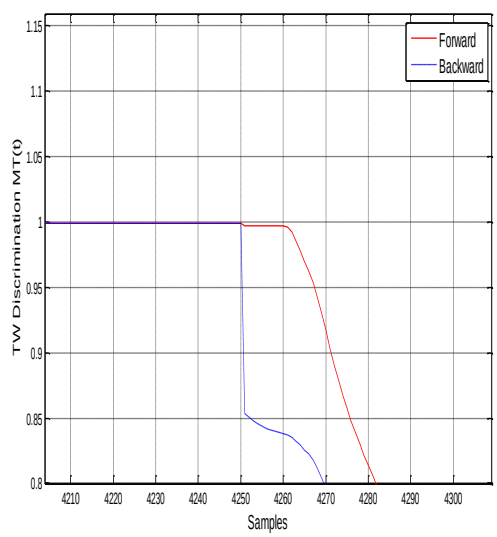

Figure 5.1(b), MT(t) for L1 of LA-G fault on B.B.

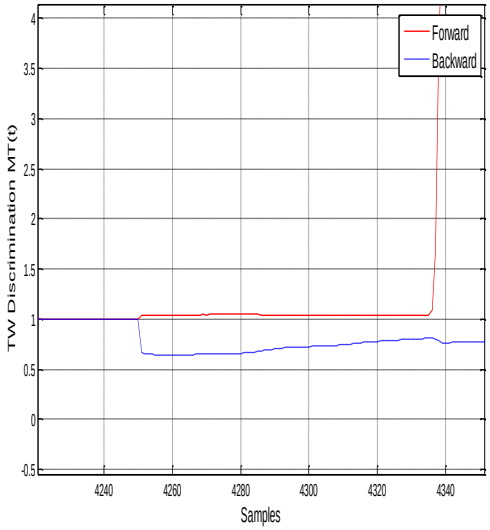

Figure 5.1(c), MT(t) for L2 of LA-G fault on B.B.

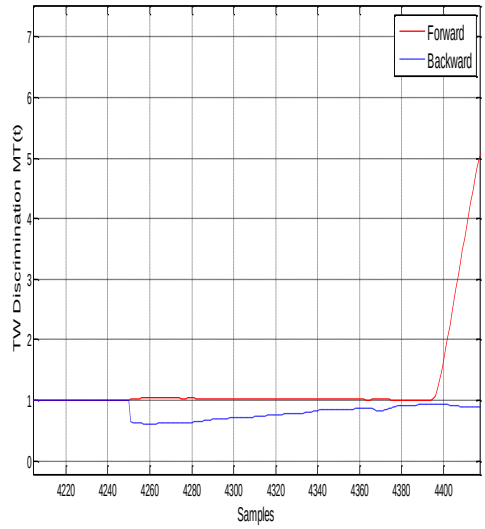

Figure 5.1(d), MT(t) for L2 of LA-G fault on B.B.

$$FT = \begin{vmatrix} 21.8918 & 1.4241 & 0.1111 \\ 9.6375 & 0.9671 & 0.0129 \\ 9.8033 & 1.1873 & 0.0824 \end{vmatrix} \qquad (5\text{-}1)$$

All items in column 1 is by far greater than the their correspondent in the other 2 columns ,however columns 2 and 3 are almost similar. Tf ≠ Tb for all 3 lines are unequal.

B) R=10 Ω

Figure 5.2(a,b,c & d) and Matrix 5-2 show the effect of applying phase A to ground fault on Cairo busbar .Fault inception angle is 0.0425 and fault resistance is 10 ohms.

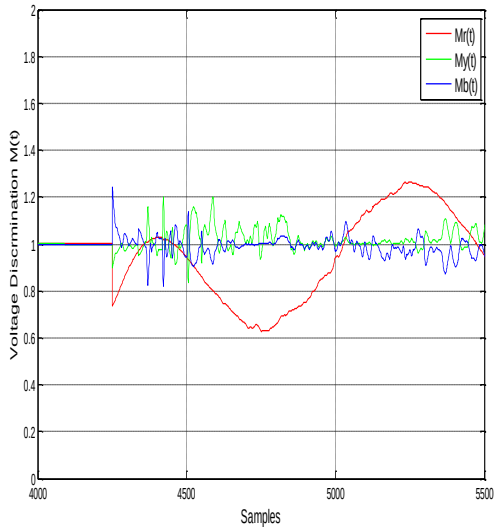

Figure 5.2(a), M(t) of LA-G fault on B.B.

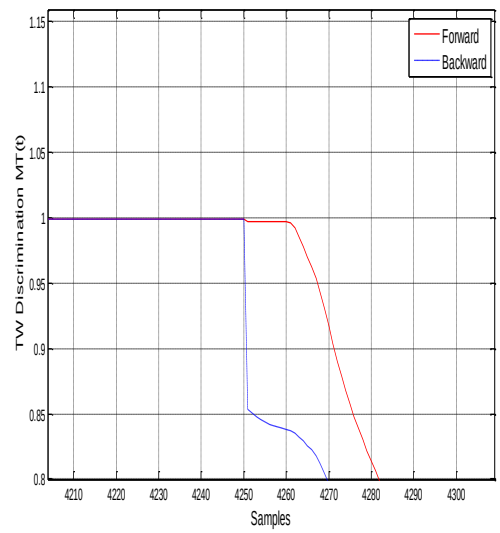

Figure 5.2(b), MT(t) for L1 of LA-G fault on B.B.

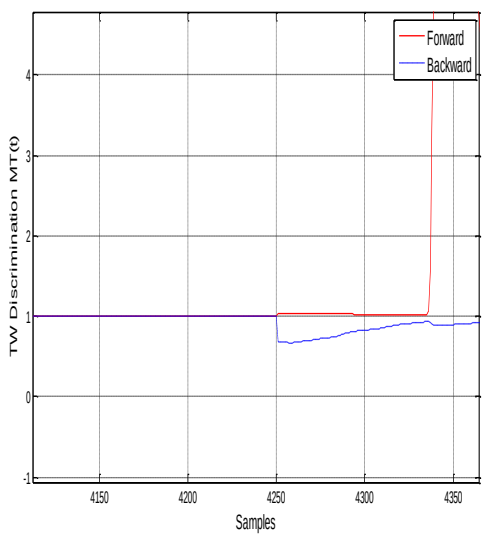

Figure 5.2(c), MT(t) for L2 of LA-G fault on B.B.

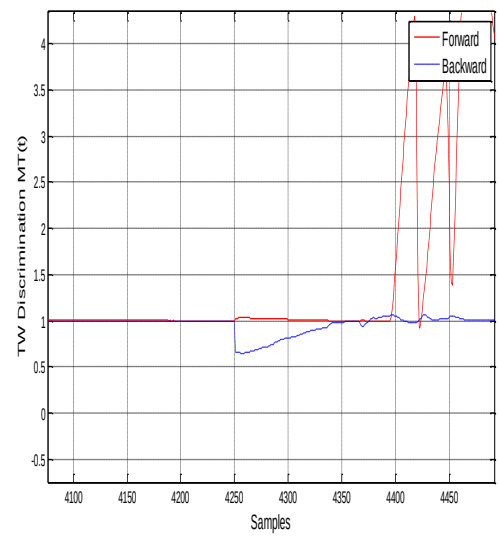

Figure 5.2(d), MT(t) for L3 of LA-G fault on B.B.

$$FT = \begin{vmatrix} 0.3828 & 0.0473 & 0.1177 \\ 0.3828 & 0.0007 & 0.1152 \\ 0.4185 & 0.0075 & 0.1397 \end{vmatrix} \qquad (5\text{-}2)$$

All items in column 1 are by far greater than their correspondent in the other 2 columns, however columns 2 and 3 are almost similar. Tf ≠ Tb for all 3 lines are unequal.

5-4-1-2 L-L-G B.B fault

A) R=0 Ω

Figure 5.3(a,b,c & d) and Matrix 5-3 show the effect of applying phase A to phase C to ground fault on Cairo busbar. Fault inception angle is 0.0425 and fault resistance is neglected.

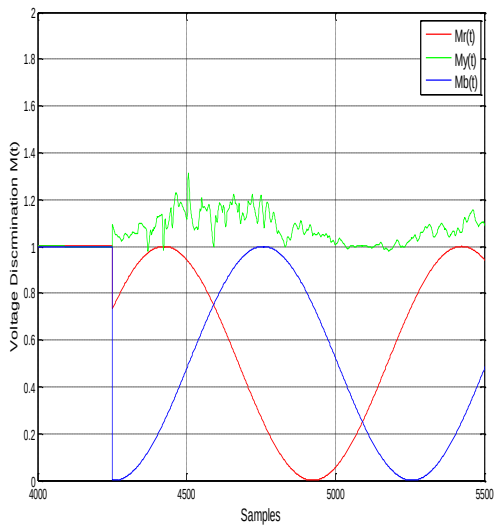

Figure 5.3(a), M(t) of LA-C-G fault on B.B.

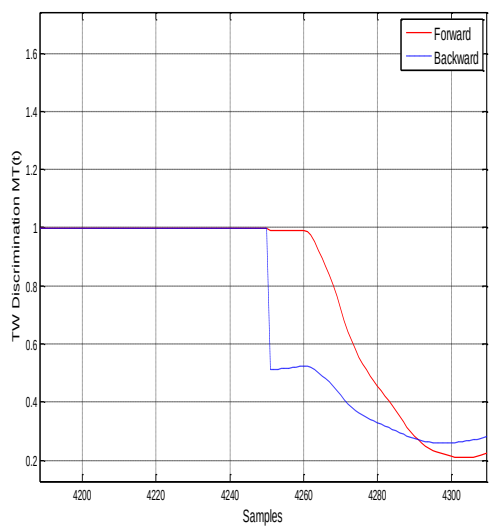

Figure 5.3(b), MT(t) for L1 of LA-C-G fault on B.B.

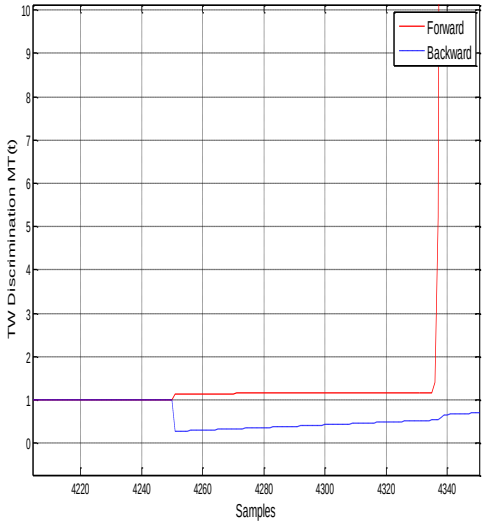

Figure 5.3(c), MT(t) for L2 of LA-C-G fault on B.B.

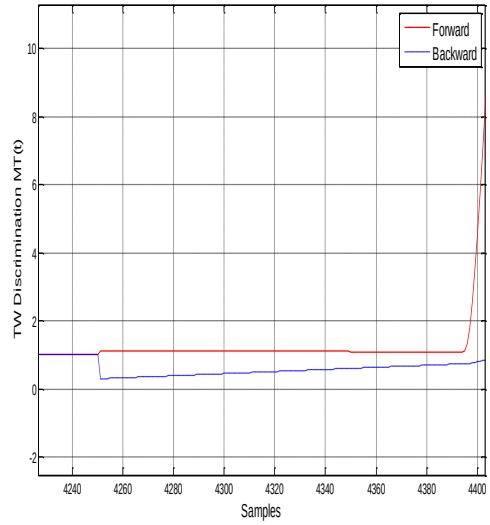

Figure 5.3(d), MT(t) for L3 of LA-C-G fault on B.B.

$$FT = \begin{vmatrix} 25.7954 & 0.6781 & 14.2054 \\ 11.9633 & 0.4796 & 6.6553 \\ 12.4275 & 0.6208 & 7.1252 \end{vmatrix} \qquad (5\text{-}3)$$

All items in columns 1 and 3 are by far greater than their correspondent in column 2. Tf ≠ Tb for all 3 lines are unequal.

B) R=10 Ω

Figure 5.4(a,b,c & d) and Matrix 5-4 show the effect of applying phase A to phase C to ground fault on Cairo busbar. Fault inception angle is 0.525 and fault resistance 10 ohms.

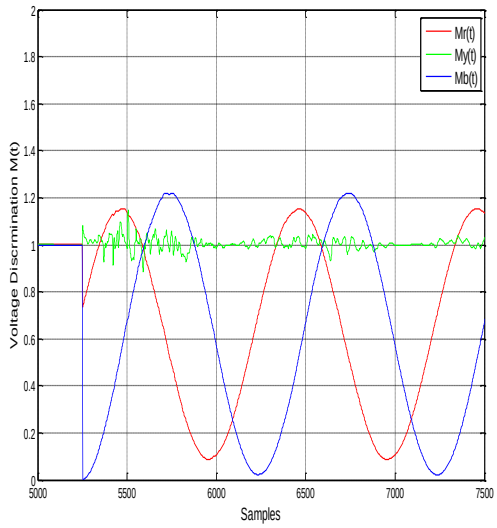

Figure 5.4(a), M(t) of LA-C-G fault on B.B.

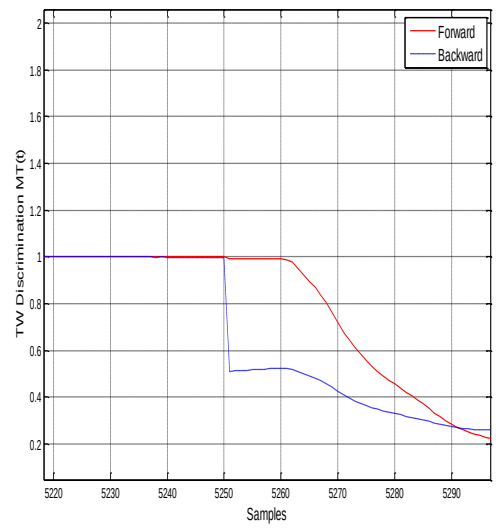

Figure 5.4(b), MT(t) for L1 of LA-C-G fault on B.B.

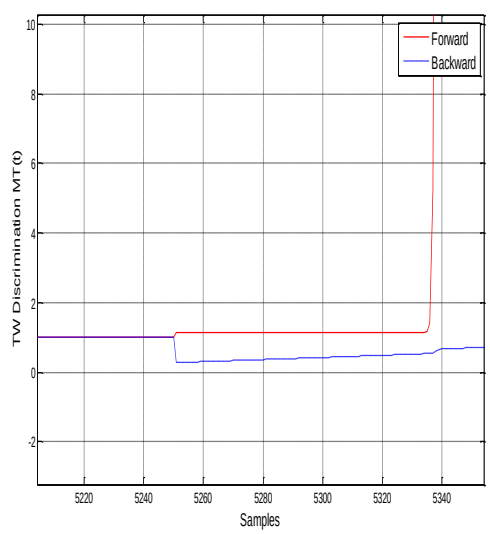

Figure 5.4(c), MT(t) for L2 of LA-C-G fault on B.B.

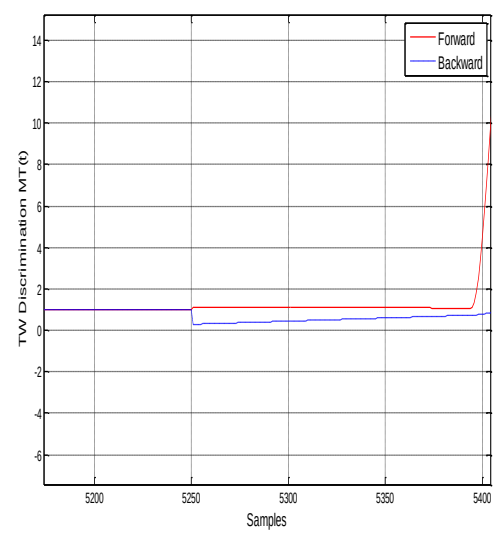

Figure 5.4(d), MT(t) for L3 of LA-C-G fault on B.B.

$$FT = \begin{vmatrix} 17.5465 & 0.1104 & 15.9380 \\ 8.8249 & 0.0770 & 7.0213 \\ 9.3975 & 0.0898 & 7.5252 \end{vmatrix} \qquad (5\text{-}4)$$

All items in columns 1 and 3 is by far greater than their correspondent in column 2. Tf ≠ Tb for all 3 lines are unequal.

5-4-1-3 L-L B.B fault

Figure 5.5(a,b,c & d) and Matrix 5-5 show the effect of applying phase A to phase C fault on Cairo busbar. Fault inception angle is 0.0425.

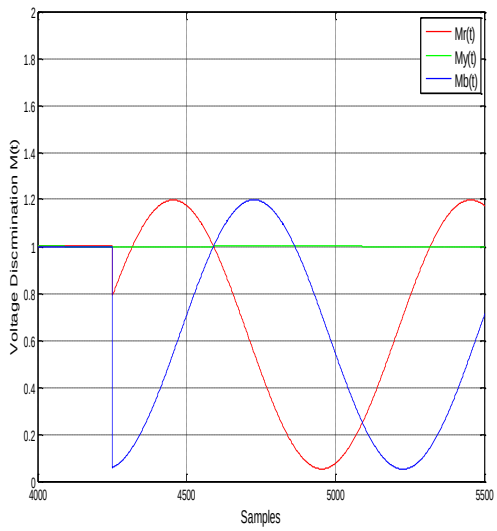

Figure 5.5(a), M(t) of LA-C fault on B.B.

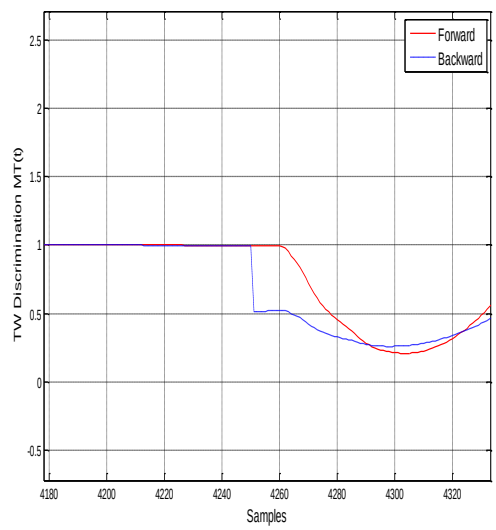

Figure 5.5(b), MT(t) for L1 of LA-C fault on B.B.

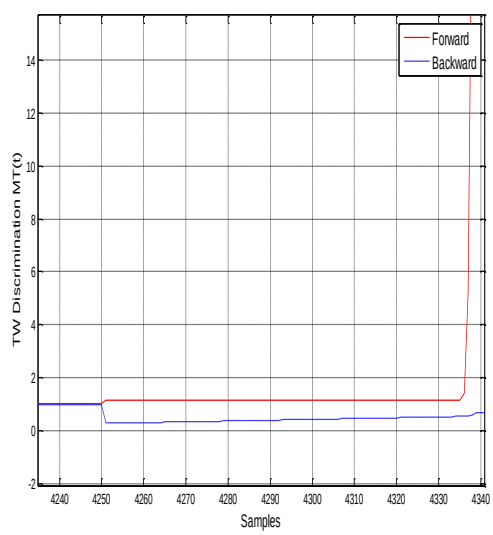

Figure 5.5(c), MT(t) for L2 of LA-C fault on B.B.

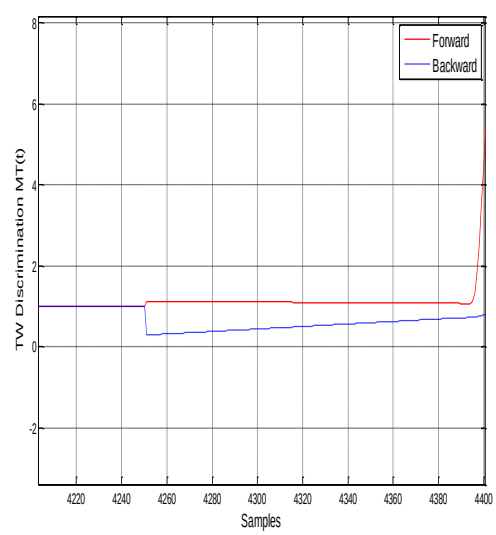

Figure 5.5(d), MT(t) for L3 of LA-C fault on B.B.

$$FT = \begin{vmatrix} 19.2747 & 0.0001 & 14.4268 \\ 9.6100 & 0.0000 & 6.3878 \\ 10.1904 & 0.0000 & 6.8783 \end{vmatrix} \qquad (5\text{-}5)$$

All items in columns 1 and 3 is by far greater than their correspondent in column 2., yet unlike L-L-G fault column 2 stuck to almost zeros. Tf ≠ Tb for all 3 lines are unequal.

5-4-1-4 L-L-L B.B fault

Figure 5.6(a,b,c & d) and Matrix 5-6 show the effect of applying 3 phases fault on Cairo busbar. Fault inception angle is 0.0425.

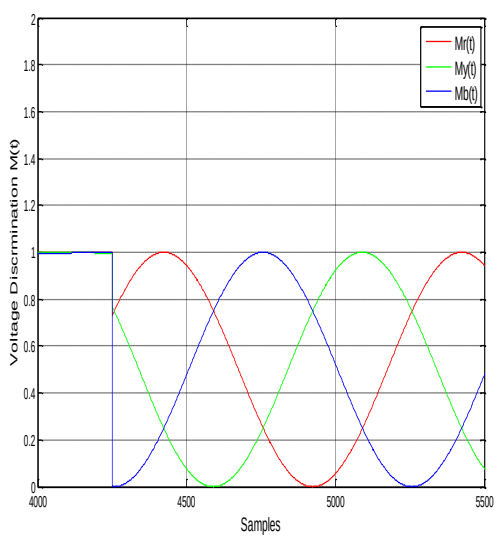

Figure 5.6(a), M(t) of LA-B-C fault on B.B.

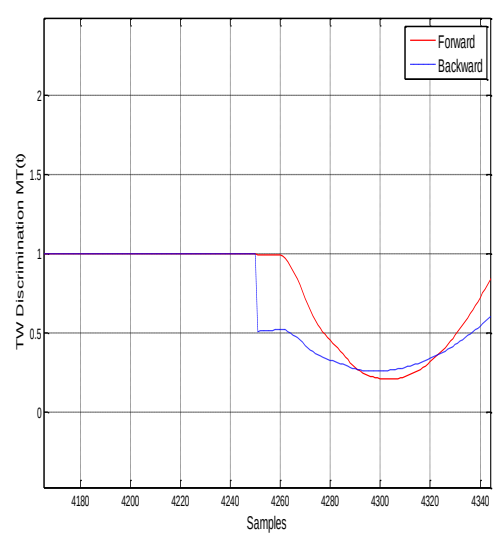

Figure 5.6(b), MT(t) for L1 of LA-B-C fault on B.B.

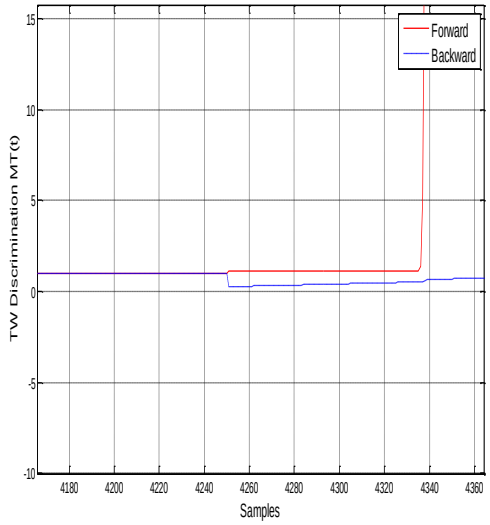

Figure 5.6(c), MT(t) for L2 of LA-B-C fault on B.B.

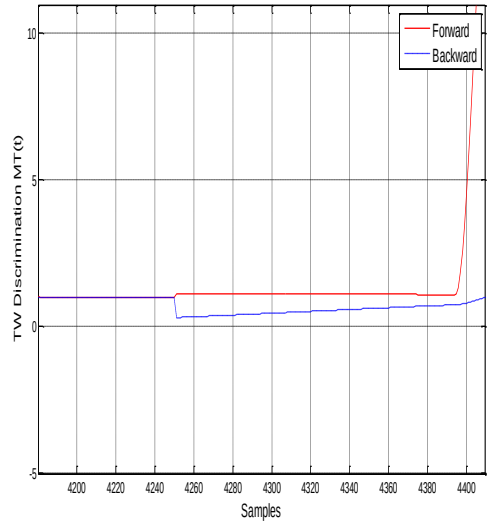

Figure 5.6(d), MT(t) for L3 of LA-B-C fault on B.B.

$$FT = \begin{vmatrix} 37.1824 & 38.4336 & 15.7328 \\ 17.0188 & 17.5850 & 7.7721 \\ 18.1139 & 18.7360 & 8.3231 \end{vmatrix} \qquad (5\text{-}6)$$

All items in all rows are relatively high and none of them is significantly higher than its correspondent in the others 2 columns. Tf ≠ Tb for all 3 lines are unequal.

5-4-2 Line faults

Discrimination technique is essential to limit the disconnected area tightly to its defected region and avoid false tripping. Relay techniques can implement the transmission lines back up protection function.

In the next section Discrimination technique will be applied over all fault cases located in the middle of a moderate length line of almost 125 km (fault is 62 km away of the relay).

5-4-2-1 L-G Line fault

Figure 5.7(a,b,c & d) and Matrix 5-7 show the effect of applying phase A to ground fault in the middle of Cairo – Korimat line. Fault inception angle is 0.0425 and fault resistance is negligible.

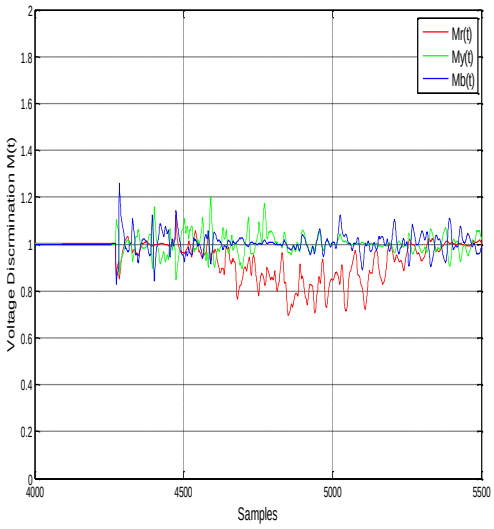

Figure 5.7(a), M(t) of LA-G fault on L2.

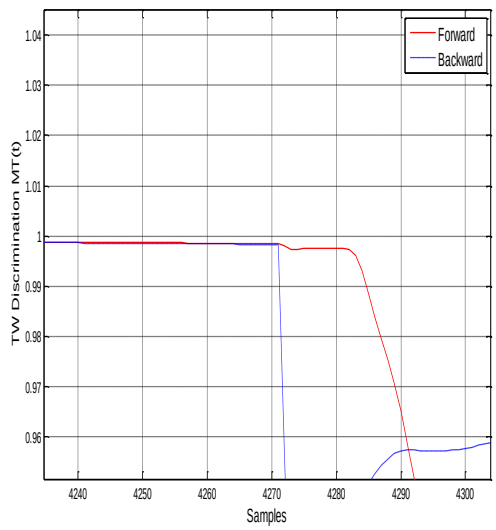

Figure 5.7(b), MT(t) for L1 of LA-G fault on L2.

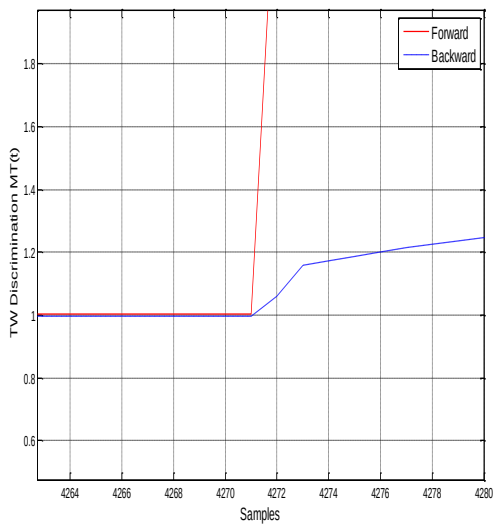

Figure 5.7(c), MT(t) for L2 of LA-G fault on L2.

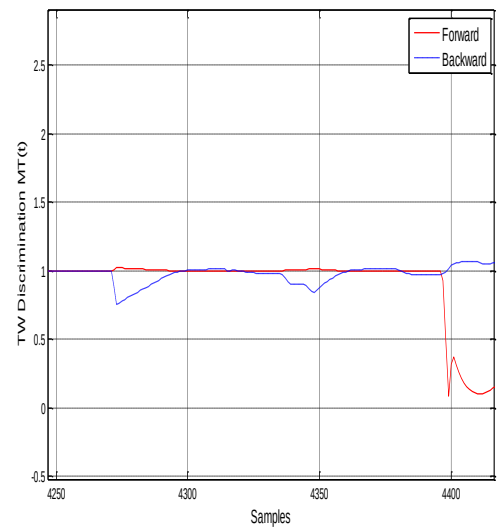

Figure 5.7(d), MT(t) for L3 of LA-G fault on L2.

$$FT = \begin{vmatrix} 0.0298 & 0.0612 & 0.0030 \\ 59.2203 & 0.087 & 0.1012 \\ 0.0113 & 0.0148 & 0.0044 \end{vmatrix} \qquad (5\text{-}7)$$

Second item in column 1 is by far greater than its correspondent in the other 2 columns, however all items in columns 2 and 3 are almost similar. Tf_2 equals to Tb_2, but Tf_1 unequal to Tb_1, also Tf_3 unequal to Tb_3.

5-4-2-3 L-L-G Line fault

Figure 5.8(a,b,c & d) and Matrix 5-8 show the effect of applying phase A to phase C to ground fault in the middle of Cairo – Korimat line. Fault inception angle is 0.0425 and fault resistance is negligible.

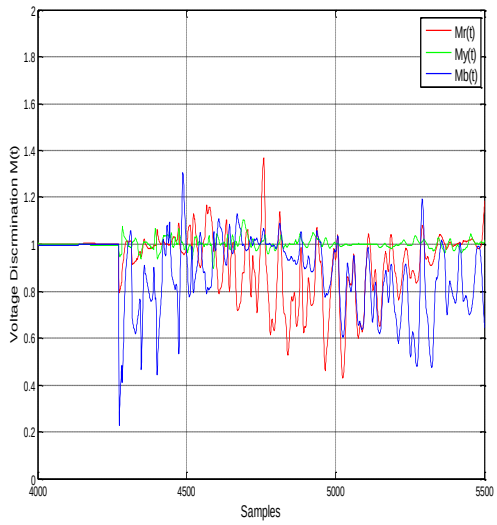

Figure 5.8(a), M(t) of LA-C-G fault on L2.

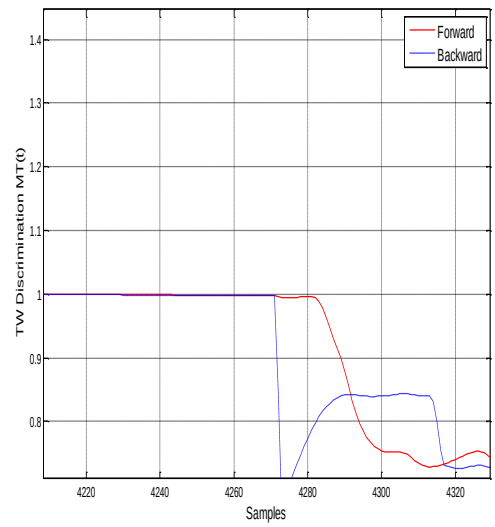

Figure 5.8(b), MT(t) for L1 of LA-C-G fault on L2.

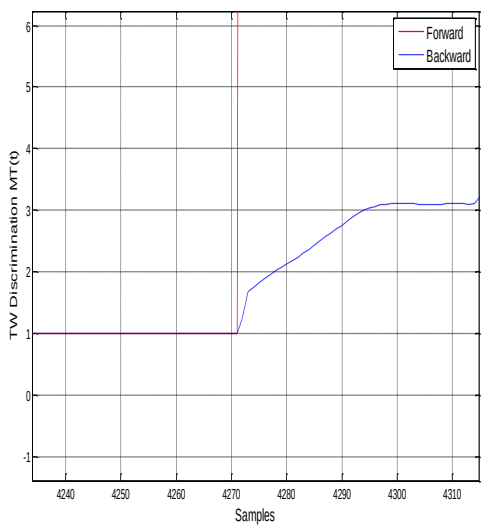

Figure 5.8(c), MT(t) for L2 of LA-C-G fault on L2.

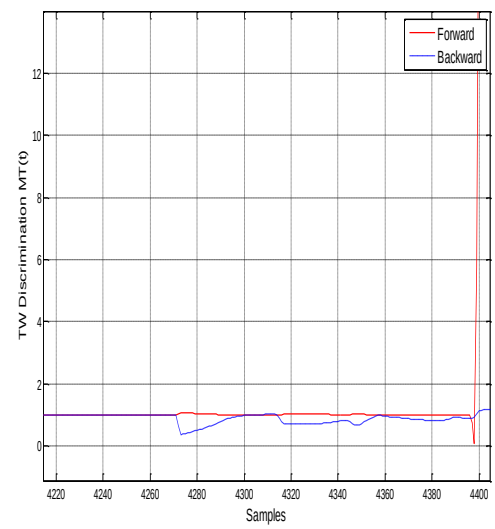

Figure 5.8(d), MT(t) for L3 of LA-C-G fault on L2.

$$FT = \begin{vmatrix} 0.4157 & 0.0049 & 0.0239 \\ 92.5877 & 0.0031 & 77.2895 \\ 0.1542 & 0.0040 & 0.0833 \end{vmatrix} \qquad (5\text{-}8)$$

Second item in columns 1 and 3 is by far greater than their correspondent in column 2. Tf_2 equals to Tb_2, but Tf_1 unequal to Tb_1, also Tf_3 unequal to Tb_3.

5-4-2-3 L-L Line fault

Figure 5.9(a,b,c & d) and Matrix 5-9 show the effect of applying phase A to phase C fault in the middle of Cairo – Korimat line. Fault inception angle is 0.0425.

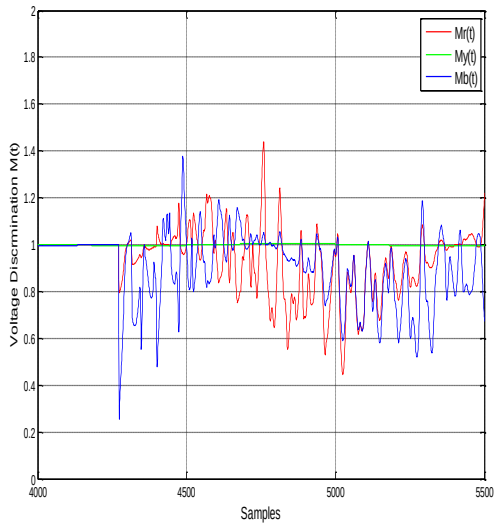

Figure 5.9(a), M(t) of LA-C fault on L2.

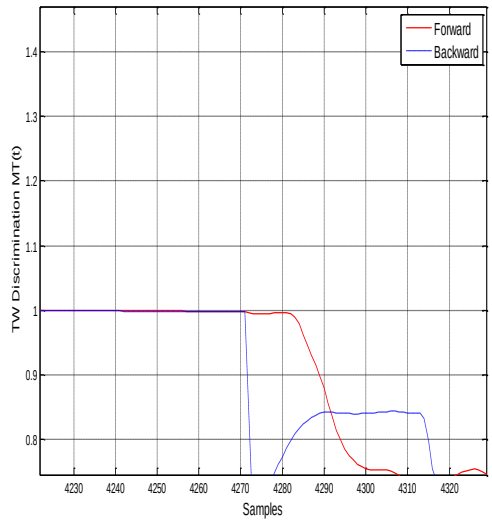

Figure 5.9(b), MT(t) for L1 of LA-C fault on L2.

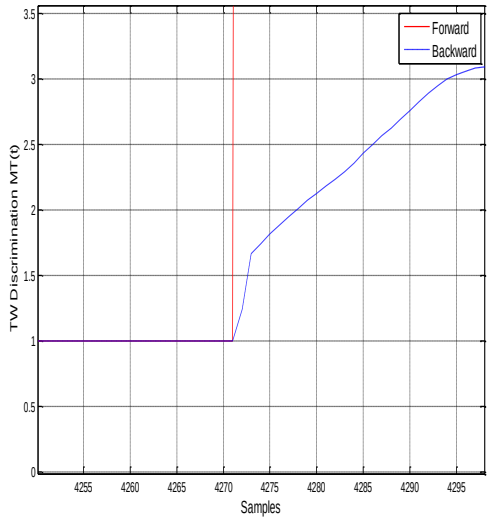

Figure 5.9(c), MT(t) for L2 of LA-C fault on L2.

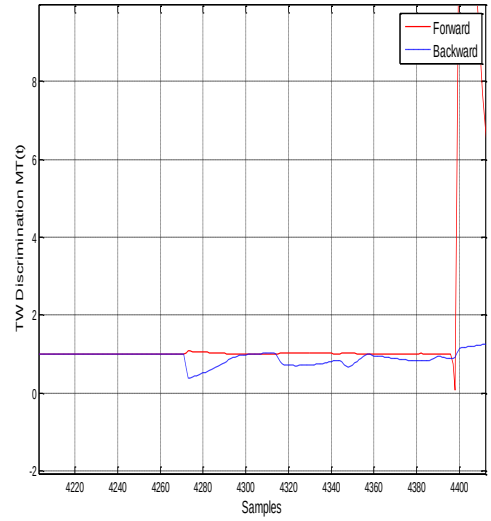

Figure 5.9(d), MT(t) for L3 of LA-C fault on L2.

$$FT = \begin{vmatrix} 0.5329 & 0.0001 & 0.1179 \\ 71.1732 & 0.0000 & 81.8326 \\ 0.1841 & 0.0000 & 0.0544 \end{vmatrix} \qquad (5\text{-}9)$$

Second item in columns 1 and 3 is by far greater than their correspondent in column 2, yet unlike L-L-G fault column 2 stuck to almost zero. Tf_2 equals to Tb_2, but Tf_1 unequal to Tb_1, also Tf_3 unequal to Tb_3.

5-4-2-4 L-L-L Line fault

Figure 5.10(a,b,c & d) and Matrix 5-10 show the effect of applying 3 phases fault in the middle of Cairo – Korimat line. Fault inception angle is 0.0425.

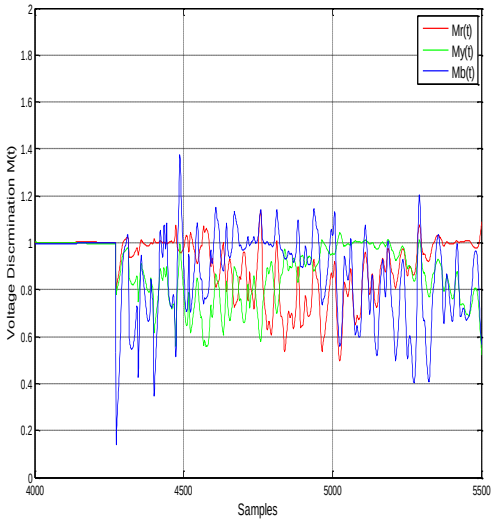

Figure 5.10(a), M(t) of LA-B-C fault on L2.

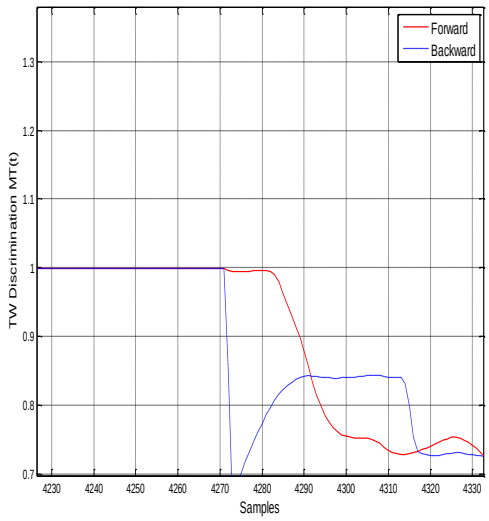

Figure 5.10(b), MT(t) for L1 of LA-B-C fault on L2.

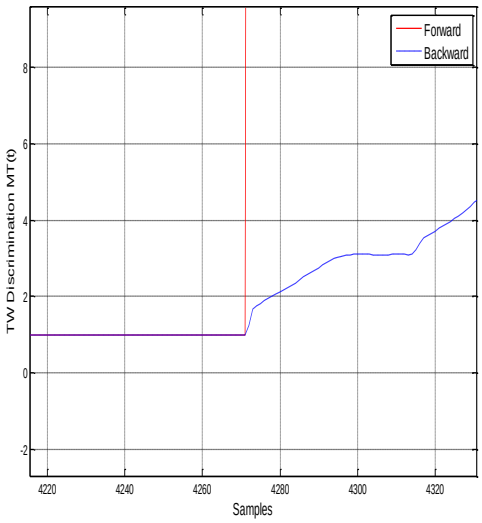

Figure 5.10(c), MT(t) for L2 of LA-B-C fault on L2.

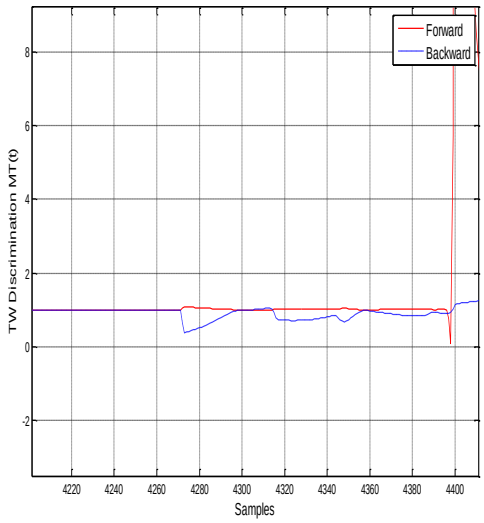

Figure 5.10(d), MT(t) for L3 of LA-B-C fault on L2.

$$FT = \begin{vmatrix} 0.4802 & 0.5480 & 0.2087 \\ 167.8277 & 189.0601 & 79.7150 \\ 0.0068 & 0.0818 & 0.1826 \end{vmatrix} \qquad (5\text{-}10)$$

All items in the second row are relatively supreme and non of them is significantly higher than its correspondent in the others 2 columns. Tf_2 equals to Tb_2, but Tf_1 unequal to Tb_1, also Tf_3 unequal to Tb_3

5-4-3 Farther distance fault

In the next section discrimination technique will be applied over some fault cases located in the middle of longer line of almost 209 km (fault is 105 km away of the relay).

It is expected to have a similar behavior to the shorter line mentioned in the last section.

5-4-3-1 L-G Long line fault

A) R=0 Ω

Figure 5.11(a,b,c & d) and Matrix 5-11 show the effect of applying phase A to ground fault in the middle of Cairo – Samalut line. Fault inception angle is 0.0425 and fault resistance is negligible.

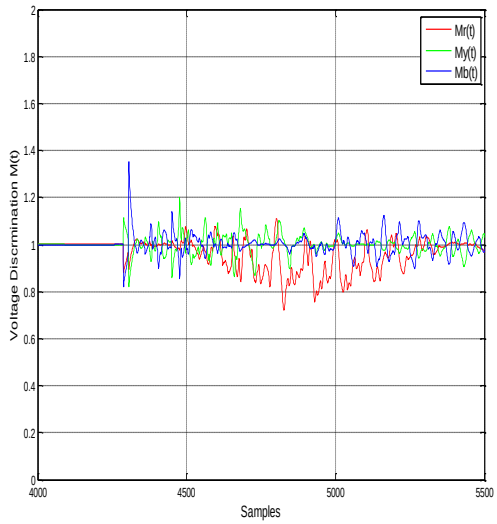

Figure 5.11(a), M(t) of LA-G fault on L3.

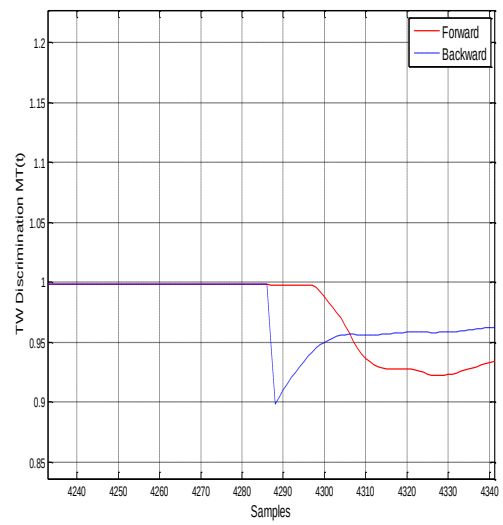

Figure 5.11(b), MT(t) for L1 of LA-G fault on L3.

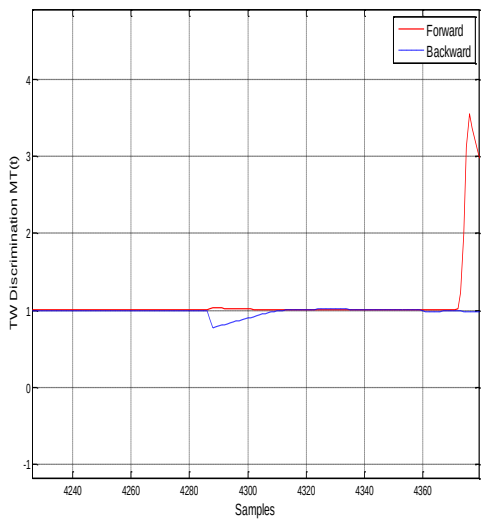

Figure 5.11(c), MT(t) for L2 of LA-G fault on L3.

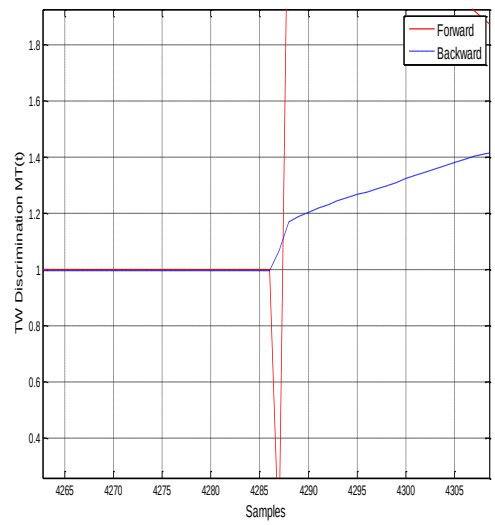

Figure 5.11(d), MT(t) for L3 of LA-G fault on L3.

$$FT = \begin{vmatrix} 0.0125 & 0.0451 & 0.0457 \\ 0.0109 & 0.0216 & 0.0283 \\ 30.1675 & 0.0676 & 0.0981 \end{vmatrix} \qquad (5\text{-}11)$$

Third item in column 1 is by far greater than its correspondent in the other 2 columns, however all items in columns 2 and 3 are almost similar. Tf_3 equals to Tb_3, but Tf_1 unequal to Tb_1, also Tf_2 unequal to Tb_2.

B) R=10 Ω

Figure 5.12(a,b,c & d) and Matrix 5-12 show the effect of applying phase A to ground fault in the middle of Cairo – Samalut line. Fault inception angle is 0.525 and fault resistance is 10 ohms.

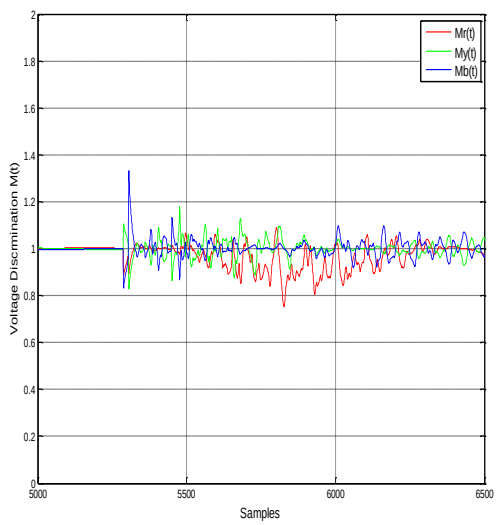

Figure 5.12(a), M(t) of LA-G fault on L3.

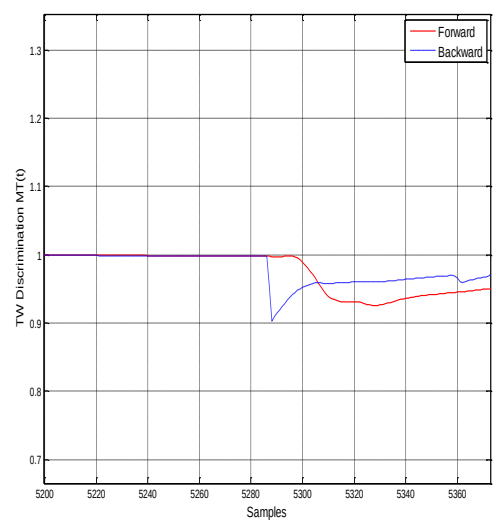

Figure 5.12(b), MT(t) for L1 of LA-G fault on L3.

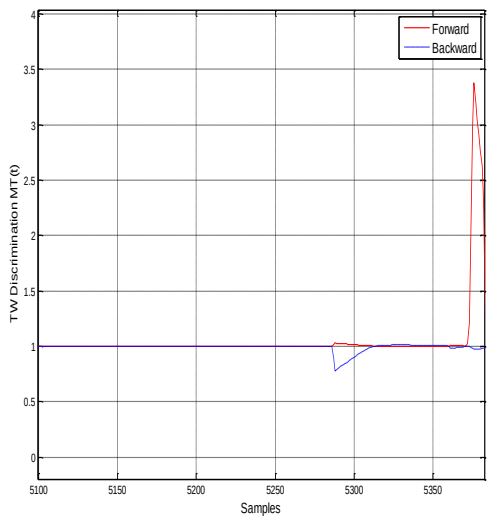

Figure 5.12(c), MT(t) for L2 of LA-G fault on L3.

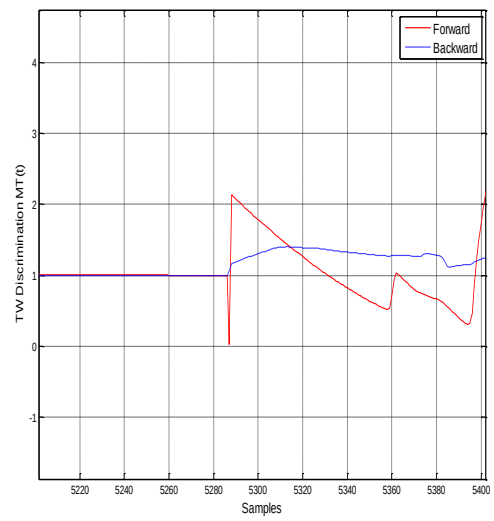

Figure 5.12(d), MT(t) for L3 of LA-G fault on L3.

$$FT = \begin{vmatrix} 0.1307 & 0.0207 & 0.0433 \\ 0.0241 & 0.0124 & 0.0279 \\ 17.9001 & 0.0372 & 0.0931 \end{vmatrix} \qquad (5\text{-}12)$$

Third item in column 1 is by far greater than its correspondent in the other 2 columns ,however all items in columns 2 and 3 are almost similar. Tf_3 equals to Tb_3, but Tf_1 unequal to Tb_1, also Tf_2 unequal to Tb_2.

5-4-3-2 L-L-G Long line fault

Figure 5.13(a,b,c & d) and Matrix 5-13 show the effect of applying phase A to phase C to ground fault in the middle of Cairo – Samalut line. Fault inception angle is 0.525 and fault resistance is 10 ohms.

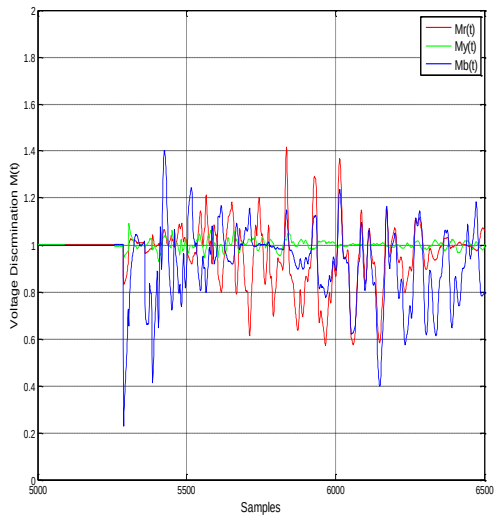

Figure 5.13(a), M(t) of LA-C-G fault on L3.

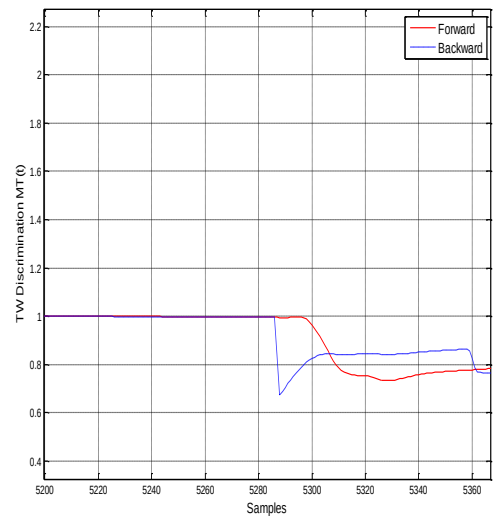

Figure 5.13(b), MT(t) for L1 of LA-C-G fault on L3.

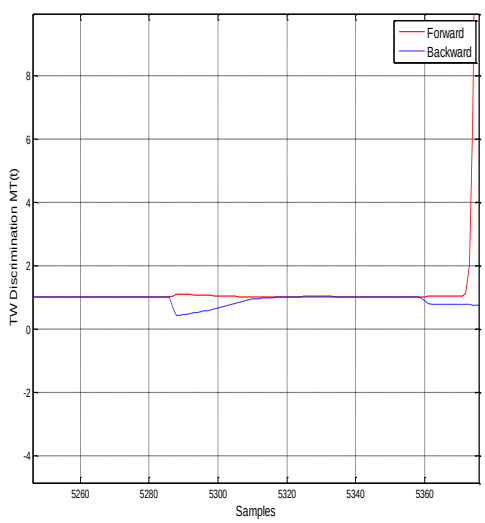

Figure 5.13(c), MT(t) for L2 of LA-C-G fault on L3.

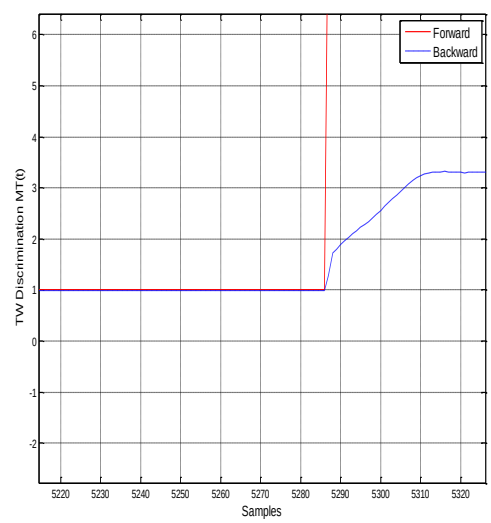

Figure 5.13(d), MT(t) for L3 of LA-C-G fault on L3.

$$FT = \begin{vmatrix} 0.2258 & 0.0214 & 0.0900 \\ 0.0050 & 0.0103 & 0.09069 \\ 32.9240 & 0.0346 & 52.7070 \end{vmatrix} \qquad (5\text{-}13)$$

Third item in columns 1 and 3 is by far greater than their correspondent in column 2. Tf_3 equals to Tb_3, but Tf_1 unequal to Tb_1, also Tf_2 unequal to Tb_2.

5-4-3 Special fault cases

In rare cases faults can occur in very special condition such as critical fault location, extraordinary high fault resistance and distinguished inception angles. Those conditions affect the wave form and vary it from the normal fault cases mentioned before; therefore proposed techniques will be applied on fault with such conditions in the next section.

Line to ground fault is the most conventional type that occurs in the transmission lines, also the severity of its effect is the lowest between all, and therefore the special faults studies are going to emphasize on such fault type.

5-4-3-1 Very close faults

Faults happened closed to the busbar have almost the same effect to that happened on the busbar itself however it is not accepted in the EHV network protection to react with both faults similarly. Discrimination technique should manage to differentiate between them.

In order to check to how extend the relay will succeed in that; the proposed tools were applied over a fault placed in the middle of Cairo-Cairo west transmission line (16 Km) which provides faults far by only 8 km away from the relay.

A) L-G closed faults, R=0 ohm

Figure 5.14(a,b,c & d) and Matrix 5-14 show the effect of applying phase A to ground fault in the middle of Cairo – Cairowest line. Fault inception angle is 0.0425 and fault resistance is negligible.

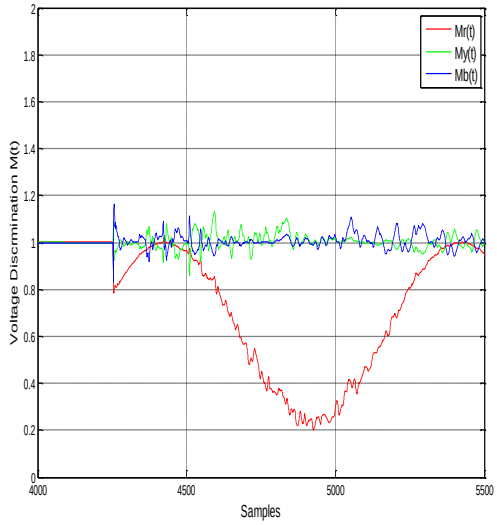

Figure 5.14(a), M(t) of LA-G fault on L1.

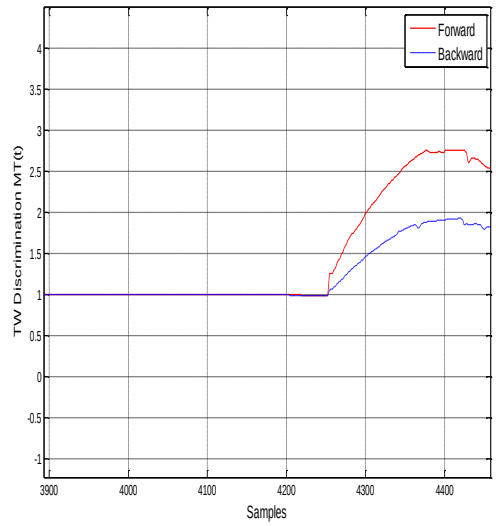

Figure 5.14(b), MT(t) for L1 of LA-G fault on L1.

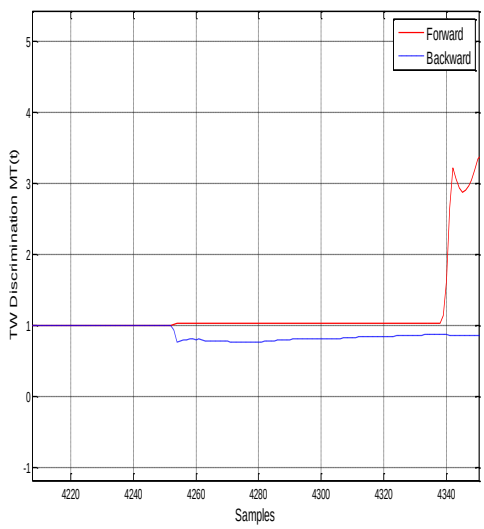

Figure 5.14(c), MT(t) for L2 of LA-G fault on L1.

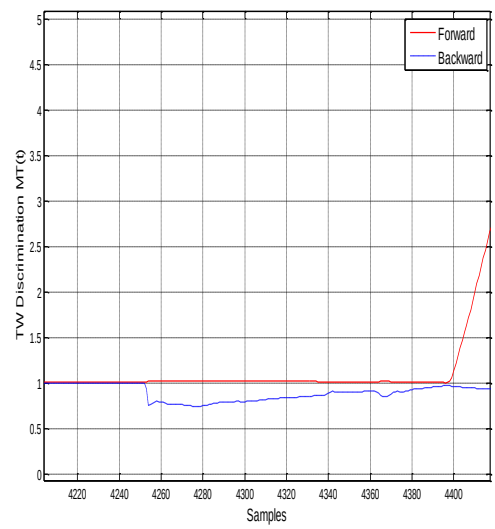

Figure 5.14(d), MT(t) for L3 of LA-G fault on L1.

$$FT = \begin{vmatrix} 51.4275 & 0.0203 & 0.0291 \\ 1.8373 & 0.3607 & 0.1209 \\ 2.3437 & 0.5303 & 0.1252 \end{vmatrix} \qquad (5\text{-}14)$$

First item in column 1 is by far greater than its correspondent in the other 2 columns ,however all items in columns 2 and 3 are almost similar. Tf_1 equal to Tb_1, but Tf_2 unequal to Tb_2 also Tf_3 unequal to Tb_3.

B) L-G closed faults ,R=10 ohm

Figure 5.15(a,b,c & d) and Matrix 5-15 show the effect of applying phase A to ground fault in the middle of Cairo – Cairowest line. Fault inception angle is 0.0525 and fault resistance is 10 ohms.

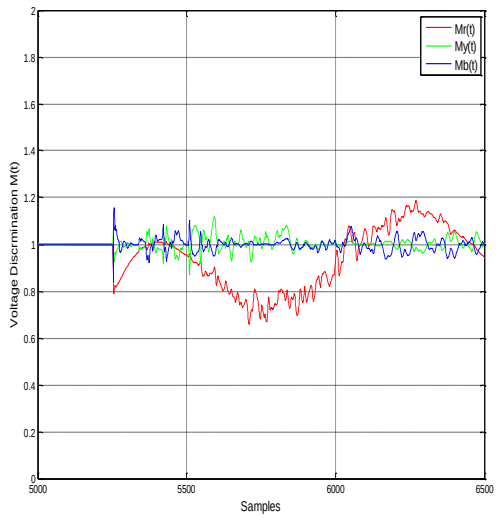

Figure 5.15(a), M(t) of LA-G fault on L1.

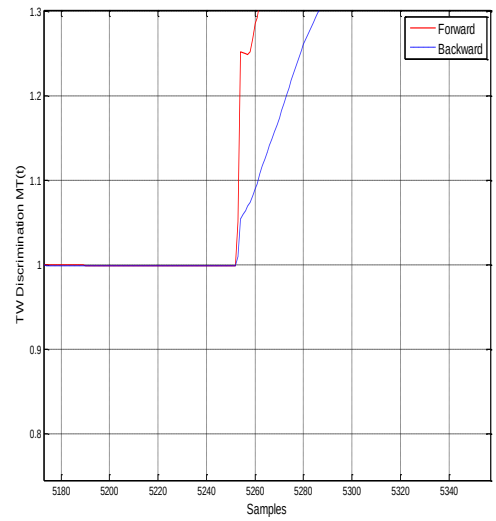

Figure 5.15(b), MT(t) for L1 of LA-G fault on L1.

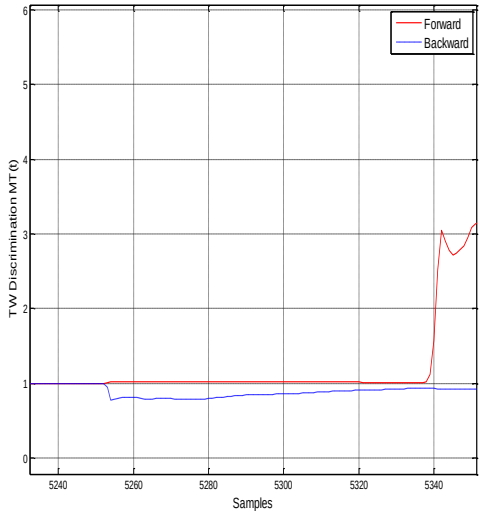

Figure 5.15(c), MT(t) for L2 of LA-G fault on L1

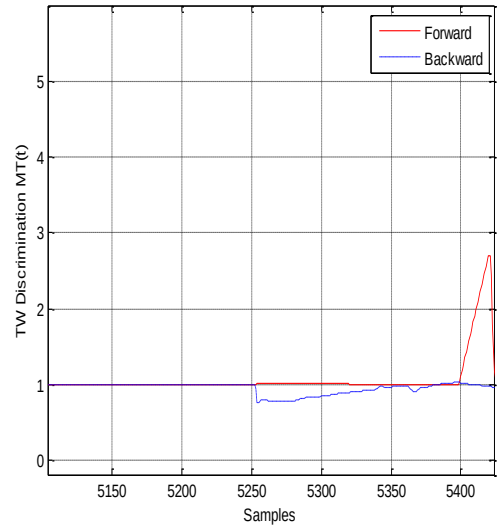

Figure 5.14(d), MT(t) for L3 of LA-G fault on L1.

$$FT = \begin{vmatrix} 6.5938 & 0.0042 & 0.0082 \\ 0.3374 & 0.0086 & 0.0860 \\ 0.3513 & 0.0174 & 0.1204 \end{vmatrix} \qquad (5\text{-}15)$$

First item in column 1 is by far greater than its correspondent in the other 2 columns ,however all items in columns 2 and 3 are almost similar. Tf_1 equal to Tb_1, but Tf_2 unequal to Tb_2 also Tf_3 unequal to Tb_3.

5-4-3-2 High fault resistance

High fault resistance has an effect of attenuating the amplitude of the discrimination signals calculated and therefore it is essential to check the proposed relay against it.

A) B.B L-G fault with high resistance.

Figure 5.16(a,b,c & d) and Matrix 5-16 show the effect of appling phase A to ground fault on cairo busbar.Fault inception angle is 0.0525 and fault resistance is 100 ohms.

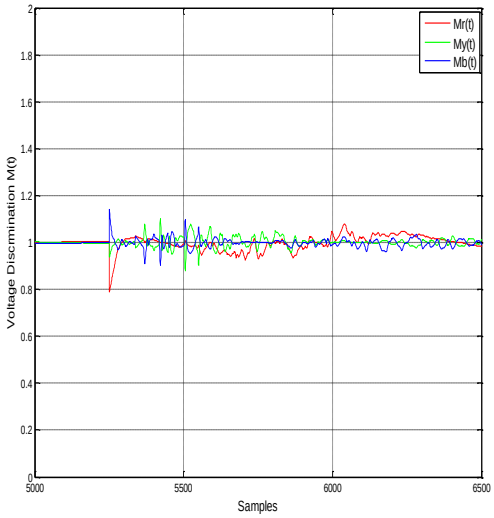

Figure 5.16(a), M(t) of LA-G fault on B.B.

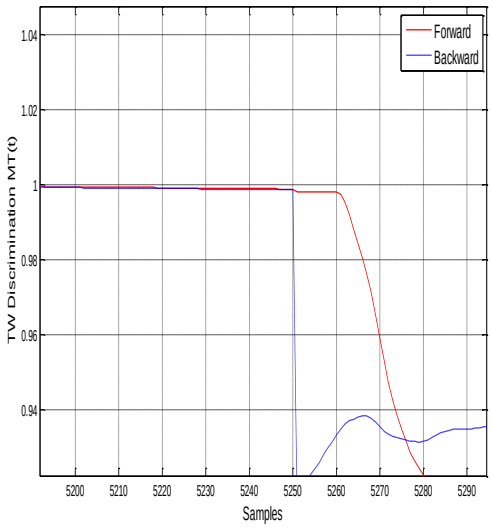

Figure 5.16(b), MT(t) for L1 of LA-G fault on B.B.

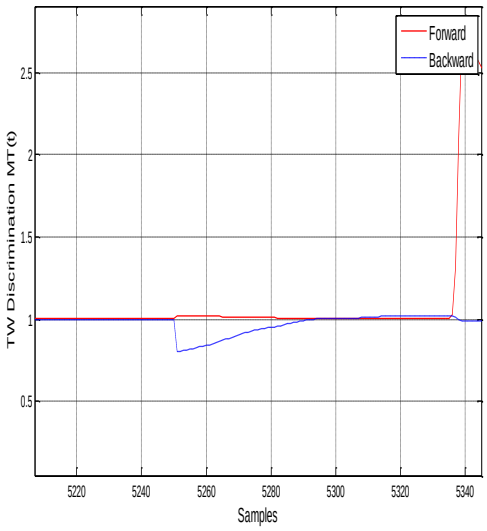

Figure 5.16(c), MT(t) for L2 of LA-G fault on B.B.

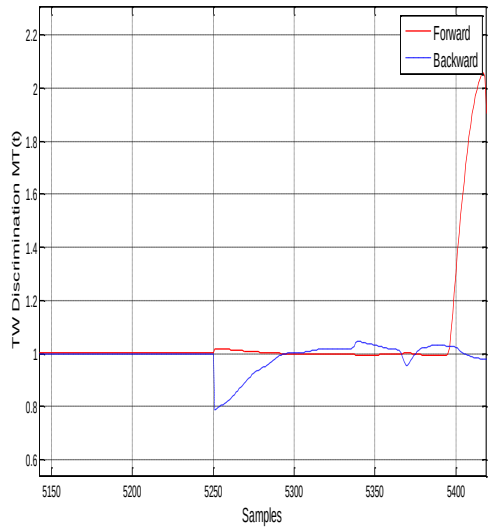

Figure 5.16(d), MT(t) for L3 of LA-G fault on B.B.

$$FT = \begin{vmatrix} 0.1417 & 0.0126 & 0.0109 \\ 0.0925 & 0.0054 & 0.0111 \\ 0.0926 & 0.0060 & 0.0137 \end{vmatrix} \qquad (5\text{-}16)$$

All items in column 1 is by far greater than their correspondent in the other 2 columns.It is remarkable that all deviation matrix values is significantly lower than that resulted from same fault with negligible resistance. Tf_1 equal to Tb_1, but Tf_2 unequals to Tb_2 also Tf_3 unequals to Tb_3.

B) Transmission line L-G fault with high resistance.

Figure 5.17(a,b,c & d) and Matrix 5-17 show the effect of applying phase A to ground fault in the middle of Cairo – Korimat line. Fault inception angle is 0.0525 and fault resistance is 100 ohm.

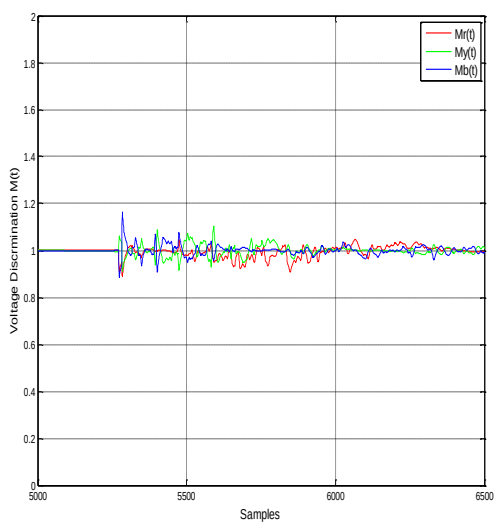

Figure 5.17(a), M(t) of LA-G fault on L2.

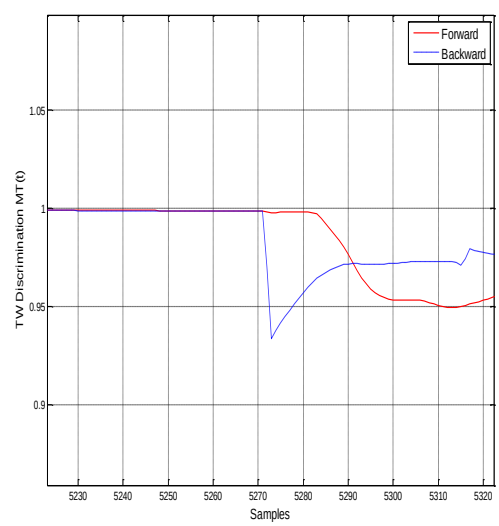

Figure 5.17(b), MT(t) for L1 of LA-G fault on L2.

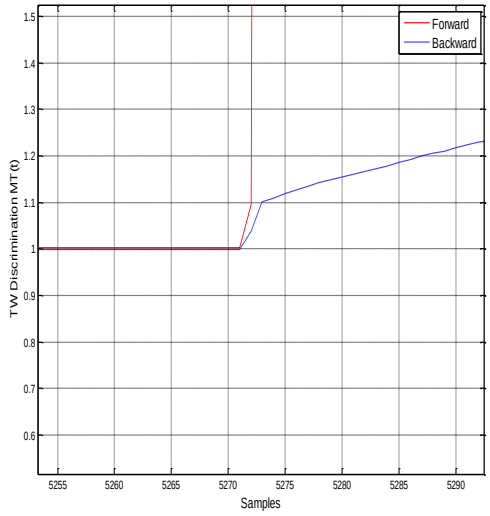

Figure 5.17(c), MT(t) for L2 of LA-G fault on L2.

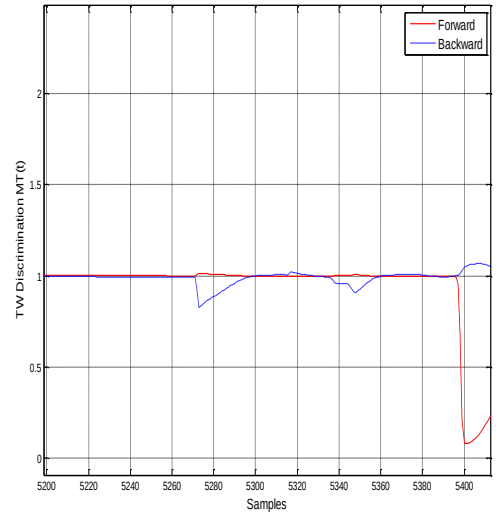

Figure 5.17(d), MT(t) for L3 of LA-G fault on L2.

$$FT = \begin{vmatrix} 0.0887 & 0.0048 & 0.0095 \\ 3.1261 & 0.0027 & 0.0202 \\ 0.0171 & 0.0011 & 0.0010 \end{vmatrix} \qquad (5\text{-}17)$$

Second item in column 1 is by far greater than its correspondent in the other 2 columns. Tf ≠ Tb for all 3 lines are unequal.

5-4-3-2 Critical inception angles.

Faults are going to be tested under a very special inception angles like Peaks and zero crossing points of wave signal.

A) B.B L-G fault at inception in peak point.

Figure 5.18(a,b,c & d) and Matrix 5-18 show the effect of applying phase A to ground fault on Cairo busbar. Fault inception angle is 0.04 and fault resistance is negligible.

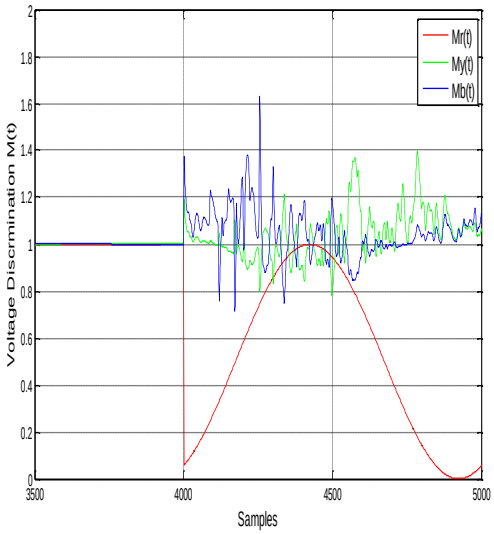

Figure 5.18(a), M(t) of LA-G fault on B.B.

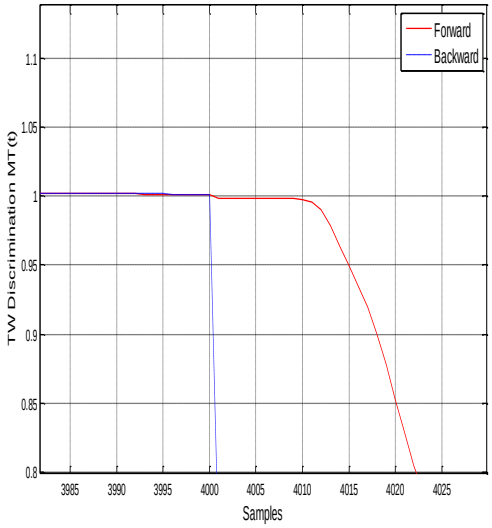

Figure 5.18(b), MT(t) for L1 of LA-G fault on B.B.

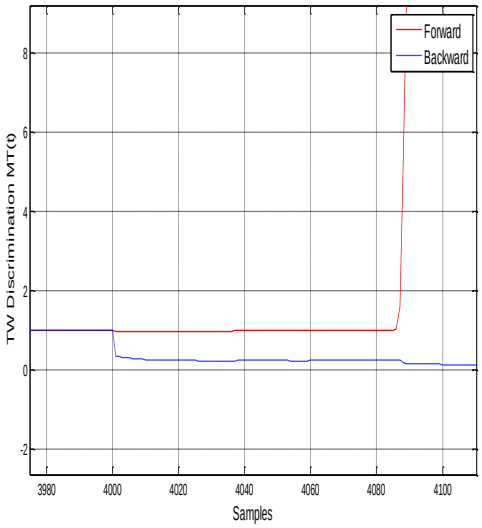

Figure 5.18(c), MT(t) for L2 of LA-G fault on B.B.

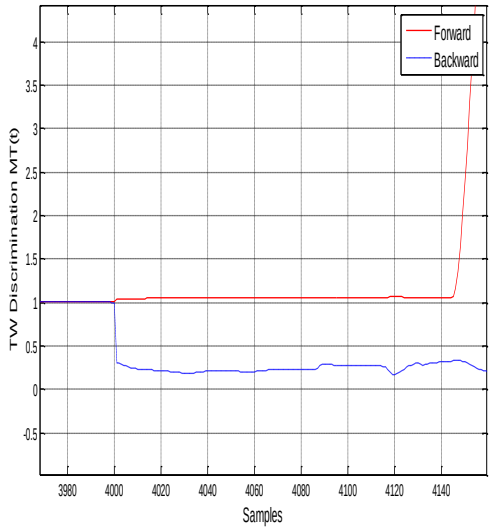

Figure 5.18(d), MT(t) for L3 of LA-G fault on B.B.

$$FT = \begin{vmatrix} 10.6552 & 0.9076 & 0.3665 \\ 4.9822 & 0.7108 & 0.2344 \\ 5.1484 & 0.8521 & 0.2470 \end{vmatrix} \qquad (5\text{-}18)$$

First item in column 1 is by far greater than its correspondent in the other 2 columns. Tf ≠ Tb for all 3 lines are unequal.

B) B.B L-G fault at inception in zero crossing point.

Figure 5.19(a,b,c & d) and Matrix 5-19 show the effect of applying phase A to ground fault on Cairo busbar. Fault inception angle is 0.045 and fault resistance is 10 ohm.

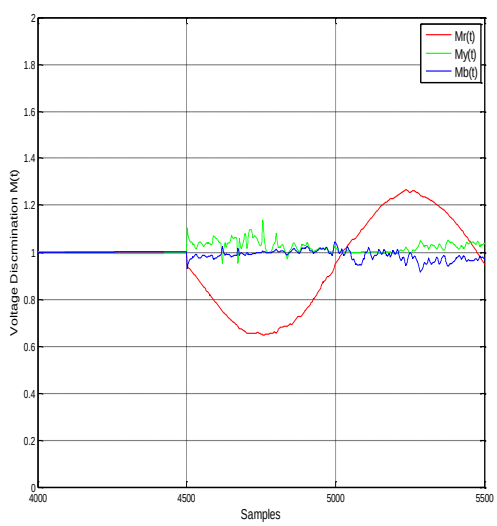

Figure 5.19(a), M(t) of LA-G fault on B.B.

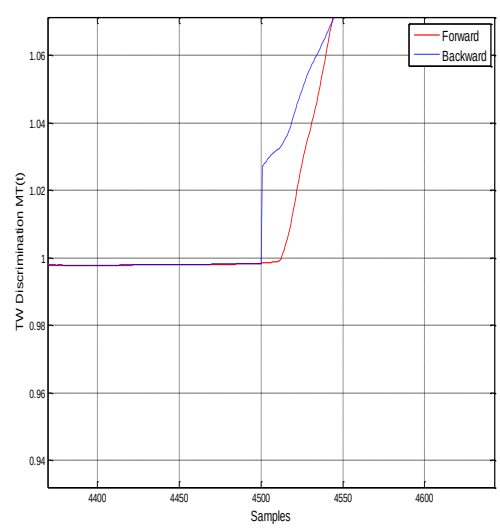

Figure 5.19(b), MT(t) for L1 of LA-G fault on B.B.

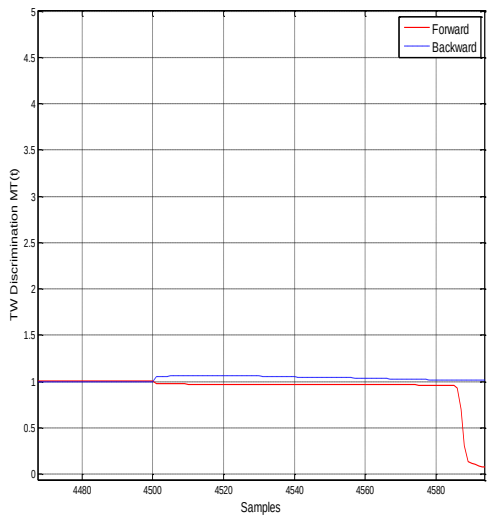

Figure 5.19(c), MT(t) for L2 of LA-G fault on B.B.

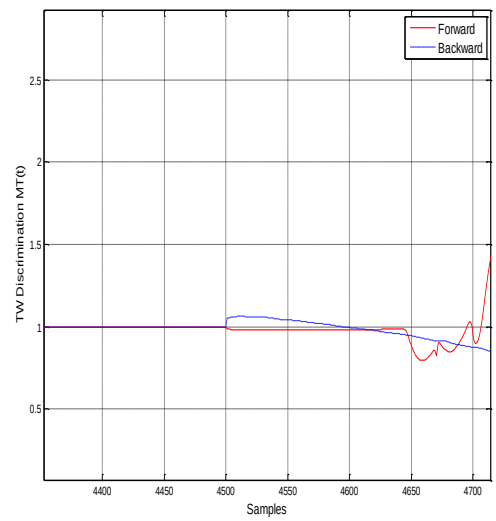

Figure 5.19(d), MT(t) for L3 of LA-G fault on B.B.

$$FT = \begin{vmatrix} 0.3718 & 0.0357 & 0.1340 \\ 0.4262 & 0.0098 & 0.1313 \\ 0.4121 & 0.0210 & 0.1556 \end{vmatrix} \qquad (5\text{-}19)$$

All items in column 1 is by far greater than their correspondent in the other 2 columns. Tf ≠ Tb for all 3 lines are unequal.

C) Line L-G fault at inception in peak point.

Figure 5.20(a,b,c & d) and Matrix 5-20 show the effect of applying phase A to ground fault in the middle of Cairo – Korimat line. Fault inception angle is 0.04 and fault resistance is neglected.

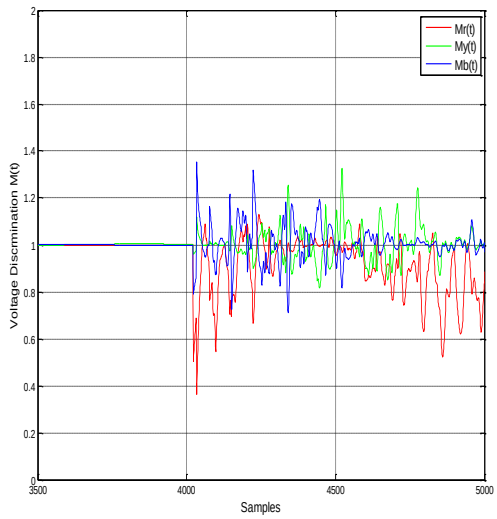

Figure 5.20(a), M(t) of LA-G fault on L2.

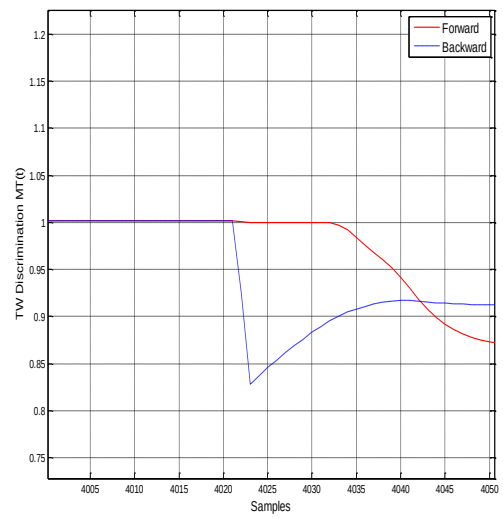

Figure 5.20(b), MT(t) for L1 of LA-G fault on L2.

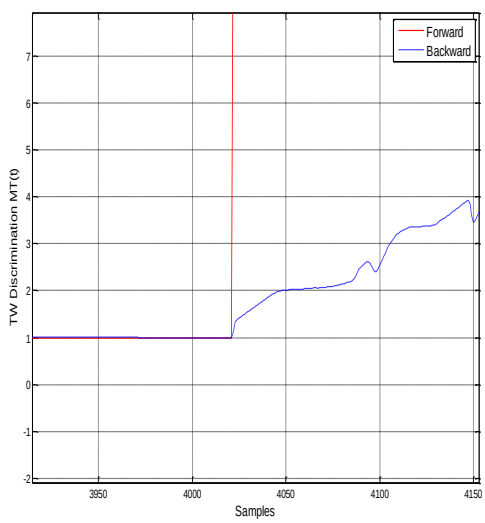

Figure 5.20(c), MT(t) for L2 of LA-G fault on L2.

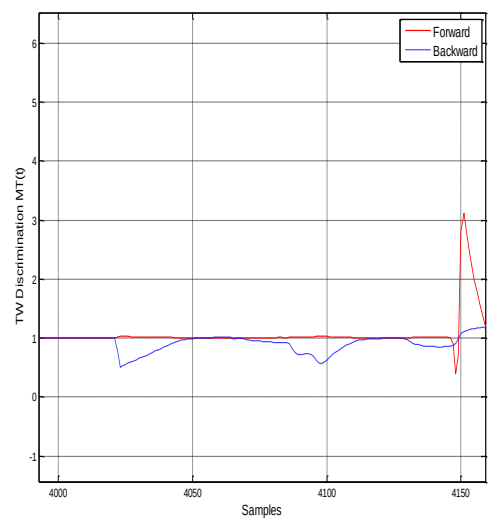

Figure 5.20(d), MT(t) for L3 of LA-G fault on L2.

$$FT = \begin{vmatrix} 0.0095 & 0.0593 & 0.0600 \\ 32.8044 & 0.0862 & 0.0989 \\ 0.0280 & 0.0201 & 0.0014 \end{vmatrix} \qquad (5\text{-}20)$$

Second item in column 1 is by far greater than its correspondent in the other 2 columns, however all items in columns 2 and 3 are almost similar. Tf_2 equals to Tb_2, but Tf_1 unequal to Tb_1, also Tf_3 unequal to Tb_3.

D) Line L-G fault at inception in zero crossing point.

Figure 5.21(a,b,c & d) and Matrix 5-21 show the effect of applying phase A to ground fault in the middle of Cairo – Korimat line. Fault inception angle is 0.045 and fault resistance is neglected.

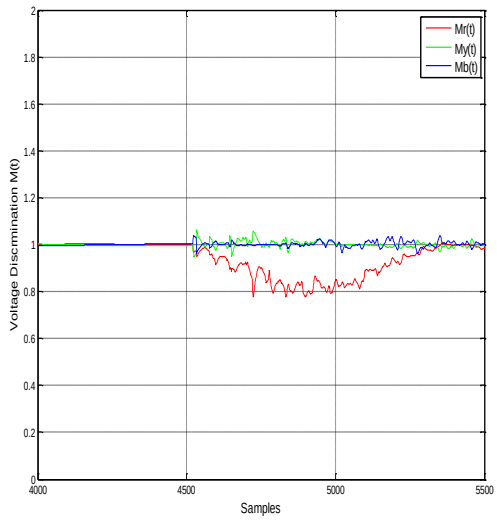

Figure 5.21(a), M(t) of LA-G fault on L2.

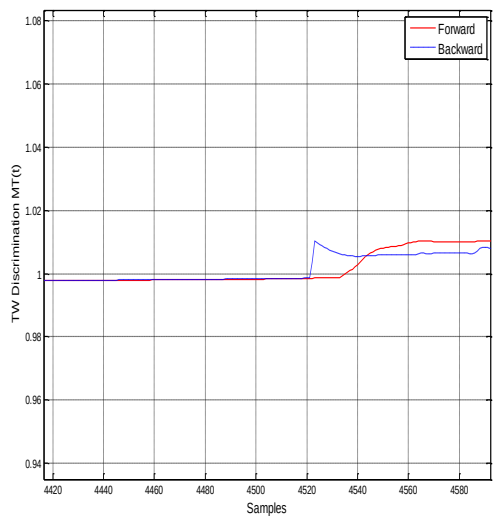

Figure 5.21(b), MT(t) for L1 of LA-G fault on L2.

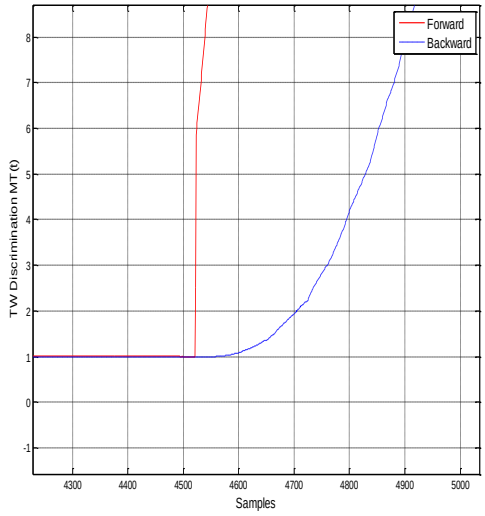

Figure 5.21(c), MT(t) for L2 of LA-G fault on L2.

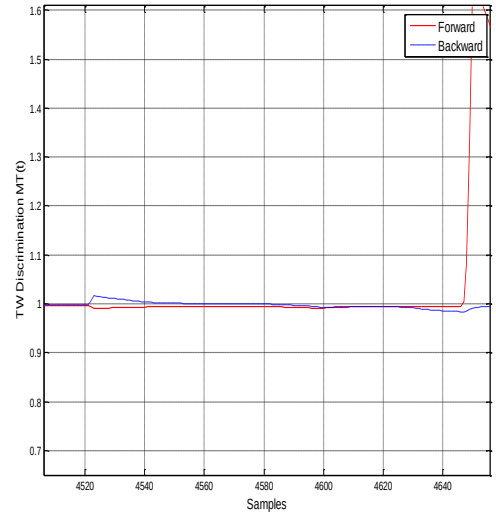

Figure 5.21(d), MT(t) for L3 of LA-G fault on L2.

$$FT = \begin{vmatrix} 0.0443 & 0.0632 & 0.0570 \\ 72.8323 & 0.0777 & 0.0953 \\ 0.0053 & 0.0105 & 0.0058 \end{vmatrix} \qquad (5\text{-}21)$$

Second item in column 1 is by far greater than their correspondent in the other 2 columns. Tf_2 equal to Tb_2, but Tf_1 unequal to Tb_1 also Tf_3 unequal to Tb_3. It is quite obvious that the travelling wave detected in the zero crossing point faults is minimal.

5-5 Summary:

A certain network was chosen carefully and simulated using its actual parameters by ATP software. Variables like fault type, fault location, fault inception angle and fault resistance were changed in each time then cases were studied and results were generated.

It was proved that applying all 3 techniques in certain cascading gives the opportunity to detect the fault condition and have entire details on it such as fault occurrence exact moment, fault type and location yet, some problems appears while simulating faults in zero crossing points where the travelling waves signal drops to minimal level. This defect can cause troubles in the relay sensitivity.

In the next chapter all tools are going to be experimentally tested on a lab model to check to how extend those techniques are applicable in reality.

Chapter 6 Practical Relay Application Over a Lab Model

5-1 Introduction

In this chapter a practical application for the new suggested relay is presented, where a 380 V lab model is simulating an actual 500 KV network, EHV transmission line is used. The model consists of identical PI-sections, where each section represents a transmission line of 25 Km long, a 380 V three phase balanced source is used as a supply and a three phase induction motors with a gear box is representing a dynamic load. The line mutual coupling for both inductance and capacitance are considered.

A terminal node in the line model is representing a distribution busbar where the source will be connected to it to feed the motors located in the other terminal of the transmission line.

Analysis will be held on both transmission line and busbar in healthy case and also during fault that can be applied on the model.

Such experiment aims to investigate practically the capability of the suggested relay to detect the fault instant accurately besides confirming the fault type and it's location in the network.

6-2 Lab model structure

Figures 6-1 (a) and (b) show photographic images of the whole lab model, and the DAQ card used, while Figure (6-2) explains the connection of the equipments. A three phase induction motor is being used as a load, the single

ended three phase current and voltage signals are fed via calibrated current and voltage transformers to a high speed interface card at a sampling frequency of 10 KHz, while The protection techniques is executed using Lab-View [38] [App.E].

Figure6-1(a), 380 V lab model for 500 KV Transmission line

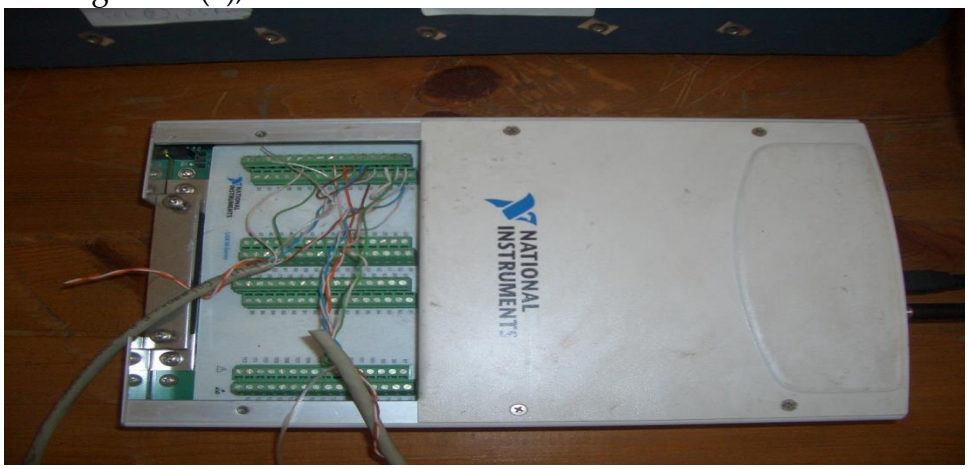

Figure6-1(b), NI-Interface card used in Lab

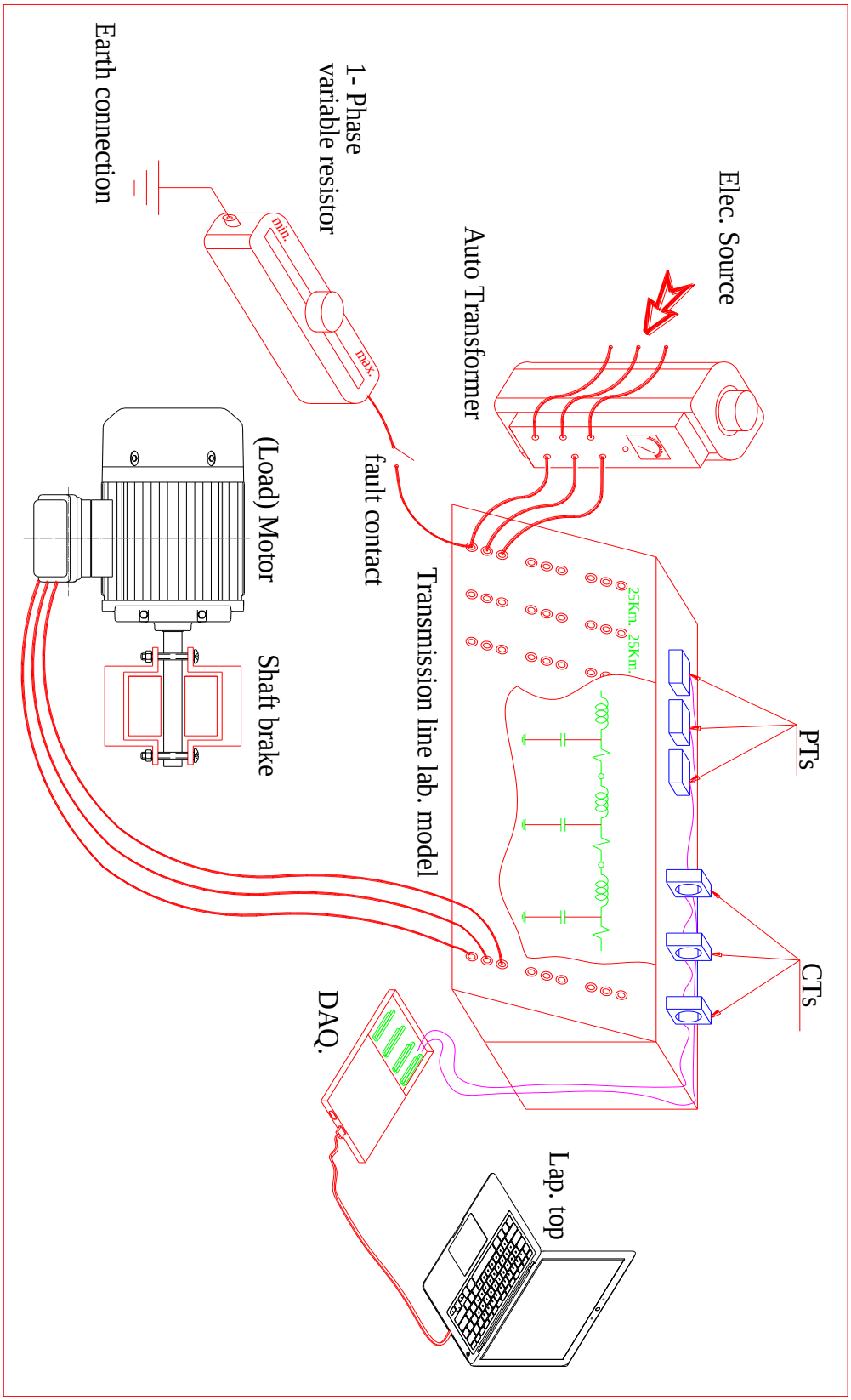

Fig. 6-2, Equipments connection.

6-2-1 Normal Operation

Voltage of the phase under investigation (phase A) together with its complementary generated wave were plotted against time of five complete cycles in figure 6-3(a) where the red plot represents received actual phase voltage and the black plot represents the created complementary signal.

Three phase currents detected were plotted in figure 6-3(b) against the same scale used with voltage. Also the unity discrimination signal resulting from applying the programmed Cos-Sin protection technique was demonstrated in figure 6-3(c).

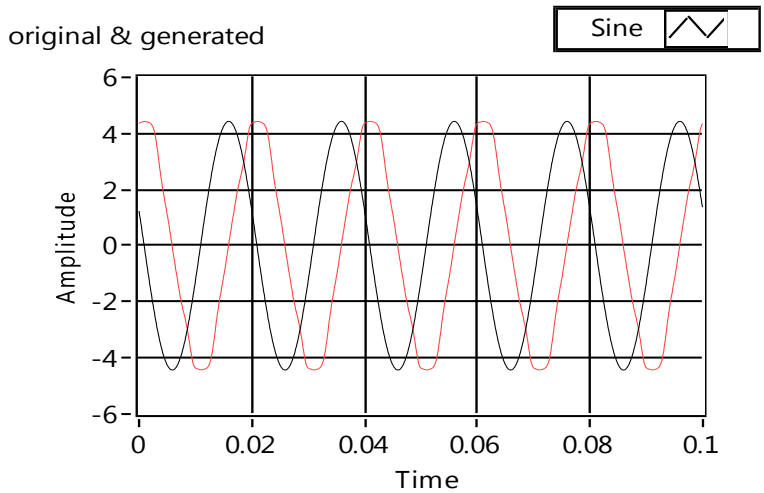

Figure 6-3(a), Input phase voltage and complementary generated signal during normal conditions.

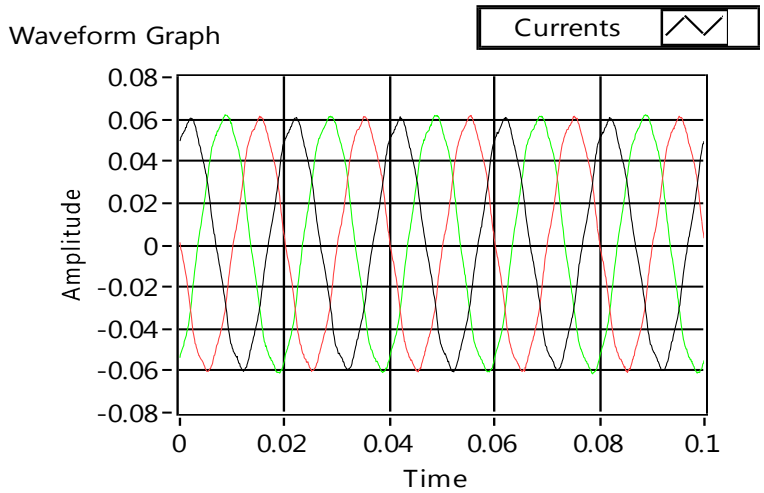

Figure 6-3(b), System 3 phase current signal during normal conditions.

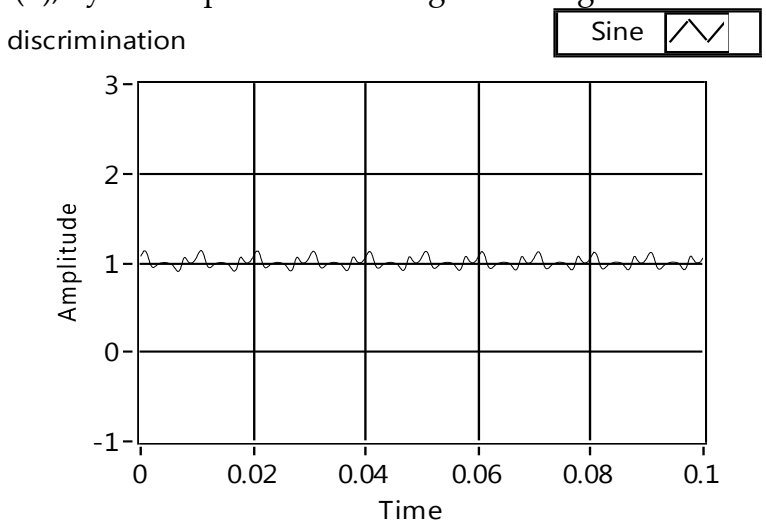

Figure 6-3(c), Discrimination signal resulting from applying the Cos- Sin technique.

Sampling error, load nature and bad source waveform cause that ripples that appears in the unity signal shown in figure 6-3(c), yet the discrimination signal keep oscillating around the value of one which means that in normal cases the average of discrimination signal is almost unity.

To overcome such oscillation appears in real modeling the threshold value should be adjusted to accommodate that ripples therefore limits of values 0.8 and 1.2 is used.

6-2-2 Fault conditions

The proposed technique was tested during a SLG fault applied on phase A. The fault was imposed on two different locations to examine the suggested discrimination technique that its results are going to be shown discussed in the next section.

6-2-2-1 Busbar fault

Fault first location was chosen on the point where source is feeding the transmission line model and then the load in a way that this node fault represents the busbar fault. The Cos-Sin tool was examined during the bus failure, where the phase voltage and generated signals are shown in red and black in Figure 6-4(a) respectively whereas the corresponding discrimination signal is introduced in figure 6-4(b).

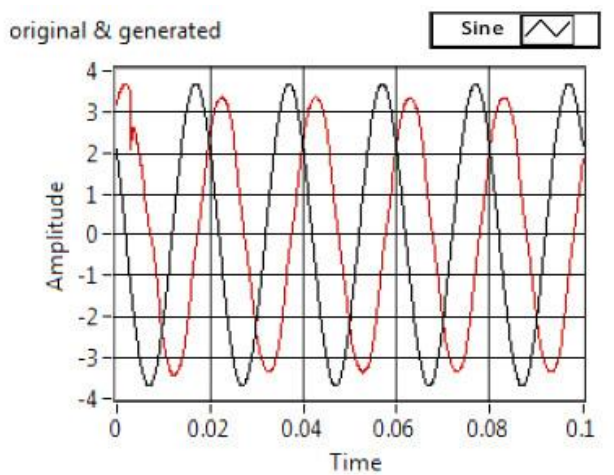

Figure 6-4(a), Input phase voltage and complementary generated signal during busbar fault conditions.

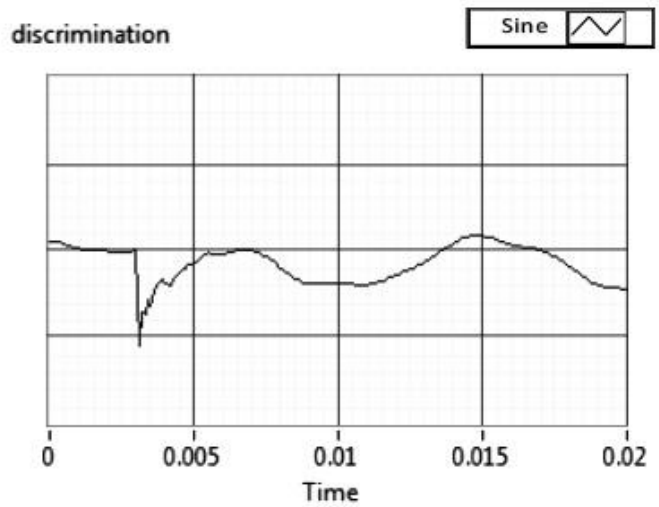

Figure 6-4(b), Discrimination signal resulting from busbar fault.

It appears clearly from the above graphs that after the fault moment the discrimination signal deviated from unity severely following the mismatch happened between the original detected phase voltage and the generated with 90° degree shifted signal. Average value over a one complete cycle is by far less than one unlike the mere cycle average computed before the fault instant with healthy conditions where it produces unity value.

6-2-2-2 Line fault

The other fault location was selected at a certain point on the transmission line model that is far by 50 km away from the first one. The Cos-Sin tool was checked again during that line point failure, where the phase voltage and generated signals are shown in red and black in Figure 6-5(a) respectively whereas the corresponding discrimination signal is introduced in figure 6-5(b).

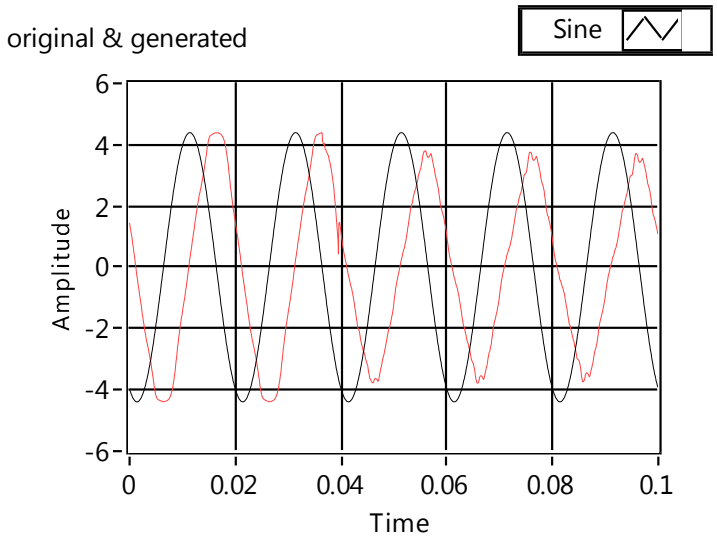

Figure 6-5(a), Input phase voltage and complementary generated signal during line fault conditions.

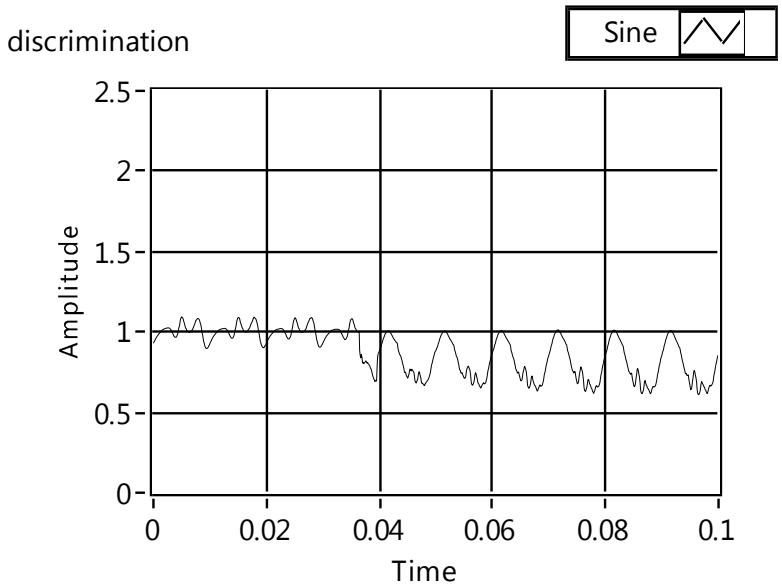

Figure 6-5(b), discrimination signal resulting from line fault.

From the above graphs it is obvious that both voltage and discrimination curves of line fault have the same behavior to that of busbar. Same deviation with almost similar characteristics happened that might cause a confusion in the fault location, therefore a supplementary criteria that is utilizing travelling wave

phenomena was practically tested to discriminate and identify the location of the fault.

6-2-3 Practical modeling for fault discrimination criteria

This modeling required a separate program on the lab view to extract the forward and backward travelling waves, apply the proposed technique on them and plot the resultant graphs. Graphs were captured in no fault condition and in different fault locations in order to represent the effect of each.

6-2-3-1 No fault

Figure 6-6 represents extracted travelling waves after implementing the proposed protection technique in normal case where the forward and backward processed signals are shown in red and black respectively, they were plotted against five complete cycle's time.

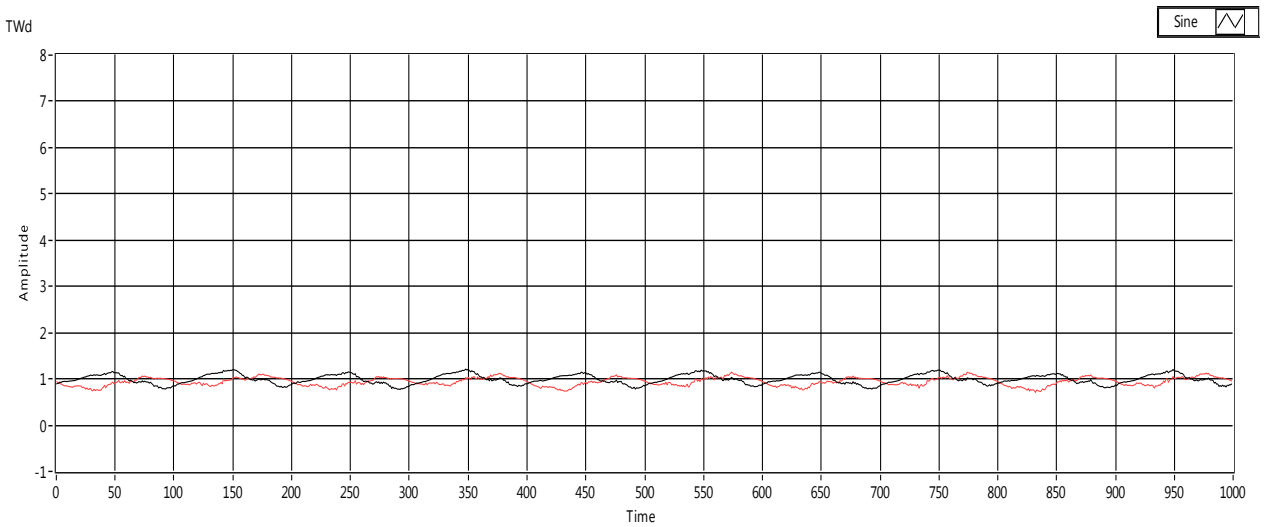

Figure 6-6, Forward and backward graphs of processed traveling wave in no fault condition.

The graph shows that despite the little fluctuations appeared, both plots stuck around unity.

6-2-3-2 fault condition

Figure 6-7 (a) & (b) represent the travelling wave signals after applying the discrimination protection technique steps during the fault moments forward and backward processed signals are shown in red and black respectively, they were plotted against five complete cycle's time. Figure 6-7(a) related to the fault happened 50 km away from the busbar where the measuring equipment are connected while figure 6-7(b) belongs to a fault occurred on the bar it self . Both forward and backward processed signals are shown in red and black respectively and they were plotted against five complete cycle's time.

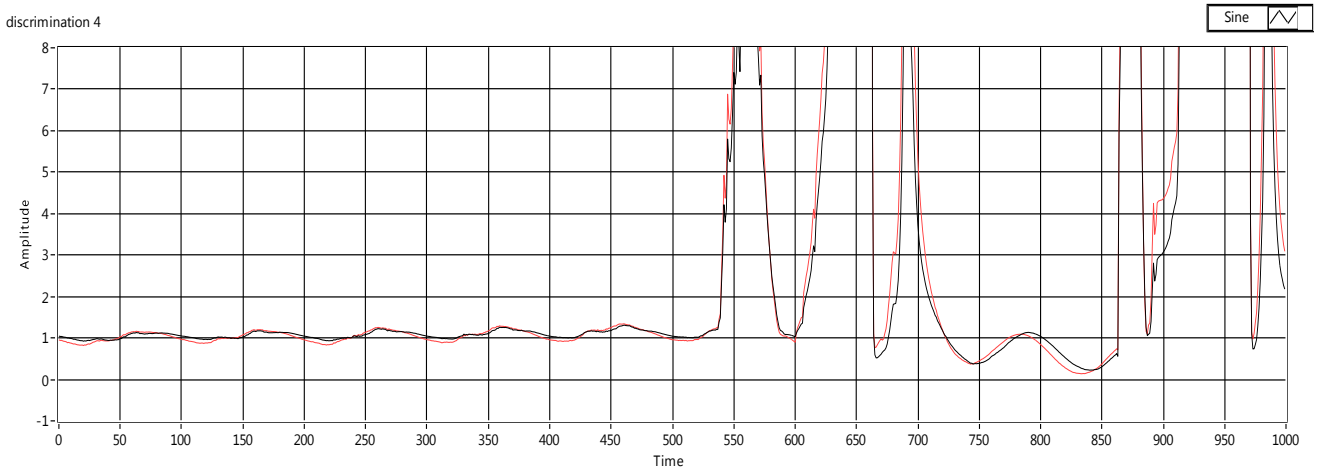

Figure 6-7(a), Forward and backward graphs of processed traveling wave in transmission line fault.

The graph shows that, at the exact moment of fault both plots deviate together severely from unity.

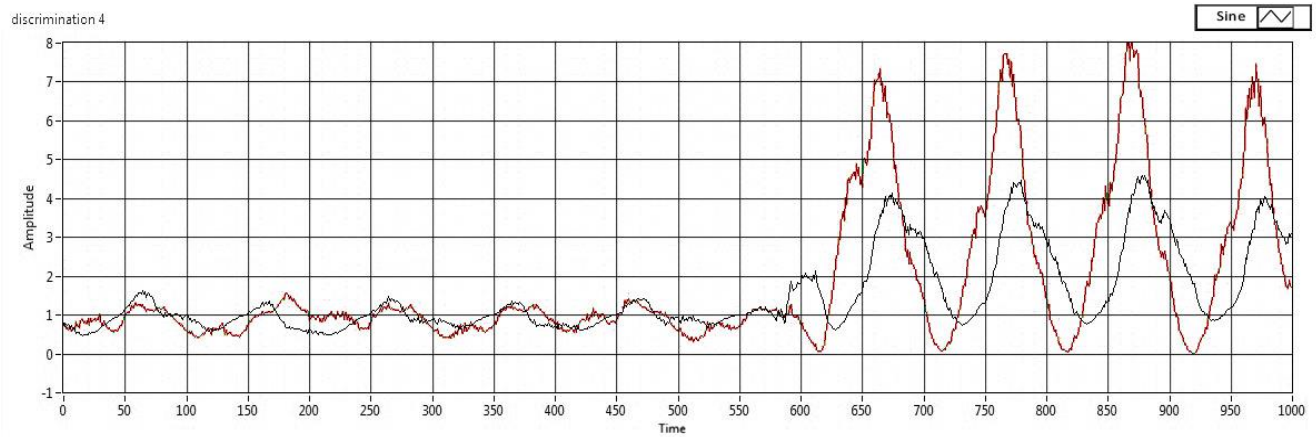

Figure 6-7(b), Forward and backward graphs of processed traveling wave in busbar fault.

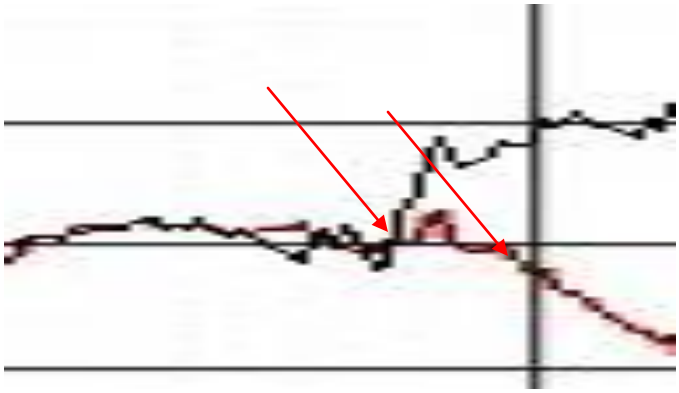

The graph shows that, at the fault, both plots deviate separately from unity.

To sum up, it appears clearly from the above graphs that just after the fault moment the forward and back ward processed travelling waves deviate heavily from the unity state and that happens wherever the fault locate however, no shift between the drifting moments of the curves was noticed when the fault occurs on the transmission line and on the other hand, a remarkable shift was found when the fault hit the busbar which provide a clear discrimination indicator and refer to the fault location precisely.

6-3 Conclusion

In this chapter, the fault detection and discrimination criterion discussed and applied in previous chapters were practically executed on a 380 V experimental lab model, this practical execution showed farther success, where the following points are concluded

- Proposed Cos-Sin protection Technique could be practically used as a tool for fault detection in EHV busbar.
- The application of fault discrimination feature is a powerful, simple and successful feature for fault discrimination.
- The application of such techniques is simple and needs no complicated interfacing as we can use a quite low sampling frequency (10 KHz).

In the next few pages an overall conclusion for applying the above mentioned protection tools is introduced, the contribution of the new technique is shown and further work suggestions are given.

Chapter 7 CONCLUSION

7.1 Conclusions and contributions

In the previous discussed chapters some protection techniques were explained in details. The operating sequence of such techniques produced a new suggested digital relay then the outgoing of the performance of that relay during simulation steps were clearly shown in both tabulated results and output waveforms. In this chapter, conclusions derived from analyzing the outcome results are presented.

The thesis's targets are to introduce a relay that fits mainly EHV networks and is specialized in protecting the grid busbars.

The suggested relay is connected to the busbar itself so that it can monitor the bus voltage accurately and follow any change happened, it also connected to all the transmission lines attached to that busbar via current transformers and by that it can perform its criteria in a certain sequence.

No matter the number of transmission lined connected to the bus or their lengths, the proposed digital relay was found to be capable of doing the protection assignment needed as the following:

- The relay manage to detect the fault presence
- The relay is able to identify the faulted phases.
- It can easily provide the exact fault type that occurred in the network.

- The relay succeeds in discriminating between faults that happened on the busbars to those located on the transmission lines even in the cases with a very closed transmission line faults.

Thesis contribution can be stated as the following:

1. Highlight the (Cos-Sin) tool that can detect and utilize high frequency transient components associating fault conditions to identify fault presence. The suggested tool has the advantages of being simple, needs no complex mathematical equations and can be safely applied to both the voltage and current signals besides any signal that may arise from any combination of both signals.
2. The (Cos-Sin) tool was successfully applied in EHV small network as it was tested on both transmission lines and busbar. The output result, waveforms and averages were plotted and tabulated.
3. The proposed tool is reinforced by extra two supplementary techniques that are based on Cos-Sin concept as well. The whole three criteria mentioned below furnish convenient protection reliability when operating in certain sequence where they reform the proposed digital relay.
    - Fault Detection Criterion detects fault presence and determines the faulted phases by using a discriminating signal M(t) and a threshold ζ that is controlled by relay user to adopt with incoming signal ripples.
    - Fault Analysis Criterion determines the faulted line and fault type by using a new discriminating signal Mi(t)and its average deviation value δMi(t) over a certain period which was optimized in this thesis as one complete cycle.

- Fault Discrimination Criterion uses the concept of traveling Waves theory to determine the faulted Line and busbar faults, that is done by determining the deviating instants of both the forward and backward signals, given by MTf(t) and MTb(t)respectively, it is used mainly to detect busbar faults and to avoid wrong decisions that may appear in the previous criterion due to far end faults through high resistances.

4. The proposed digital relay that is applied to the Egyptian unified 500 KV system proved its capability of protecting Cairo busbar against all type of faults. It managed in determining the type of fault and the faulted phases accurately.
5. The digital relay succeeded also in sensing faults that located on the transmission lines attached to monitored busbar and despite the presence of multi lines with various lengths, the relay is able to tell which line is defected. It also can discriminate between busbar fault and very closed line faults which is very difficult due to the similarity in their effects.
6. A practical application for the suggested relay is presented using a transmission line lab model with 500 KV network parameters and analysis held on both transmission line and busbar in healthy and fault cases proved the capability of the suggested relay to detect the fault instant accurately besides confirming the fault type and it's location in reality.

7.2 Future work

Based on the work implemented in this dissertation, the future recommended research topic can include the possibility of obtaining a protective relay package that can be safely used with EHV transmission networks

depending on the new suggested Cos-Sin tool. Also application of such method on protecting other electrical equipments such as rotating machinery or transformers is valid.

References

[1]. Harjinder Singh Sidhu, *"High Speed Digital Protection of EHV Transmission Lines Using Traveling Waves"*, Thesis (M.Sc.), University of Saskatchewan, 2004.

[2]. Mladen Kezunovic, *"The Electrical Engineering Handbook-9.Fundamentals of Power System Protection"*, Department of Electrical Engineering, Texas A & M University, College Station, Texas, USA, 2005.

[3]. Alireza Tavakoli Ghainani, "*Digital Protection Scheme for Distance Relaying of a Six-Phase Power System*", Thesis (Ph.D.), University of Teknologi, Malaysia, 2010.

[4]. Ashraf Ibrahim Megahed, "*Neural Network Based Digital Differential Relay for Synchronous Generator*", Thesis (Ph.D.), University of Calgary, Alberta, 1998.

[5]. Sunil S Rao, *"Switch Gear and Protection"*, 10th edition 1992.

[6]. Levi Portillo Urdaneta, *"A Methodology for Performance and Compatibility Evaluation of an All-Digital Substation Protection"*, Thesis (M.Sc.), Texas A & M University, 2006.

[7]. J. Lewis Blackburn, Thomas J. Domin, *"Protective Relaying Principles and Applications-10.Busbar Protection", Third Edition, 2006.*

[8]. Alstom guide, *"Network Protection and Automation Guide", 2011.*

[9]. Abdelsalam Mohamed Elhaffar, *"Power Transmission Line Fault Location Based on Current Traveling Waves"*, Thesis (Ph.D.), Helsinki University of Technology, 2008.

[10]. Daw Saleh Sasi Mohammed, *"Travelling Wave Method for Transmission System Fault Location"*, Thesis (M.Eng.), Universiti Teknologi Malaysia, 2009.

[11]. L.G Weiss, *"Wavelet and Wideband Correlation Processing"*, IEEE PS magazine Vol 11, January 1994, pp 13-32.

[12]. A.P.Sakis Meliopoulos, Chien-Hsing Lee, *" An Alternative Method for Transient Analysis via Wavelets"*, IEEE transactions on power delivery, vol. 15, no. 1, january 2000, pp 114-121.

[13]. L.C.W.Frerk, *"Power System Protection-13. Busbar Protection", Volume 3, 1995.*

[14]. Daniel Nack, *"Reliability of Substation Configurations- Typical Bus Configurations",* Iowa State University, 2005.

[15]. Les Hewitson, Mark Brown, Ben Ramesh, *"Practical Power Systems Protection-16. Switchgear (busbar) protection", 2004.*

[16]. A.K. Raja, Amit P. Srivastava, Manish Dwivedi, *"Power Plant Engineering-12.Busbar protection", 2006.*

[17]. Y.C. Kang, S.H. Kang and P.A. Crossley, *"Design, Evaluation and Implementation of a Busbar Differential Protection Relay Immune to the Effects of Current Transformer Saturation"* IEE Proc.-Gener. Transm. Distrib., Vol. 151, No. 3, pp. 305-312 May 2004.

[18]. Y.C. Kang, J.S. Yun, B.E. Lee, S.H. Kang, S.I. Jang and Y.G. Kim, *"Busbar Differential Protection in Conjunction with a Current Transformer Compensating Algorithm"*, IET Gener. Transm. Distrib., 2008, 2, (1), pp. 100 –109.

[19]. Mohamed E. El-Hawary , *"Electrical Power Systems ,Design and Analysis-9. Busbar Protection" ,Technical University of Nova Scotia,*1995.

[20]. C.Russel mason (General Electric guide), *"The Art and Science of Protective Relays-3. Protective Relay Types"*, 1956.

[21]. P. M. Anderson, *"Power System Protection, Power Math Associates, Inc.-16. Bus Differential Protection"*, 1999.

[22]. ME Masoud,E H Shehab El-din and Mostafa Eissa , *"Power System Protection",* Helwan university,2012.

[23]. David W. P. Thomas, Ricardo J. O. Carvalho and Elisete T. Pereira, "Fault *Location in Distribution Systems Based on Traveling Waves",* Bologna PowerTech. Conferece, 2003.

[24]. D.C. Idoniboyeobu, P. O. Ohiero, *"High Speed Protection of Extra High Voltage (EHV) Transmission Lines Using Digital Traveling Waves",* International Journal of Academic Research, vol.3. no.5, Sep., 2011, pp. 430-438.

[25]. M.E. Masoud, E.H. Shehab El_din and Ali M. El-Rifaie *" A new transient detection tool for extra high speed relays"* , MEPCON 2003.

[26]. M.E. Masoud, E.H. Shehab El_din and Ali M. El-Rifaie *" A New Supervising Relay for Extra High Voltage Transmission Lines Protection "* , MEPCON 2003.

[27]. Egyptian Electrical Authority , *"Annual Report of Electrical Statistics*", 2010-2011, Cairo, Egypt.

[28]. Alternating Transient Program (ATP) help, Version 2010.

[29]. Ali M. El-Rifaie, *"A Supervising Relay for Extra High Voltage Transmission Networks"*, Thesis (M.Sc.), Helwan University, 2003.

[30]. Vajira Pathirana, *"A Power System Protection Scheme Combining Impedance Measurement and Travelling Waves"*, Thesis (Ph.D.), The University of Manitoba, Canada, 2004.

[31]. L.M. Wedepohl *" Application of Matrix Method to the Solution of Travelling Wave Phenomena in Polyphase Power Systems"* Proc. IEEE, Vol.110, PP 2200-2216, 1963.

[32]. Xinzhou Dong, Shiyong Wang, Shenxing Shi, *"Research on Characteristics of Voltage Fault Traveling Waves of Transmission Line"*, Modern Electric Power Systems, Wroclaw, Poland, 2010.

[33]. Abdelsalam Elhaffar, Matti Lehtonen, *"Multi-End Traveling Wave Fault Location Based on Current Traveling Waves"*, 16th PSCC, Glasgow, Scotland, July, 2008.

[34]. Cansın Y. Evrenoso˜glu, Ali Abur, *"Fault Location in Distribution Systems with Distributed Generation"*, 15th PSCC, Liege, August, 2005.

[35]. Darren Spoor, Jian Guo Zhu, *"Improved Single-Ended Traveling-Wave Fault-Location Algorithm Based on Experience with Conventional Substation Transducers",* IEEE transactions on power delivery, vol. 21, no. 3, pp 1714-1720,.july 2006.

[36]. Anuradha s Deshpande, Grishma S. Shah ,*" Transmission Line Protection based on Travelling Waves"*, WSEAS Transactions on circuits and systems, issue 12, volume 10, december 2011.

[37]. MatLab user's help, version R2008a, Mathworks Inc., 2008.

[38]. Software control of M series NI data acquisition card, Version 2010, National Instrumentation Incorporated.

Appendix [A]

Typical Line Configuration and Parameters

The parameters of the transmission line may be generally divided into two groups. Power frequency parameters, which are required in order to study load flow, system stability and fault levels. Higher frequency parameters, which are needed for studying the effect of striking voltage, switching and faults during the earliest time. The line geometrical configuration given in Figure A-1 of 500 KV tower and conductors such as tower height and width, arms lengths, ground wires and conductors geometry are shown in Table A-1, these parameters are fed to the EMTP line-constant program, the line constant program will provide us by both the capacitance matrix "C"(A-1), the impedance matrix "Z"(A-2),the impedance matrix for symmetrical parameters "Z\ "(A-3), and the transformation matrix "T"(A-4) which will be used in turns to estimate the line parameters such as resistance, inductance and capacitance for any specific frequency. In addition, the model parameters including characteristic impedance, wave velocity, wave attenuation are also given where their values where computed under a 50 HZ frequency value Table A-2 [29].

$$C = \begin{vmatrix} 1.759347\ E\text{-}08 & & \\ -2.601989E\text{-}09 & 1.798530E\text{-}08 & \\ -7.398215E\text{-}010 & -2.601989E\text{-}09 & 1.759347\ E\text{-}08 \end{vmatrix} \text{ Farads/ Mile (A-1)}$$

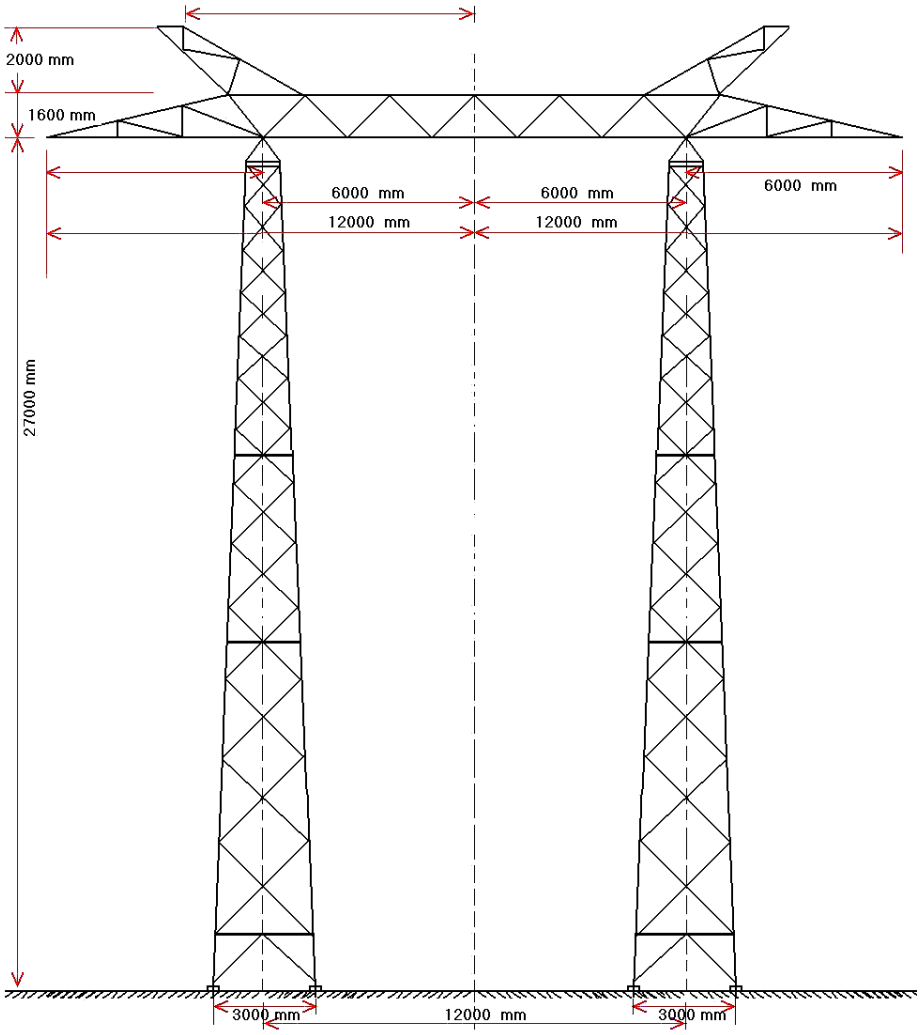

Figure A.1, Construction configuration of Egyptian

500 KV transmission line

Parameters	value
Skin Effect	0.5
Number of conductors per bundle	3
Resistance (ohm/mile)	0.1045
Conductor diameter (inches)	1.189
Height of the conductor at the tower (feet)	82.0
Height of the conductor at mid span (feet)	52.0
Horizontal conductor displacement (feet)	-39.4
Sub-conductor separation (inches)	15.7
Sub-conductor angle to horizontal (degrees)	30.0
Frequency (HZ)	50.0
Number of shield wires	2
Resistance of shield wire (ohm/mile)	0.1308
Diameter of shield wire (inches)	0.4331
Horizontal displacement of shield wire (feet)	-27.1
Height of the shield wire at the tower (feet)	100.4
Height of the shield wire at mid span (feet)	70.5
Earth resistivity (ohms-meter)	100.0

Table A.1, Input Data for Flat Line Constant program.

$$\mathbf{Z} = \begin{vmatrix} 0.07238262 + J\,0.6604298 & & \\ 0.0356379 + J\,0.1955710 & 0.07121915 + J\,0.6486030 & \\ 0.0343739 + J\,0.1427735 & 0.03563797 + J\,0.1955710 & 0.07238262 + J\,0.6604298 \end{vmatrix} \ \mathbf{\Omega} \text{ / Mile} \quad \text{(A-2)}$$

$$\mathbf{Z}^{\backslash}_{\substack{\mathbf{0}\\ \mathbf{1}\\ \mathbf{2}}} = \begin{vmatrix} 0.1442428 + J\,1.012431 & & \\ -0.01184339 - J\,0.006799 & 0.03328154 + J\,0.0206359 & \\ 0.0118047 - J\,0.006857 & 0.0367781 + J\,0.478515 & 0.0345120 + J\,0.018504 \end{vmatrix} \ \mathbf{\Omega} \text{ / Mile} \quad \text{(A-3)}$$

$$T = (1/3) \begin{vmatrix} 1.7457 & 1.7125 & 1.7457 \\ -2.1213 & 0.0000 & 2.1213 \\ -1.1130 & 2.5592 & -1.1130 \end{vmatrix} \qquad \text{(A-4)}$$

The model parameters provided by the constant line program are shown in table A-2.

Parameter	Zero Mode	Positive Mode
Surge Impedance(ohm)	486.3-j4.0039	278.4-j2.1975
Attenuation(db/mile)	1.27509E-03	5.74018E-04
Velocity (miles/sec)	1.49793E+05	1.82396E+05
Wavelength (miles)	2.99586E+03	3.64792E+03
Resistance (ohm/mile)	1.42428E-01	3.67782E-02
Reactance (ohm/mile)	1.01243E00	4.78516E-01
Susceptance(mho/mile)	4.32332E-06	6.19062E-06

Table 7.2, Model parameters of typical 500 KV transmission line.

Appendix [B]

Travelling waves equations

All conductors of a transmission line have resistances and inductances distributed uniformly along the length of the line. It is, however, assumed in most applications that the resistance and inductance of a conductor is lumped and is, therefore, replaced by a single value. This is also true for the conductance and capacitance of a conductor.

Transmission lines can not be analyzed with lumped parameters, when the length of the line is considerably small compared to the wavelength of the signal applied to the line. Power lines, which are more than 50 km long, are considered to have distributed parameters. These lines have the following properties:

1. Voltages and currents travel on the line.
2. The velocity of propagation of these waves is finite.

One meter sections of a power transmission line can be represented by the circuits shown in Figure E.1.

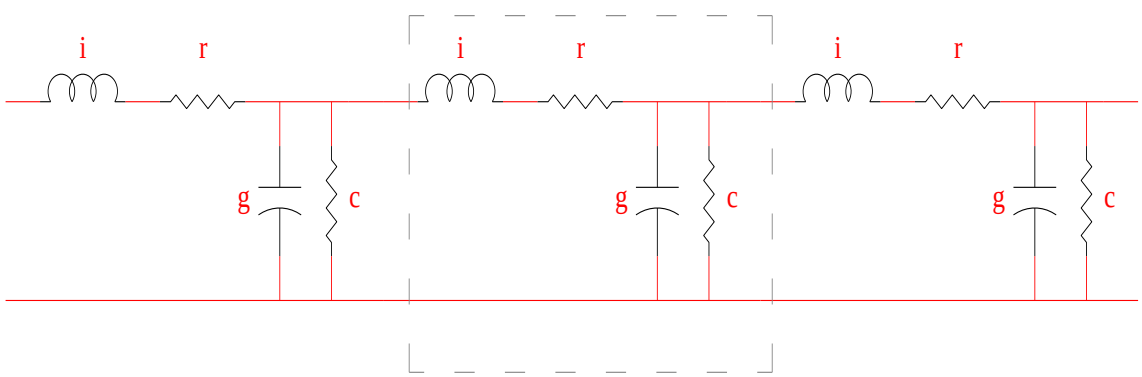

Figure B.1, Representation of transmission line.

Consider a small section of length, dx of a transmission line, as shown in Figure B.2 . Assume that resistance, inductance, capacitance and conductance remain constant along the length of the transmission line and do not change with time where $Z = r + j\omega l$ and $Y = g + j\omega c$.

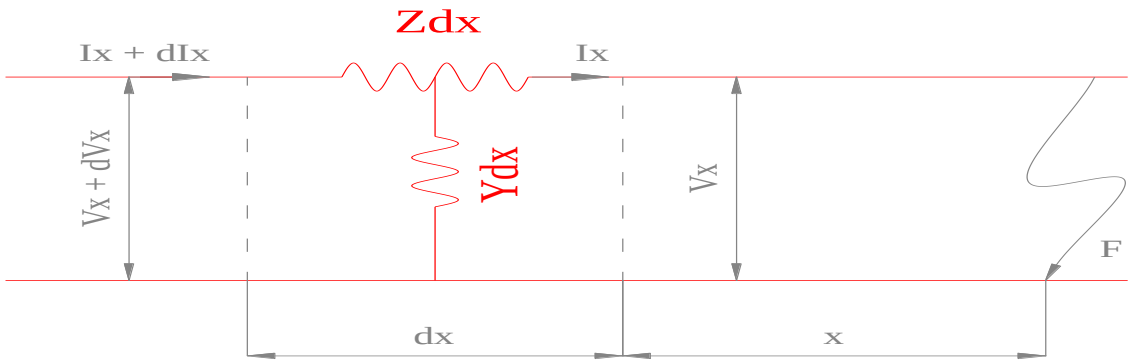

Figure B.2. Schematic diagram of a line increment.

The following differential relationships can be written across the elemental section:

$$dV_x = I_x \cdot Zdx \text{ or } dV_x / dx = ZI_x \qquad \text{(B-1)}$$

$$dI_x = V_x \cdot Ydx \text{ or } dI_x / dx = YV_x \qquad \text{(B-2)}$$

Differentiating Eq. (1) with respect to x

$$d^2V_x / dx^2 = Z \cdot dI_x / dx \qquad \text{(B-3)}$$

Substituting the value of dI_x / dx from Eq. (2) in Eq.(3),

$$d^2V_x / dx^2 = YZV_x \qquad \text{(B-4)}$$

This is a nonlinear differential equation whose general solution can be written as follows:

$$V_x = C_1 e^{\gamma x} + C_2 e^{-\gamma x} \qquad \text{(B-5)}$$

Where, $\gamma = \sqrt{YZ}$ $\gamma = \sqrt{}$ yz and is called as the propagation constant

C1 and C2 are arbitrary constants to be evolved.

Differentiating Eq. (5) with respect to x,

$$dV_x / dx = C_1 \gamma e^{\gamma x} + C_2 \gamma e^{-\gamma x} = ZI_x \qquad \text{(B-6)}$$

$$I_x = (C_1 / Z_o) e^{\gamma x} + (C_2 / Z_o) e^{-\gamma x} \qquad \text{(B-7)}$$

Where, $Z_o = \sqrt{Z/Y}$ and is called as the characteristic impedance of the line and is given as:

$$Z\circ = \begin{vmatrix} 500.0 & 0.0 & 0.0 \\ 0.0 & 280.0 & 0.0 \\ 0.0 & 0.0 & 280.0 \end{vmatrix} \Omega$$

The constants C1 and C2 may be evaluated by using the end conditions, i.e. when x = 0, *V*x = *V*f and *I*x =*I*f.

Substituting these values in Eqs (5) and (7) gives,

$$V_f = C_1 + C_2 \qquad \text{(B-8)}$$

$$I_f = (C_1 + C_2) / Z_o \qquad \text{(B-9)}$$

Which upon solving yield

$$C_1 = (V_f + Z_o I_f) / 2 \qquad \text{(B-10)}$$

$$C2 = (V_f + Z_o I_f) / 2 \qquad \text{(B-11)}$$

Where,*V*f and *I*f are post fault voltage and current respectively.

Substituting the values of C1 and C2 in Eqs (5) and (7) gives,

$$V_x = ((V_f + Z_o I_f)/2) e^{\gamma x} + ((V_f - Z_o I_f)/2) e^{-\gamma x} \qquad \text{(B-12)}$$

$$I_x = ((V_f / Z_o + I_f)/2) e^{\gamma x} + ((V_f / Z_o - I_f)/2) e^{-\gamma x} \qquad \text{(B-13)}$$

Now, γ is a complex number which can be expressed as:

$$\gamma = \alpha + j\beta \qquad \text{(B-14)}$$

Where,

α = attenuation constant

β = phase constant

Hence, instantaneous value of *V*x (t) can be written as,

$$V_x = \left(\left(V_f + Z_o I_f\right)/2\right)e^{\alpha x}e^{j(\omega t+\beta x)} + \left(\left(V_f - Z_o I_f\right)/2\right)e^{-\alpha x}e^{-j(\omega t+\beta x)} \quad \text{(B-15)}$$

Similarly, *I*x (t) can be written as,

$$I_x = \left(\left(V_f / Z_o + I_f\right)/2\right)e^{\alpha x}e^{j(\omega t+\beta x)} + \left(\left(V_f / Z_o - I_f\right)/2\right)e^{-\alpha x}e^{-j(\omega t+\beta x)} \quad \text{(B-16)}$$

Eqns.(15 & 16) are the travelling wave equations at any point on the line at a distance x from the fault point. Now *V*x consists of two terms each of which is a function of two variables– time and distance. Thus they represent two travelling waves, i.e.

$$V_x = V_f + V_b \quad \text{(B-17)}$$

Where,

$V_f = \left(\left(V_f + Z_o I_f\right)/2\right)e^{\alpha x}e^{j(\omega t+\beta x)}$ and is called as forward travelling voltage wave.

$V_b = \left(\left(V_f - Z_o I_f\right)/2\right)e^{-\alpha x}e^{-j(\omega t+\beta x)}$ and is called as backward travelling voltage wave. Similarly,

$$I_x = I_f + I_b \quad \text{(B-18)}$$

Where,

$I_f = \left(\left(V_f / Z_o + I_f\right)/2\right)e^{\alpha x}e^{j(\omega t+\beta x)}$ and is called as forward travelling current wave.

$I_b = \left(\left(V_f / Z_o - I_f\right)/2\right)e^{-\alpha x}e^{-j(\omega t+\beta x)}$ and is called as reverse travelling current wave. Hence using the above equations, forward and backward travelling waves for all phases can be found.

Using the transformation, forward and backward travelling waves of three phases are being transformed into $0\ \alpha\ \beta$ modal components.The transformation is given as:

$$\left[V_{0\alpha\beta}\right] = \left[K\right]\cdot\left[V_{abc}\right] \qquad \text{(B-19)}$$

and

$$\left[I_{0\alpha\beta}\right] = \left[K\right]\cdot\left[I_{abc}\right] \qquad \text{(B-20)}$$

Where $K = (1/3)\begin{vmatrix} 1.0 & 1.0 & 1.0 \\ 1.5 & 0.0 & -1.5 \\ 0.5 & -1.0 & 0.5 \end{vmatrix}$

As the voltage at any point on the line is addition of forward and reverse travelling waves, voltage at any point on a 3-Φ transmission line is:

$$V_0 = V_0^f\left(x - v_0 t\right) + V_0^b\left(x - v_0 t\right) \qquad \text{(B-21)}$$

$$V_\alpha = V_\alpha^f\left(x - v_1 t\right) + V_\alpha^b\left(x - v_1 t\right) \qquad \text{(B-22)}$$

$$V_\beta = V_\beta^f\left(x - v_1 t\right) + V_\beta^b\left(x - v_1 t\right) \qquad \text{(B-23)}$$

And current on 3-Φ transmission line is:

$$I_0 = I_0^f + I_0^b \qquad \text{(B-24)}$$

$$I_\alpha = I_\alpha^f + I_\alpha^b \qquad \text{(B-25)}$$

$$I_\beta = I_\beta^f + I_\beta^b \qquad \text{(B-26)}$$

The discriminant function Wf and Wb associated with the forward and backward waves will be uses as the forward and backward relaying signals in the travelling wave relay where,

$$W^f = V_{0\alpha\beta} + I_{0\alpha\beta} Z_o \qquad \text{(B-27)}$$

$$W^b = V_{0\alpha\beta} - I_{0\alpha\beta} Z_o \qquad \text{(B-28)}$$

V and I are the modal voltages and currents (0, α or β components) at the relay location.

Appendix [C]

Mat-Lab Program

```
Load ATP matrix(a);

%%%%%%%%%%%%%%%%%%%
%VOLTAGE ALGORITHM%
%%%%%%%%%%%%%%%%%%%

aver=abs(a(:,2));
avey=abs(a(:,3));
aveb=abs(a(:,4));

Or=find(min(aver(1:1000))==(aver(1:1000)));
Oy=find(min(avey(1:1000))==(avey(1:1000)));
Ob=find(min(aveb(1:1000))==(aveb(1:1000)));
i=0:(length(a)-2);

% plot(a(:,1),a(:,2)','r',a(:,1),a(:,3)','y',a(:,1),a(:,4)','b')
% grid
% pause

shftr=(a(Or,1)-.02/4);
shfty=(a(Oy,1)-.02/4);
shftb=(a(Ob,1)-.02/4);

ar=sign(a(2,2)-a(1,2));
br=sign(shftr);
ay=sign(a(2,3)-a(1,3));
by=sign(shfty);
ab=sign(a(2,4)-a(1,4));
bb=sign(shftb);

for m=1:10000;
 if ar==br;
     Vdashr(m)=sin(2*pi*50*(m*0.00001-shftr));
 elseif ar~=br;
     Vdashr(m)=-sin(2*pi*50*(m*0.00001-shftr));
 else
 end

 if ay==by;
     Vdashy(m)=sin(2*pi*50*(m*0.00001-shfty));
 elseif ay~=by;
     Vdashy(m)=-sin(2*pi*50*(m*0.00001-shfty));
 else
 end

 if ab==bb;
     Vdashb(m)=sin(2*pi*50*(m*0.00001-shftb));
 elseif ab~=bb;
```

```
     Vdashb(m)=-sin(2*pi*50*(m*0.00001-shftb));
 else
 end
end



MXr=max(a(1:2000,2));
MXy=max(a(1:2000,3));
MXb=max(a(1:2000,4));

Vgenr=Vdashr'.*MXr;
Vgeny=Vdashy'.*MXy;
Vgenb=Vdashb'.*MXb;

% figure
%
plot(i',a((1:10000),2),'r',i',Vgenr,'c',i',a((1:10000),3),'y',i',Vgeny,
'g',i',a((1:10000),4),'b',i',Vgenb,'k')
% grid
% pause


% % find reflect the index of the fullfilled values (not the value it
self)

Rr=(a(1:10000,2).^2+Vgenr.^2)./MXr.^2;
DRr=find(Rr>1.025 | Rr<0.975);
Ry=(a(1:10000,3).^2+Vgeny.^2)./MXy.^2;
DRy=find(Ry>1.025 | Ry<0.975);
Rb=(a(1:10000,4).^2+Vgenb.^2)./MXb.^2;
DRb=find(Rb>1.025 | Rb<0.975);


if isempty(DRr)==0 && isempty(DRy)==0 && isempty(DRb)==0;

  if DRr(1)==DRy(1)==DRb(1);
  DRm=DRr(1);
  elseif DRr(1)==DRy(1)~=DRb(1);
  DRm=min(DRr(1),DRb(1));
  elseif DRr(1)==DRb(1)~=DRy(1);
  DRm=min(DRr(1),DRy(1));
  elseif DRy(1)==DRb(1)~=DRr(1);
  DRm=min(DRy(1),DRb(1));
  elseif DRr(1)~=DRy(1)~=DRb(1);
  DRm=min(DRr(1),DRy(1),DRb(1));
  else
  end

elseif isempty(DRr)==1 && isempty(DRy)==0 && isempty(DRb)==0;

  if DRy(1)==DRb(1);
  DRm=DRy(1);
  elseif DRy(1)~=DRb(1);
```

```
  DRm=min(DRy(1),DRb(1));
  else
  end

elseif isempty(DRy)==1 && isempty(DRr)==0 && isempty(DRb)==0;

  if DRr(1)==DRb(1);
  DRm=DRr(1);
  elseif DRr(1)~=DRb(1);
  DRm=min(DRr(1),DRb(1));
  else
  end

elseif isempty(DRb)==1 && isempty(DRr)==0 && isempty(DRy)==0;

  if DRr(1)==DRy(1);
  DRm=DRr(1);
  elseif DRr(1)~=DRy(1);
  DRm=min(DRr(1),DRy(1));
  else
  end

else
end

FcVr=Rr(DRm:DRm+1999);
FcVy=Ry(DRm:DRm+1999);
FcVb=Rb(DRm:DRm+1999);

MFVr=abs(1-mean(FcVr));
MFVy=abs(1-mean(FcVy));
MFVb=abs(1-mean(FcVb));

figure
plot(i,Rr,'r',i,Ry,'g',i,Rb,'b')
grid
% axis([3500 5000 0 2]);
axis([4000 5500 0 2]);
% axis([5000 6500 0 2]);
legend('Mr(t)','My(t)','Mb(t)');
xlabel('Samples');
ylabel('Voltage Discrmination M(t)');
% title('L1-G Busbar Fault')
% % title('L1-G Fault in middle of LineB (Cairo-Korimat) ')
pause

FcRr=Rr(DRm:DRm+1999);
FcRy=Ry(DRm:DRm+1999);
FcRb=Rb(DRm:DRm+1999);

MFRr=abs(1-mean(FcRr));
MFRy=abs(1-mean(FcRy));
MFRb=abs(1-mean(FcRb));

FT=[MFRr MFRy MFRb]
```

```
%%%%%%%%%%%%%%%%%%%%%%
% I1  %%%%%%%%%%%%%%%
%%%%%%%%%%%%%%%%%%%%%%

averi1=abs(a(:,5));
aveyi1=abs(a(:,6));
avebi1=abs(a(:,7));

Oi1r=find(min(averi1(1:1000))==(averi1(1:1000)));
Oi1y=find(min(aveyi1(1:1000))==(aveyi1(1:1000)));
Oi1b=find(min(avebi1(1:1000))==(avebi1(1:1000)));

ii1=0:(length(a)-2);
shfti1r=(a(Oi1r,1)-.02/4);
shfti1y=(a(Oi1y,1)-.02/4);
shfti1b=(a(Oi1b,1)-.02/4);

ari1=sign(a(2,5)-a(1,5));
bri1=sign(shfti1r);
ayi1=sign(a(2,6)-a(1,6));
byi1=sign(shfti1y);
abi1=sign(a(2,7)-a(1,7));
bbi1=sign(shfti1b);

for m1=1:10000;
 if ari1==bri1;
     I1dashr(m1)=sin(2*pi*50*(m1*0.00001-shfti1r));
 elseif ari1~=bri1;
     I1dashr(m1)=-sin(2*pi*50*(m1*0.00001-shfti1r));
 else
 end

 if ayi1==byi1;
     I1dashy(m1)=sin(2*pi*50*(m1*0.00001-shfti1y));
 elseif ayi1~=byi1;
     I1dashy(m1)=-sin(2*pi*50*(m1*0.00001-shfti1y));
 else
 end

 if abi1==bbi1;
     I1dashb(m1)=sin(2*pi*50*(m1*0.00001-shfti1b));
 elseif abi1~=bbi1;
     I1dashb(m1)=-sin(2*pi*50*(m1*0.00001-shfti1b));
 else
 end
end


MXI1r=max(a(1:2000,5));
MXI1y=max(a(1:2000,6));
MXI1b=max(a(1:2000,7));

I1genr=I1dashr'.*MXI1r;
I1geny=I1dashy'.*MXI1y;
```

```
I1genb=I1dashb'.*MXI1b;

I1Rr=(a(1:10000,5).^2+I1genr.^2)./MXI1r.^2;
I1Ry=(a(1:10000,6).^2+I1geny.^2)./MXI1y.^2;
I1Rb=(a(1:10000,7).^2+I1genb.^2)./MXI1b.^2;

FcI1r=I1Rr(DRm:DRm+1999);
FcI1y=I1Ry(DRm:DRm+1999);
FcI1b=I1Rb(DRm:DRm+1999);

MFI1r=abs(1-mean(FcI1r));
MFI1y=abs(1-mean(FcI1y));
MFI1b=abs(1-mean(FcI1b));

% subplot(3,4,1),plot((1:2000),FcI1r,'r');
% grid;
% subplot(3,4,2),plot((1:2000),FcI1y,'y');
% grid;
% subplot(3,4,3),plot((1:2000),FcI1b,'b');
% grid;
%
subplot(3,4,4),plot((1:2000),MFI1r,'r',(1:2000),MFI1y,'y',(1:2000),MFI1
b,'b');
% grid;
% pause

% figure
% plot(ii1.*.00001,I1Rr,'r',ii1.*.00001,I1Ry,'y',ii1.*.00001,I1Rb,'b')
% grid
% pause

%%%%%%%%%%%%%%%%%%%%%%
% I2  %%%%%%%%%%%%%%%%
%%%%%%%%%%%%%%%%%%%%%%

averi2=abs(a(:,8));
aveyi2=abs(a(:,9));
avebi2=abs(a(:,10));

Oi2r=find(min(averi2(1:1000))==(averi2(1:1000)));
Oi2y=find(min(aveyi2(1:1000))==(aveyi2(1:1000)));
Oi2b=find(min(avebi2(1:1000))==(avebi2(1:1000)));

ii2=0:(length(a)-2);
shfti2r=(a(Oi2r,1)-.02/4);
shfti2y=(a(Oi2y,1)-.02/4);
shfti2b=(a(Oi2b,1)-.02/4);

ari2=sign(a(2,8)-a(1,8));
bri2=sign(shfti2r);
ayi2=sign(a(2,9)-a(1,9));
byi2=sign(shfti2y);
abi2=sign(a(2,10)-a(1,10));
bbi2=sign(shfti2b);
```

```
for m2=1:10000;
 if ari2==bri2;
     I2dashr(m2)=sin(2*pi*50*(m2*0.00001-shfti2r));
 elseif ari2~=bri2;
     I2dashr(m2)=-sin(2*pi*50*(m2*0.00001-shfti2r));
 else
 end

 if ayi2==byi2;
     I2dashy(m2)=sin(2*pi*50*(m2*0.00001-shfti2y));
 elseif ayi2~=byi2;
     I2dashy(m2)=-sin(2*pi*50*(m2*0.00001-shfti2y));
 else
 end

 if abi2==bbi2;
     I2dashb(m2)=sin(2*pi*50*(m2*0.00001-shfti2b));
 elseif abi2~=bbi2;
     I2dashb(m2)=-sin(2*pi*50*(m2*0.00001-shfti2b));
 else
 end
end


MXI2r=max(a(1:2000,8));
MXI2y=max(a(1:2000,9));
MXI2b=max(a(1:2000,10));

I2genr=I2dashr'.*MXI2r;
I2geny=I2dashy'.*MXI2y;
I2genb=I2dashb'.*MXI2b;

I2Rr=(a(1:10000,8).^2+I2genr.^2)./MXI2r.^2;
I2Ry=(a(1:10000,9).^2+I2geny.^2)./MXI2y.^2;
I2Rb=(a(1:10000,10).^2+I2genb.^2)./MXI2b.^2;

FcI2r=I2Rr(DRm:DRm+1999);
FcI2y=I2Ry(DRm:DRm+1999);
FcI2b=I2Rb(DRm:DRm+1999);

MFI2r=abs(1-mean(FcI2r));
MFI2y=abs(1-mean(FcI2y));
MFI2b=abs(1-mean(FcI2b));

% subplot(3,4,5),plot((1:2000),FcI2r,'r');
% grid;
% subplot(3,4,6),plot((1:2000),FcI2y,'y');
% grid;
% subplot(3,4,7),plot((1:2000),FcI2b,'b');
% grid;
%
subplot(3,4,8),plot((1:2000),MFI2r,'r',(1:2000),MFI2y,'y',(1:2000),MFI2
b,'b');
% grid;
% pause
```

```
% figure
% plot(ii2.*.00001,I2Rr,'r',ii2.*.00001,I2Ry,'y',ii2.*.00001,I2Rb,'b')
% grid
% pause


%%%%%%%%%%%%%%%%%%%%%%
% I3  %%%%%%%%%%%%%%%%
%%%%%%%%%%%%%%%%%%%%%%

averi3=abs(a(:,11));
aveyi3=abs(a(:,12));
avebi3=abs(a(:,13));

Oi3r=find(min(averi3(1:1000))==(averi3(1:1000)));
Oi3y=find(min(aveyi3(1:1000))==(aveyi3(1:1000)));
Oi3b=find(min(avebi3(1:1000))==(avebi3(1:1000)));

ii3=0:(length(a)-2);
shfti3r=(a(Oi3r,1)-.02/4);
shfti3y=(a(Oi3y,1)-.02/4);
shfti3b=(a(Oi3b,1)-.02/4);

ari3=sign(a(2,11)-a(1,11));
bri3=sign(shfti3r);
ayi3=sign(a(2,12)-a(1,12));
byi3=sign(shfti3y);
abi3=sign(a(2,13)-a(1,13));
bbi3=sign(shfti3b);

for m3=1:10000;
 if ari3==bri3;
     I3dashr(m3)=sin(2*pi*50*(m3*0.00001-shfti3r));
 elseif ari3~=bri3;
     I3dashr(m3)=-sin(2*pi*50*(m3*0.00001-shfti3r));
 else
 end

 if ayi3==byi3;
     I3dashy(m3)=sin(2*pi*50*(m3*0.00001-shfti3y));
 elseif ayi3~=byi3;
     I3dashy(m3)=-sin(2*pi*50*(m3*0.00001-shfti3y));
 else
 end

 if abi3==bbi3;
     I3dashb(m3)=sin(2*pi*50*(m3*0.00001-shfti3b));
 elseif abi3~=bbi3;
     I3dashb(m3)=-sin(2*pi*50*(m3*0.00001-shfti3b));
 else
 end
end
```

```
MXI3r=max(a(1:2000,11));
MXI3y=max(a(1:2000,12));
MXI3b=max(a(1:2000,13));

I3genr=I3dashr'.*MXI3r;
I3geny=I3dashy'.*MXI3y;
I3genb=I3dashb'.*MXI3b;

I3Rr=(a(1:10000,11).^2+I3genr.^2)./MXI3r.^2;
I3Ry=(a(1:10000,12).^2+I3geny.^2)./MXI3y.^2;
I3Rb=(a(1:10000,13).^2+I3genb.^2)./MXI3b.^2;

FcI3r=I3Rr(DRm:DRm+1999);
FcI3y=I3Ry(DRm:DRm+1999);
FcI3b=I3Rb(DRm:DRm+1999);

MFI3r=abs(1-mean(FcI3r));
MFI3y=abs(1-mean(FcI3y));
MFI3b=abs(1-mean(FcI3b));

% subplot(3,4,9),plot((1:2000),FcI3r,'r');
% grid;
% subplot(3,4,10),plot((1:2000),FcI3y,'y');
% grid;
% subplot(3,4,11),plot((1:2000),FcI3b,'b');
% grid;
%subplot(3,4,12),plot((1:2000),MFI3r,'r',(1:2000),MFI3y,'y',(1:2000),MF
I3b,'b');
% grid;

FT=[MFI1r MFI1y MFI1b;MFI2r MFI2y MFI2b;MFI3r MFI3y MFI3b]

%%%%%%%%%%%%%%%%%%%%%%%%%%%%%%%%%%%%%%%%%%%%%%%%%%%%%%%%%%%%%%%%%%%%%%%%%

i=0:(length(a)-1);
Vph=[a(:,2) a(:,3) a(:,4)];
Ip1=[a(:,5) a(:,6) a(:,7)];
Ip2=[a(:,8) a(:,9) a(:,10)];
Ip3=[a(:,11) a(:,12) a(:,13)];

% % Clarke
% % K=[1 1 1;1 0 2;1 1 1]./3;
% % Karrenbauer
% % T=[1 1 1;1 -2 1;1 1 -2]./3
% % inv(j)

% DF (t) = K V(t) -  Z0 K I(t)

j=(1/3)*[1 1 1;1.5 0 -1.5;0.5 -1 0.5];

Vm=j*Vph';

Im1=j*Ip1';
```

```
Im2=j*Ip2';
Im3=j*Ip3';

Zm=[486 0 0;0 280 0;0 0 280];

%%% I1 %%%%%


Sf1=Vm-Zm*Im1;
% Sf1=Zm*Im1-Vm
Sf11=Sf1(2,:);
% figure
% plot(i.*.00001,Sf11,'r');
% grid
% pause
Sf11av=abs(Sf11);
OSf11=find(min(Sf11av(1:999))==(Sf11av(1:999)));
shftSf11=(OSf11*.00001-.02/4);
MSf11=max(Sf11(1:2000));
af1=sign(Sf11(2)-Sf11(1));
bf1=sign(shftSf11);
if af1==bf1;
    Sf11dash=sin(2*pi*50*(i*0.00001-shftSf11));
elseif af1~=bf1;
    Sf11dash=-sin(2*pi*50*(i*0.00001-shftSf11));
else
end
Sf11gen=Sf11dash*MSf11;
% plot(i.*.00001,Sf11gen,'b',i.*.00001,Sf11,'r');
% grid
RSf1=(Sf11.^2+Sf11gen.^2)./MSf11.^2;
% subplot(2,1,1),
% plot(i.*.00001,RSf1,'c');
% grid
% pause

Sb1=Vm+Zm*Im1;
Sb11=Sb1(2,:);

Sb11av=abs(Sb11);
OSb11=find(min(Sb11av(1:999))==(Sb11av(1:999)));
shftSb11=(OSb11*.00001-.02/4);
MSb11=max(Sb11(1:2000));
ab1=sign(Sb11(2)-Sb11(1));
bb1=sign(shftSb11);
if ab1==bb1;
    Sb11dash=sin(2*pi*50*(i*0.00001-shftSb11));
elseif ab1~=bb1
    Sb11dash=-sin(2*pi*50*(i*0.00001-shftSb11));
else
end
Sb11gen=Sb11dash*MSb11;
RSb1=(Sb11.^2+Sb11gen.^2)./MSb11.^2;
figure
plot(i,RSf1,'-r',i,RSb1,'--b');
% axis([5200 5550 .6 1.4]);
```

```
legend('Forward','Backward');
xlabel('Samples');
ylabel('TW Discrimination MT(t)');
% title('A8-I1')
grid

%%% I2 %%%%%


Sf2=Vm-Zm*Im2;
% Sf1=Zm*Im1-Vm
Sf21=Sf2(2,:);
% figure
% plot(i.*.00001,Sf21,'r');
% grid
% pause
Sf21av=abs(Sf21);
OSf21=find(min(Sf21av(1:999))==(Sf21av(1:999)));
shftSf21=(OSf21*.00001-.02/4);
MSf21=max(Sf21(1:2000));
af2=sign(Sf21(2)-Sf21(1));
bf2=sign(shftSf21);
if af2==bf2;
    Sf21dash=sin(2*pi*50*(i*0.00001-shftSf21));
elseif af2~=bf2;
    Sf21dash=-sin(2*pi*50*(i*0.00001-shftSf21));
else
end
Sf21gen=Sf21dash*MSf21;
% plot(i.*.00001,Sf21gen,'b',i.*.00001,Sf21,'r');
% grid
RSf2=(Sf21.^2+Sf21gen.^2)./MSf21.^2;

Sb2=Vm+Zm*Im2;
Sb21=Sb2(2,:);

Sb21av=abs(Sb21);
OSb21=find(min(Sb21av(1:999))==(Sb21av(1:999)));
shftSb21=(OSb21*.00001-.02/4);
MSb21=max(Sb21(1:2000));
ab2=sign(Sb21(2)-Sb21(1));
bb2=sign(shftSb21);
if ab2==bb2;
    Sb21dash=sin(2*pi*50*(i*0.00001-shftSb21));
elseif ab2~=bb2
    Sb21dash=-sin(2*pi*50*(i*0.00001-shftSb21));
else
end
Sb21gen=Sb21dash*MSb21;
RSb2=(Sb21.^2+Sb21gen.^2)./MSb21.^2;
figure
plot(i,RSf2,'-r',i,RSb2,'--b');
% axis([5225 5550 .9 1.1]);
legend('Forward','Backward');
xlabel('Samples');
ylabel('TW Discrimination MT(t)');
```

```
% title('A8-I1')
grid


%%% I3 %%%%%


Sf3=Vm-Zm*Im3;
% Sf1=Zm*Im1-Vm
Sf31=Sf3(2,:);
% figure
% plot(i.*.00001,Sf21,'r');
% grid
% pause
Sf31av=abs(Sf31);
OSf31=find(min(Sf31av(1:999))==(Sf31av(1:999)));
shftSf31=(OSf31*.00001-.02/4);
MSf31=max(Sf31(1:2000));
af3=sign(Sf31(2)-Sf31(1));
bf3=sign(shftSf31);
if af3==bf3;
    Sf31dash=sin(2*pi*50*(i*0.00001-shftSf31));
elseif af3~=bf3;
    Sf31dash=-sin(2*pi*50*(i*0.00001-shftSf31));
else
end
Sf31gen=Sf31dash*MSf31;
% plot(i.*.00001,Sf31gen,'b',i.*.00001,Sf31,'r');
% grid
RSf3=(Sf31.^2+Sf31gen.^2)./MSf31.^2;

Sb3=Vm+Zm*Im3;
Sb31=Sb3(2,:);

Sb31av=abs(Sb31);
OSb31=find(min(Sb31av(1:999))==(Sb31av(1:999)));
shftSb31=(OSb31*.00001-.02/4);
MSb31=max(Sb31(1:2000));
ab3=sign(Sb31(2)-Sb31(1));
bb3=sign(shftSb31);
if ab3==bb3;
    Sb31dash=sin(2*pi*50*(i*0.00001-shftSb31));
elseif ab3~=bb3
    Sb31dash=-sin(2*pi*50*(i*0.00001-shftSb31));
else
end
Sb31gen=Sb31dash*MSb31;
RSb3=(Sb31.^2+Sb31gen.^2)./MSb31.^2;
figure
plot(i,RSf3,'-r',i,RSb3,'--b');
% axis([5225 5550 .9 1.1]);
legend('Forward','Backward');
xlabel('Samples');
ylabel('TW Discrimination MT(t)');
% title('A8-I1')
grid
```

Appendix [D]

ATP

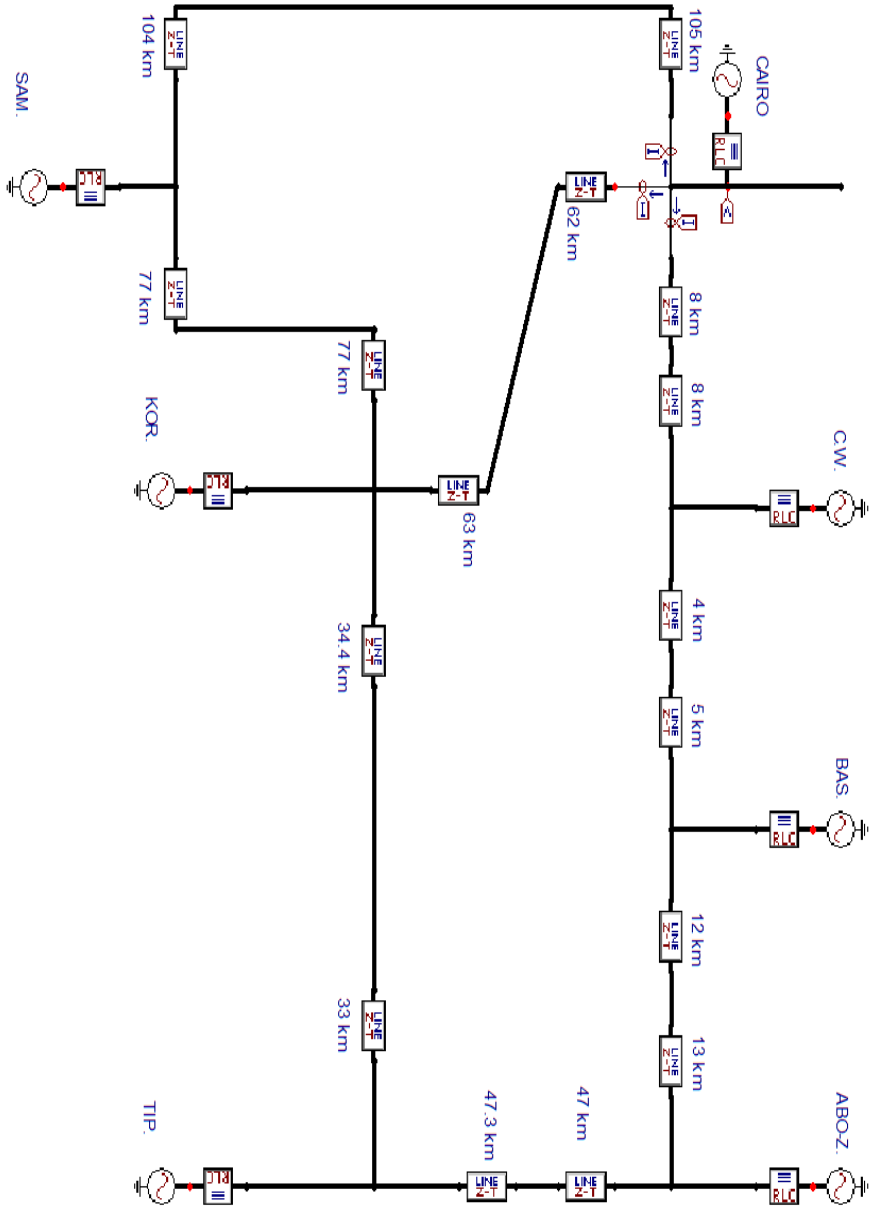

Grid simulated by ATP.

Station / Parameter	Cairo	Cairo	Basous	Abo	Tippen	Korimat	Samalut	Units
Amp.	408.248							V
Freq.	50							HZ
Phase Shift	20	20	-10	-10	0	5	0	Deg.
SC Capacity	50	20	24.4	13.26	1.2	2	20	GVA
Phases Inductance	5	12.5	10.25	18.85	208.33	125	12.5	Ohm

Table D7.1, Input Data of stations for ATP.

Lines	Cairo - Cairo West	Cairo West- Basous	Basous - Abo Zabal	Abo Zabal - Tippen	Tippen - Korimat	Korimat - Samalut	Korimat - Cairo	Samalut - Cairo	
Parameters									Units
Positive Sequence Resistance	0.0217								Ohm/Mt.
Zero Sequence Resistance	0.247								Ohm/Mt.
Positive Sequence Inductance	0.302								mH/Mt.
Zero Sequence Inductance	0.91								mH/Mt.
Positive Sequence Capacitance	3.96								µF/Mt.
Zero Sequence Capacitance	2.94								µF/Mt.
Line length	16	9	25	93	77	154	125	209	KM

Table D.2, Input Data of transmission lines for ATP.

Appendix [E]

Lab-Veiw

Lab-Veiw Block Diagram.